

Supporting Information

**Diastereoselective synthesis of the HIV protease inhibitor darunavir
and related derivatives via a titanium tetrachloride mediated
asymmetric glycolate aldol addition reaction**

Jordan M. Witte, Emmanuel Ayim, Christopher J. Sams, Jasmine B. Service, Caitlyn C. Kant,
Lillian Bambalas, Daniel Wright, Austin Carter, Kelly Moran, Isabella G. Rohrig,
Gregory M. Ferrence, and Shawn R. Hitchcock*

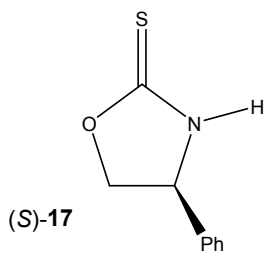
Department of Chemistry, Illinois State University, Normal, IL 617090-4160

Table of Contents

400 MHz ^1H NMR spectrum of (<i>S</i>)- 17	5
100 MHz $^{13}\text{C}\{^1\text{H}\}$ NMR spectrum of (<i>S</i>)- 17	6
400 MHz ^1H NMR spectrum of (<i>R</i>)- 17	7
100 MHz $^{13}\text{C}\{^1\text{H}\}$ NMR spectrum of (<i>R</i>)- 17	8
400 MHz ^1H NMR spectrum of (<i>S</i>)- 11	9
100 MHz $^{13}\text{C}\{^1\text{H}\}$ NMR spectrum of (<i>S</i>)- 11	10
400 MHz ^1H NMR spectrum of (<i>R</i>)- 11	11
100 MHz $^{13}\text{C}\{^1\text{H}\}$ NMR spectrum of (<i>R</i>)- 11	12
500 MHz ^1H NMR spectrum of (<i>S,S,R</i>)- 10	13
125 MHz $^{13}\text{C}\{^1\text{H}\}$ NMR spectrum of (<i>S,S,R</i>)- 10	14
400 MHz ^1H NMR spectrum of (<i>R,S,R</i>)- 10	15
100 MHz $^{13}\text{C}\{^1\text{H}\}$ NMR spectrum of (<i>R,S,R</i>)- 10	16
500 MHz ^1H NMR spectrum of 15	17
125 MHz $^{13}\text{C}\{^1\text{H}\}$ NMR spectrum of 15	18
400 MHz ^1H NMR spectrum of 18	19
100 MHz $^{13}\text{C}\{^1\text{H}\}$ NMR spectrum of 18	20
400 MHz ^1H NMR spectrum of 14	21
100 MHz $^{13}\text{C}\{^1\text{H}\}$ NMR spectrum of 14	22
400 MHz ^1H NMR spectrum of 19	23
100 MHz $^{13}\text{C}\{^1\text{H}\}$ NMR spectrum of 19	24
500 MHz ^1H NMR spectrum of 13	25

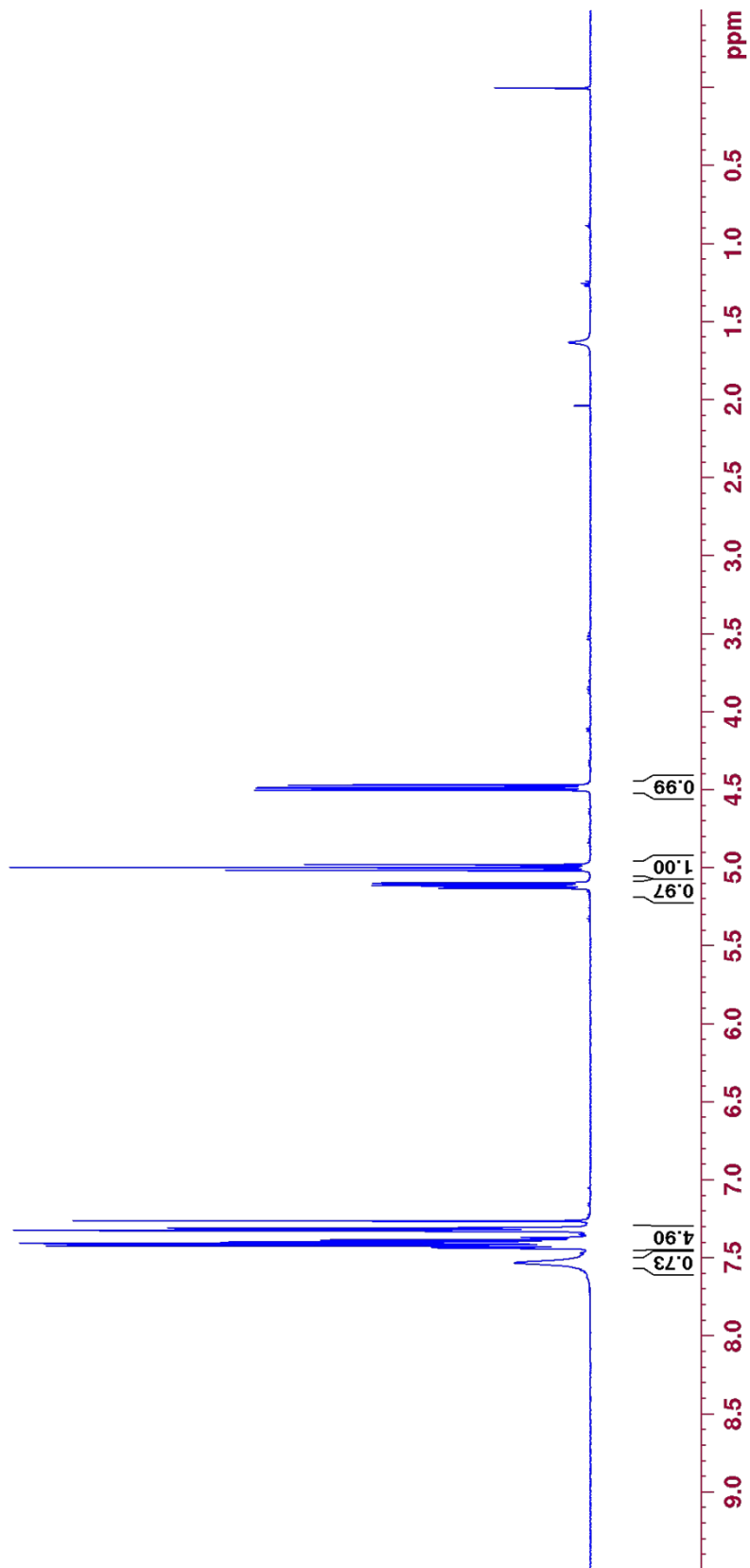
100 MHz $^{13}\text{C}\{^1\text{H}\}$ NMR spectrum of 13	26
400 MHz ^1H NMR spectrum of 20	27
100 MHz $^{13}\text{C}\{^1\text{H}\}$ NMR spectrum of 20	28
500 MHz ^1H NMR spectrum of 21	29
100 MHz $^{13}\text{C}\{^1\text{H}\}$ NMR spectrum of 21	30
500 MHz ^1H NMR spectrum of 22	31
100 MHz $^{13}\text{C}\{^1\text{H}\}$ NMR spectrum of 22	32
500 MHz ^1H NMR spectrum of 12	33
100 MHz $^{13}\text{C}\{^1\text{H}\}$ NMR spectrum of 12	34
400 MHz ^1H NMR spectrum of 23	35
100 MHz $^{13}\text{C}\{^1\text{H}\}$ NMR spectrum of 23	36
500 MHz ^1H NMR spectrum of 1	37
125 MHz $^{13}\text{C}\{^1\text{H}\}$ NMR spectrum of 1	38
500 MHz ^1H NMR spectrum of 27	39
100 MHz $^{13}\text{C}\{^1\text{H}\}$ NMR spectrum of 27	40
500 MHz ^1H NMR spectrum of 28	41
100 MHz $^{13}\text{C}\{^1\text{H}\}$ NMR spectrum of 28	42
500 MHz ^1H NMR spectrum of 30	43
100 MHz $^{13}\text{C}\{^1\text{H}\}$ NMR spectrum of 30	44
500 MHz ^1H NMR spectrum of 31	45
100 MHz $^{13}\text{C}\{^1\text{H}\}$ NMR spectrum of 31	46
500 MHz ^1H NMR spectrum of 32	47
100 MHz $^{13}\text{C}\{^1\text{H}\}$ NMR spectrum of 32	48

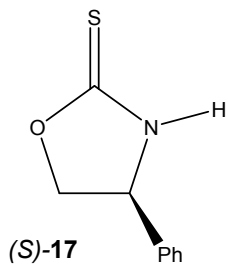
500 MHz ^1H NMR spectrum of 33	49
100 MHz $^{13}\text{C}\{^1\text{H}\}$ NMR spectrum of 33	50
500 MHz ^1H NMR spectrum of 34	51
100 MHz $^{13}\text{C}\{^1\text{H}\}$ NMR spectrum of 34	52
500 MHz ^1H NMR spectrum of 35	53
100 MHz $^{13}\text{C}\{^1\text{H}\}$ NMR spectrum of 35	54
500 MHz ^1H NMR spectrum of 36	55
100 MHz $^{13}\text{C}\{^1\text{H}\}$ NMR spectrum of 36	56
500 MHz ^1H NMR spectrum of 41	57
125 MHz $^{13}\text{C}\{^1\text{H}\}$ NMR spectrum of 41	58
500 MHz ^1H NMR spectrum of 42	59
100 MHz $^{13}\text{C}\{^1\text{H}\}$ NMR spectrum of 42	60
500 MHz ^1H NMR spectrum of 43	61
100 MHz $^{13}\text{C}\{^1\text{H}\}$ NMR spectrum of 43	62
500 MHz ^1H NMR spectrum of 44	63
100 MHz $^{13}\text{C}\{^1\text{H}\}$ NMR spectrum of 44	64
500 MHz ^1H NMR spectrum of 45	65
100 MHz $^{13}\text{C}\{^1\text{H}\}$ NMR spectrum of 45	66
500 MHz ^1H NMR spectrum of 46	67
100 MHz $^{13}\text{C}\{^1\text{H}\}$ NMR spectrum of 46	68
500 MHz ^1H NMR spectrum of 38	69
125 MHz $^{13}\text{C}\{^1\text{H}\}$ NMR spectrum of 38	70
X-ray Crystallographic Data and ORTEP for 10	71



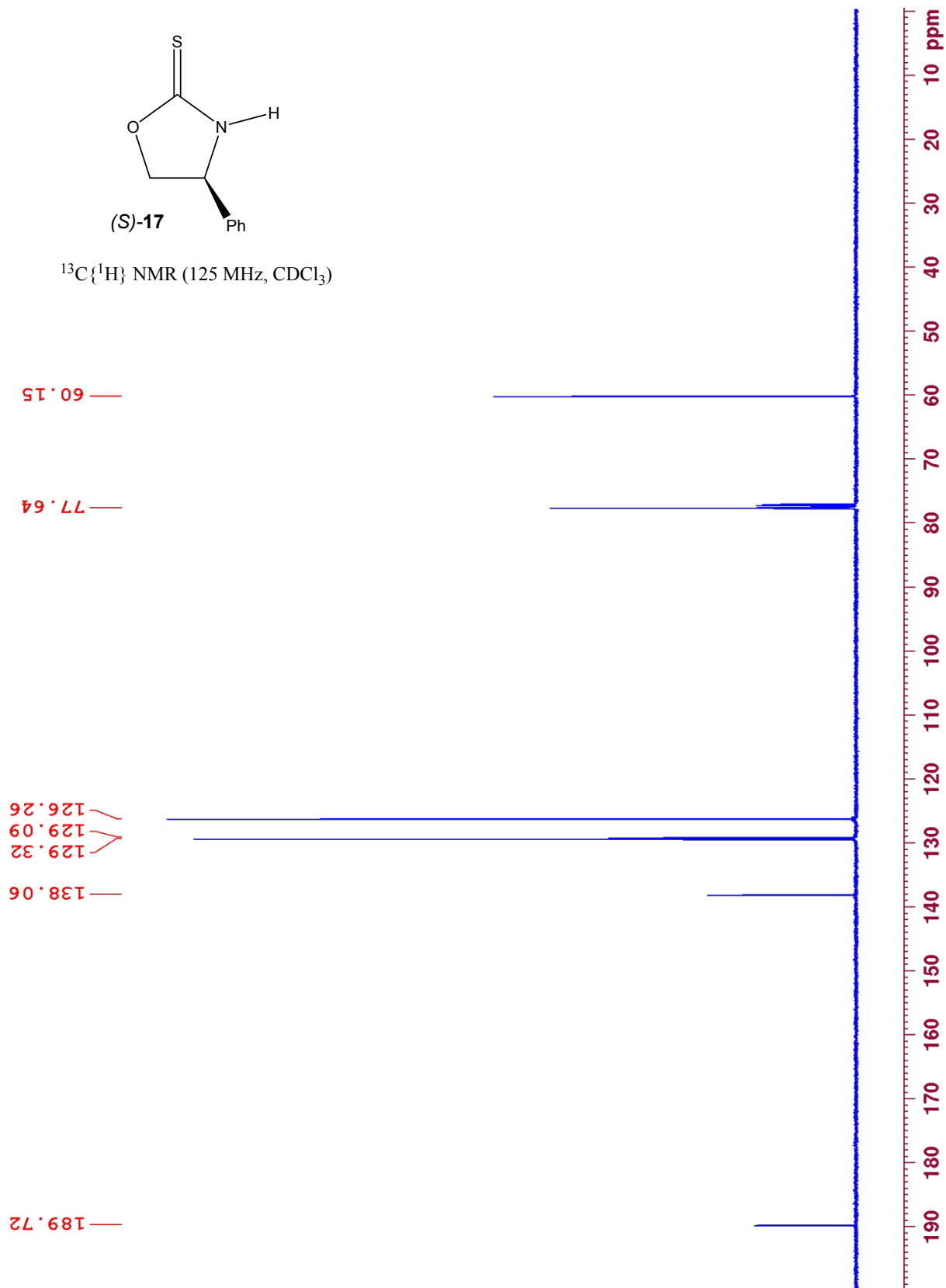
¹H NMR (500 MHz, CDCl₃)

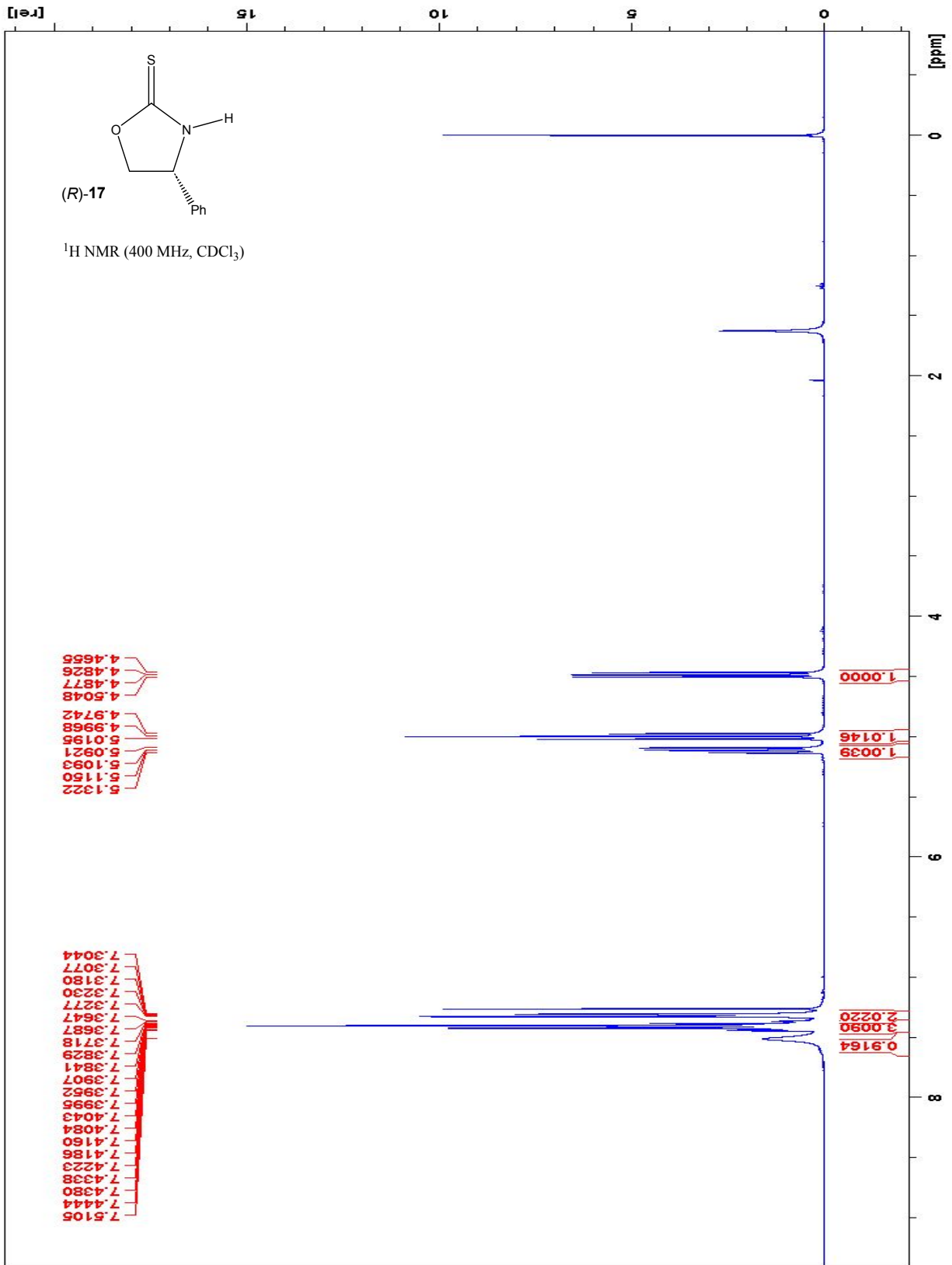
7.530
7.438
7.434
7.430
7.425
7.420
7.417
7.409
7.406
7.401
7.397
7.394
7.389
7.384
7.369
7.325
7.322
7.318
7.312
7.309
7.307
5.128
5.114
5.110
5.096
5.014
4.978
4.996
4.500
4.486
4.482
4.468

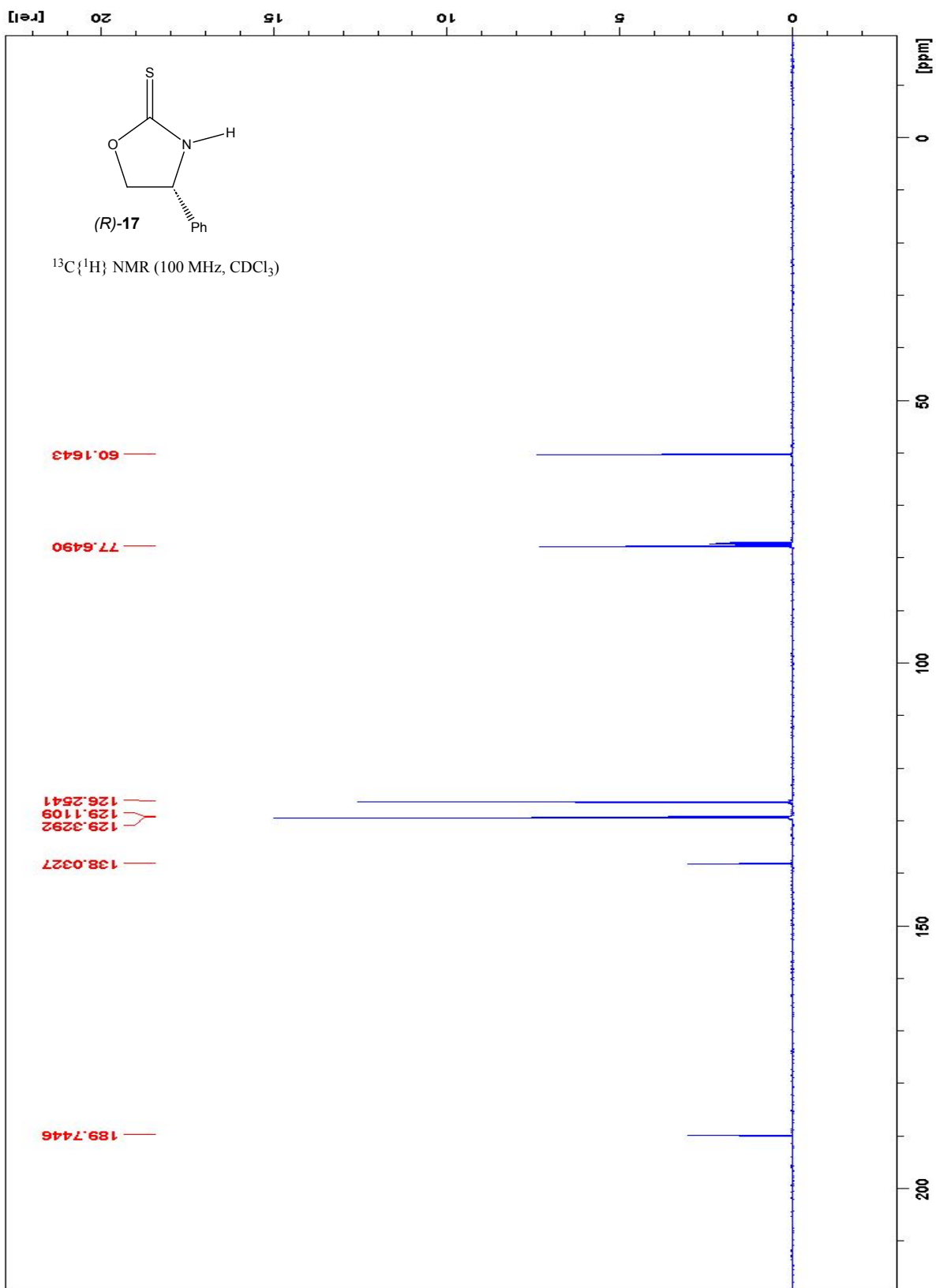


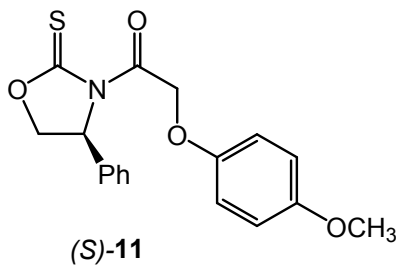


$^{13}\text{C}\{^1\text{H}\}$ NMR (125 MHz, CDCl_3)

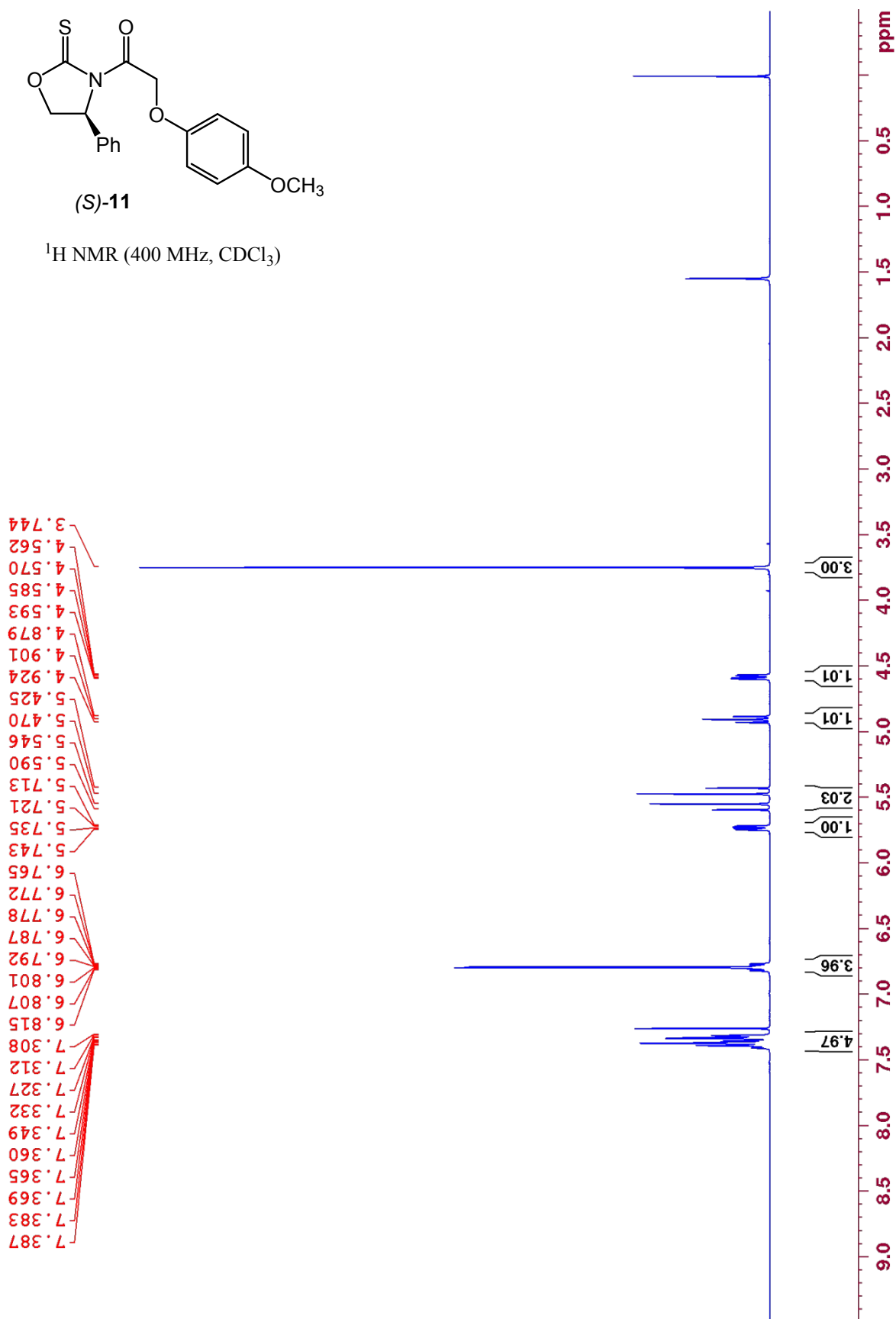


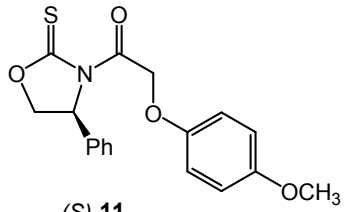




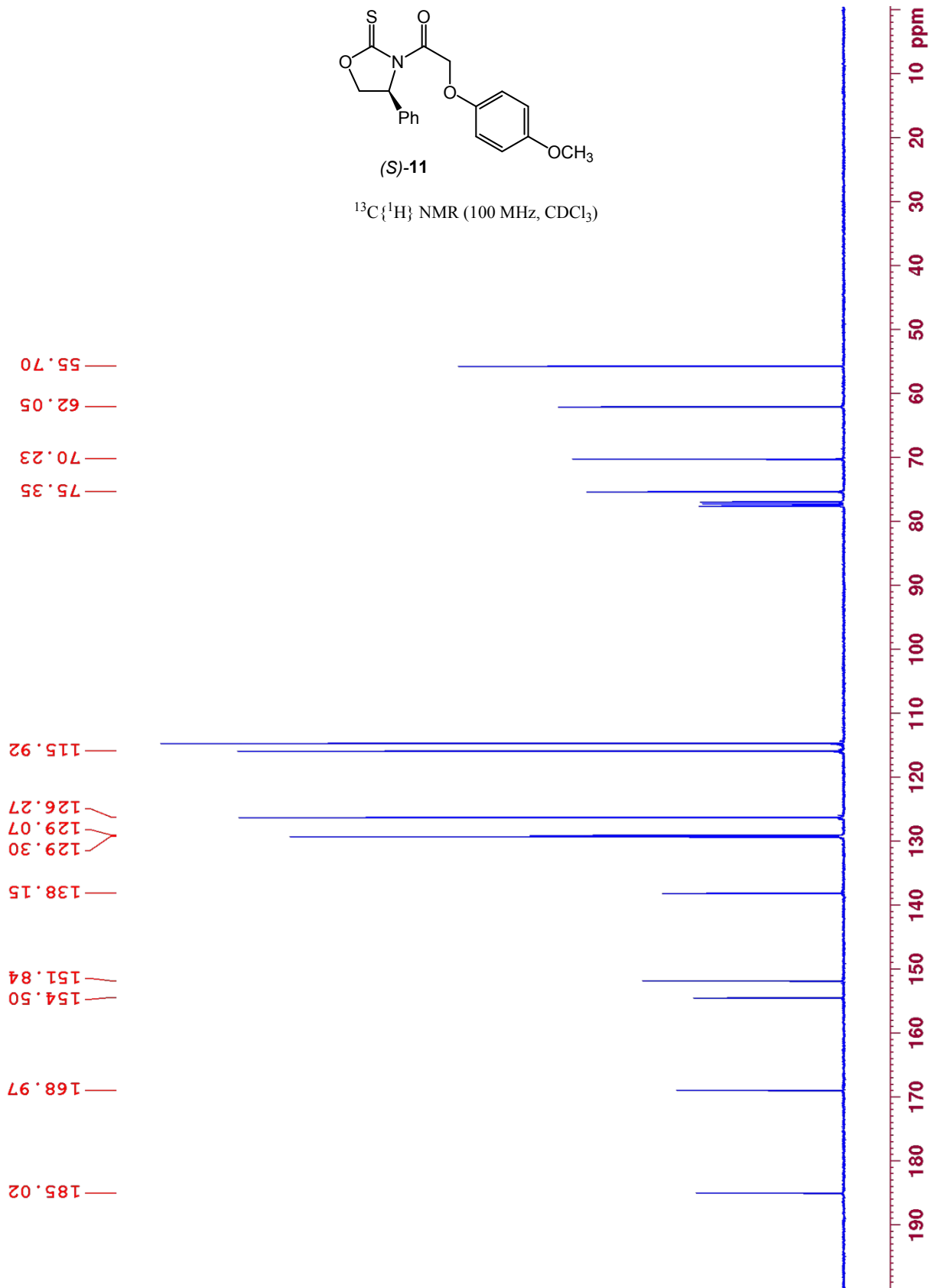


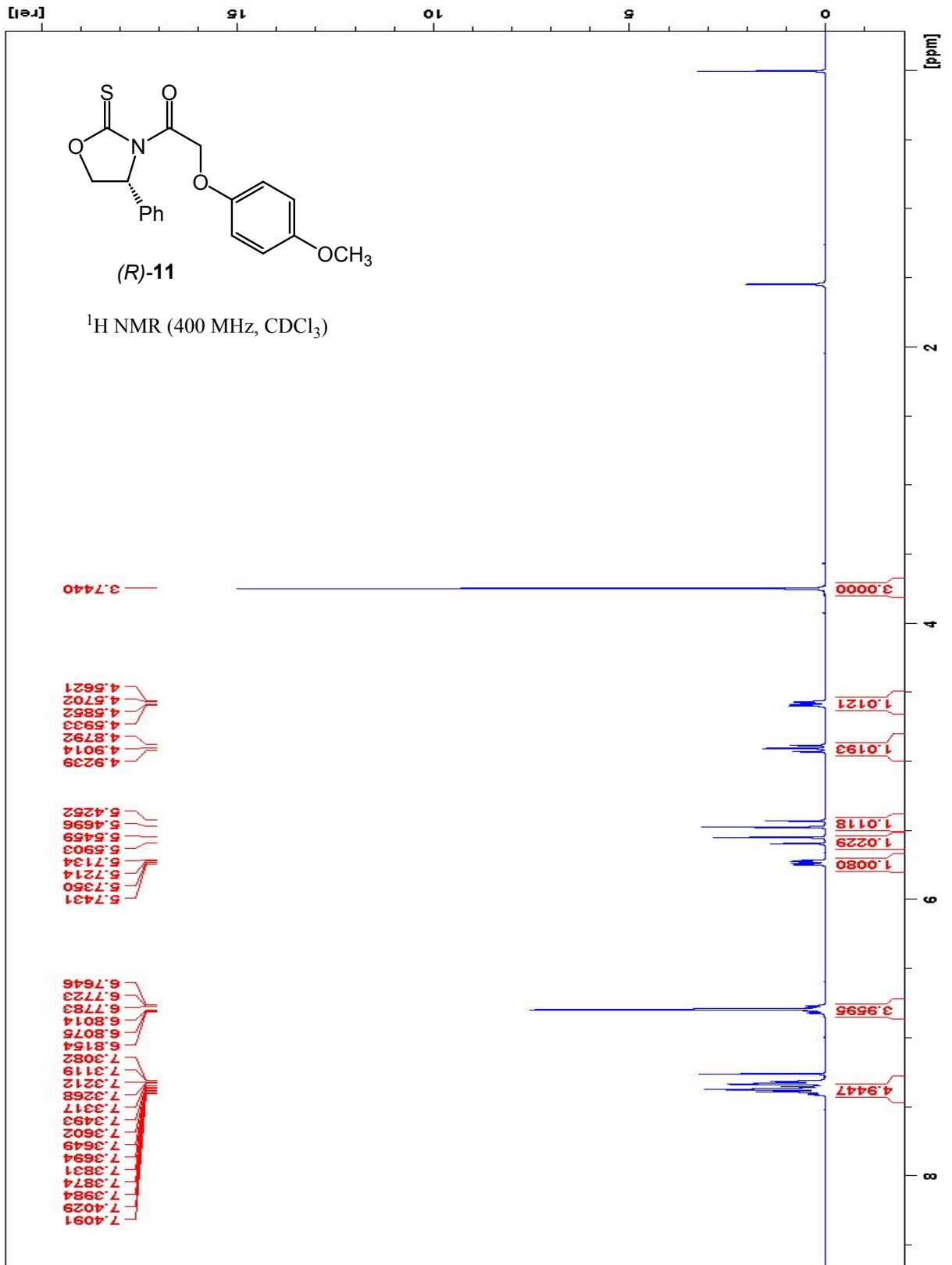
$^1\text{H NMR}$ (400 MHz, CDCl_3)

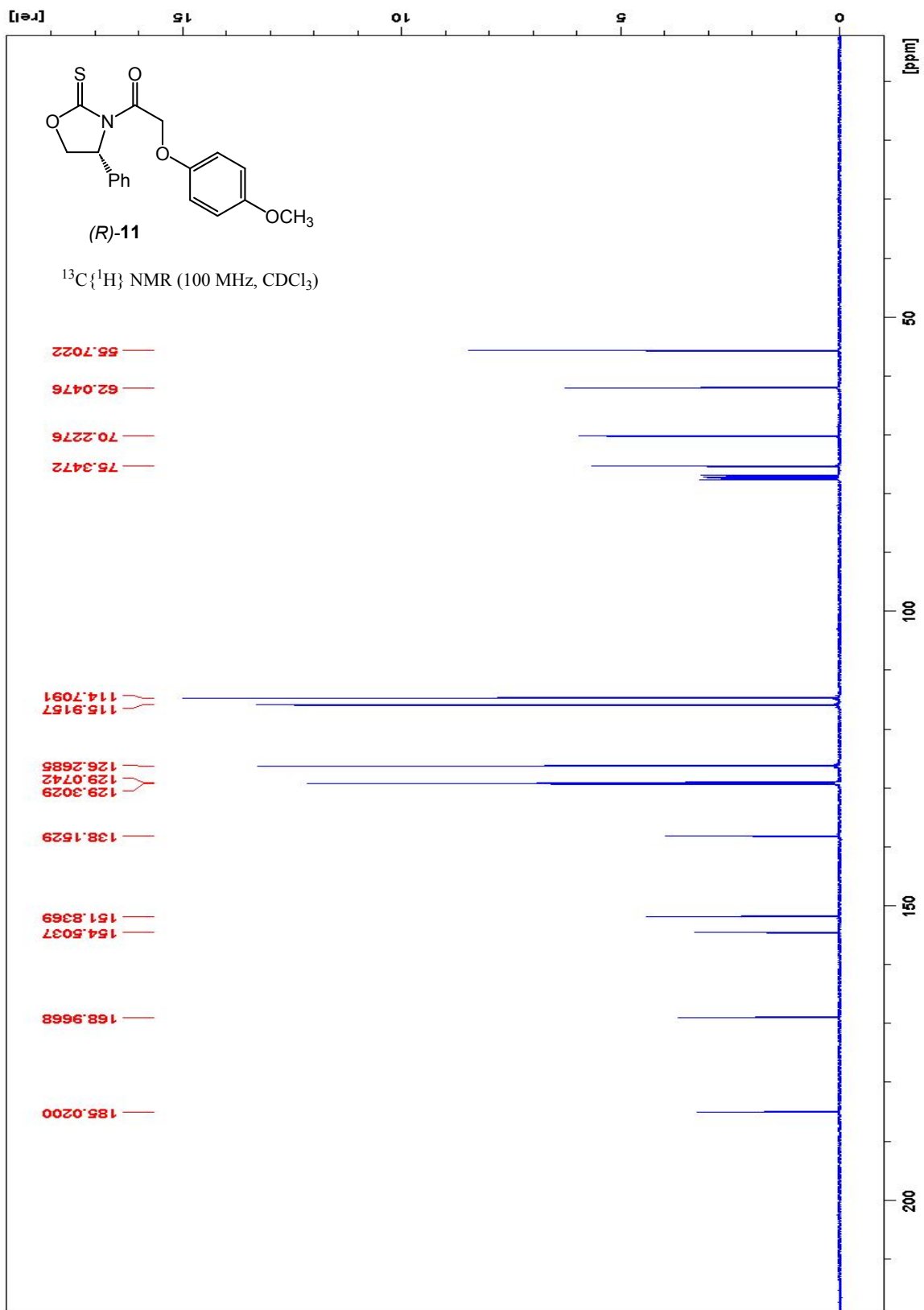


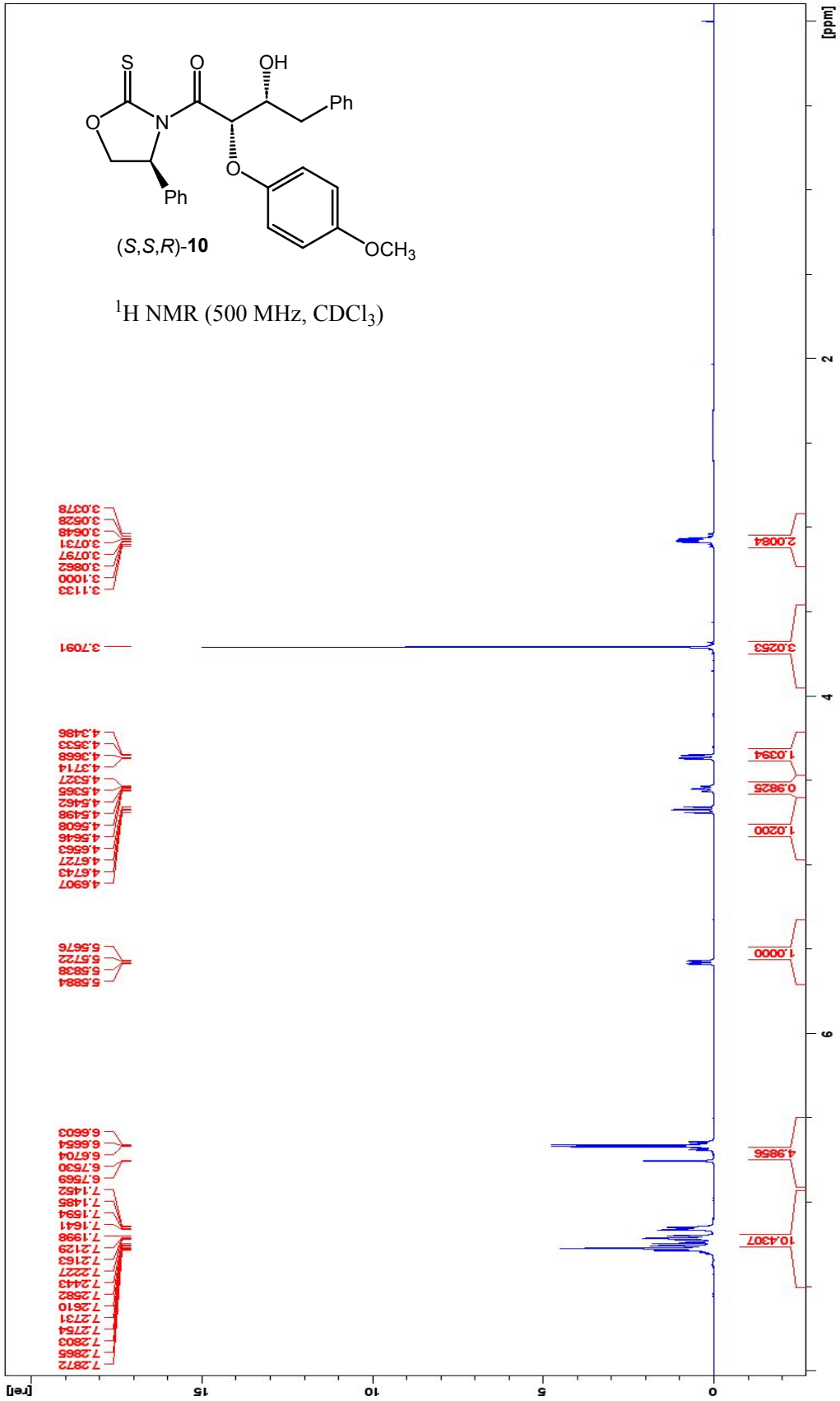


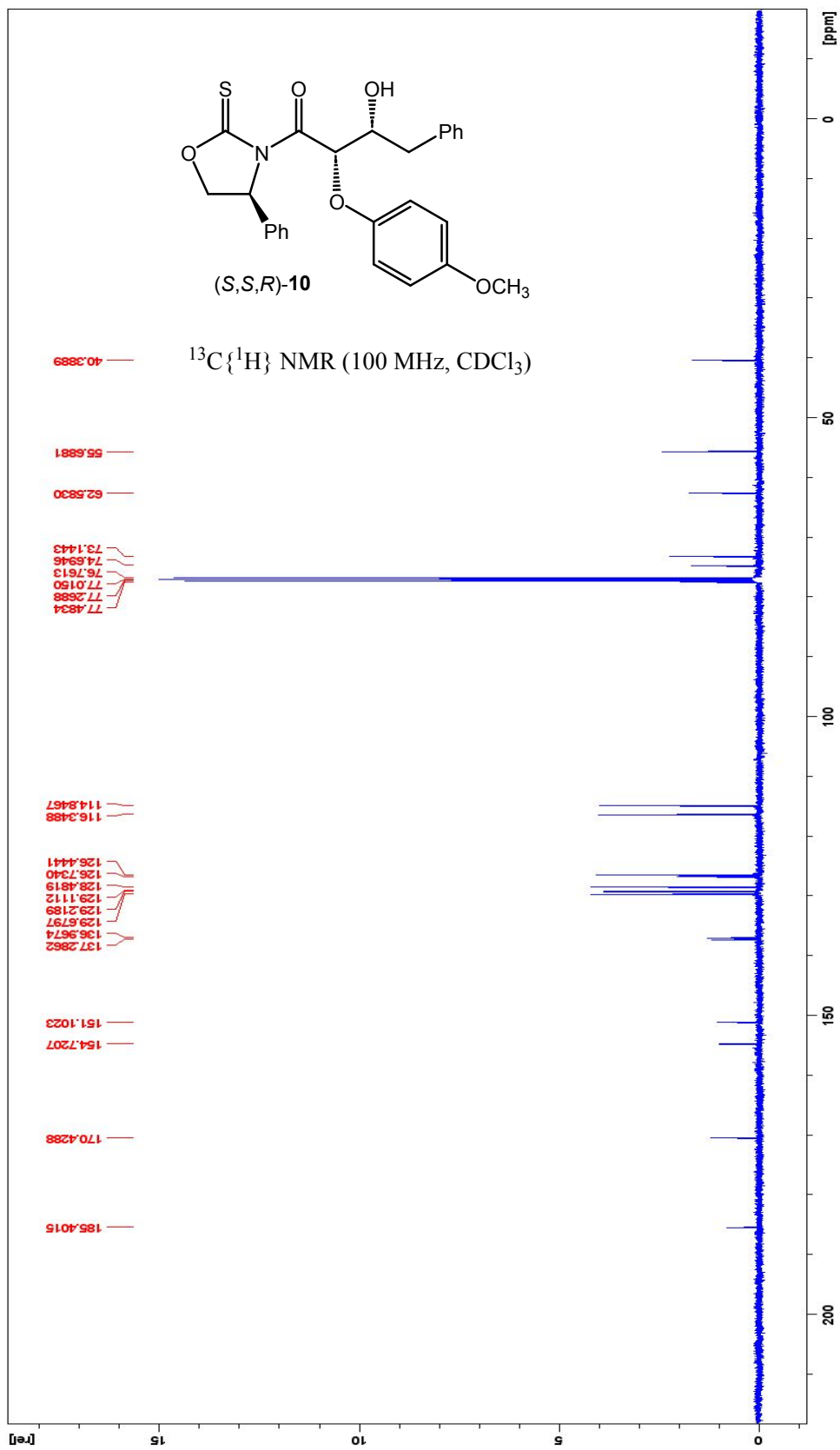
$^{13}\text{C}\{^1\text{H}\}$ NMR (100 MHz, CDCl_3)

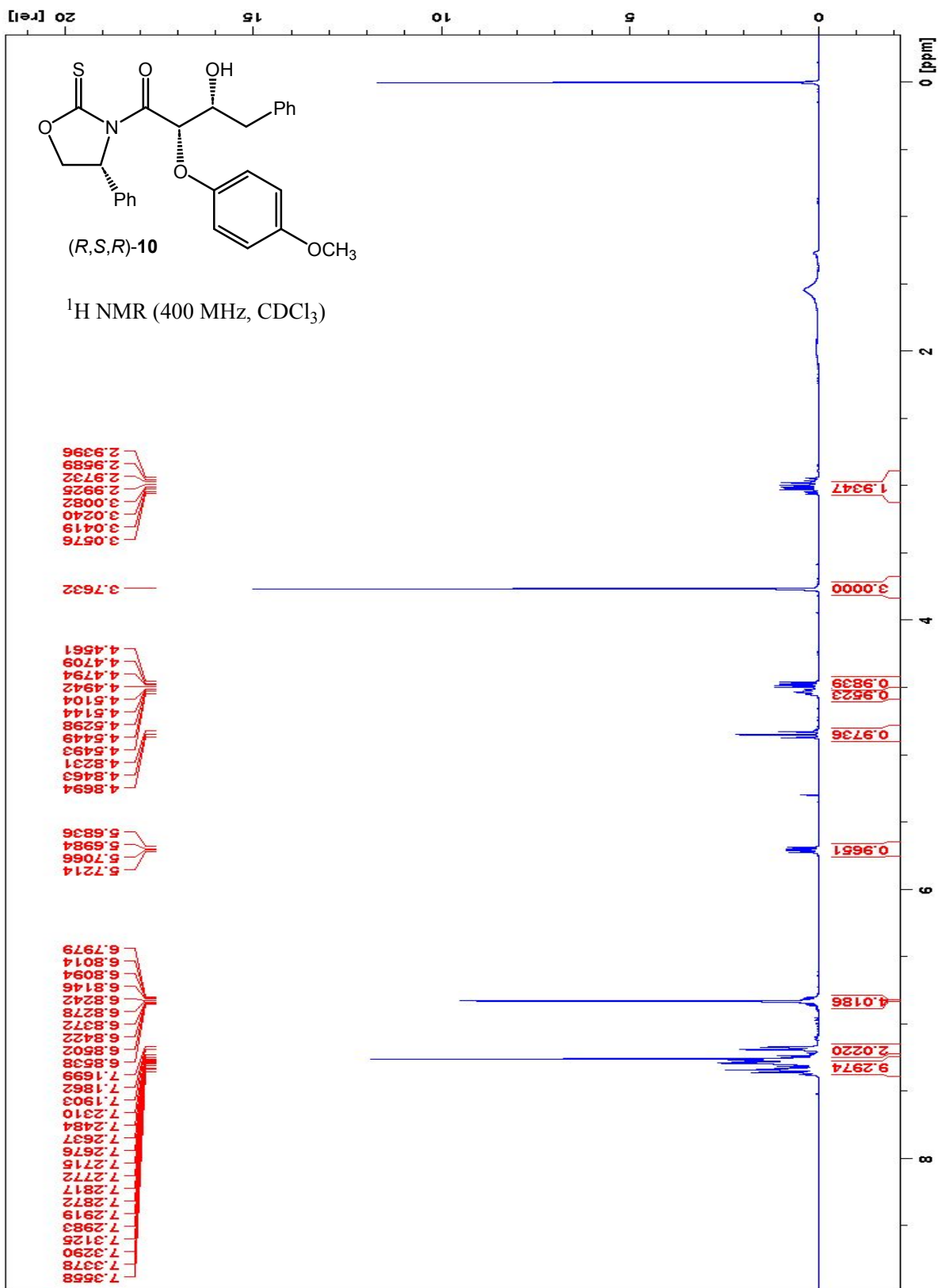


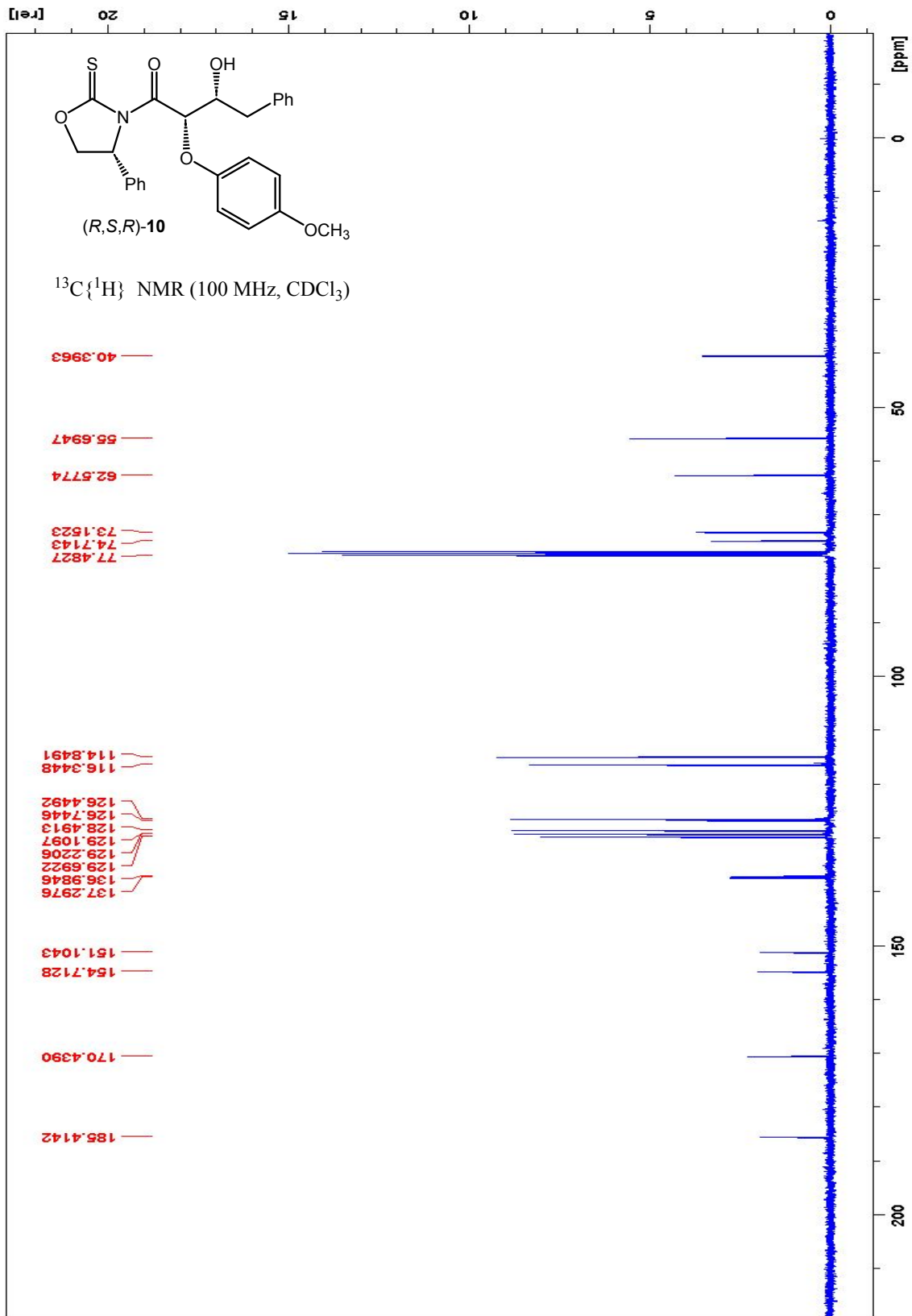


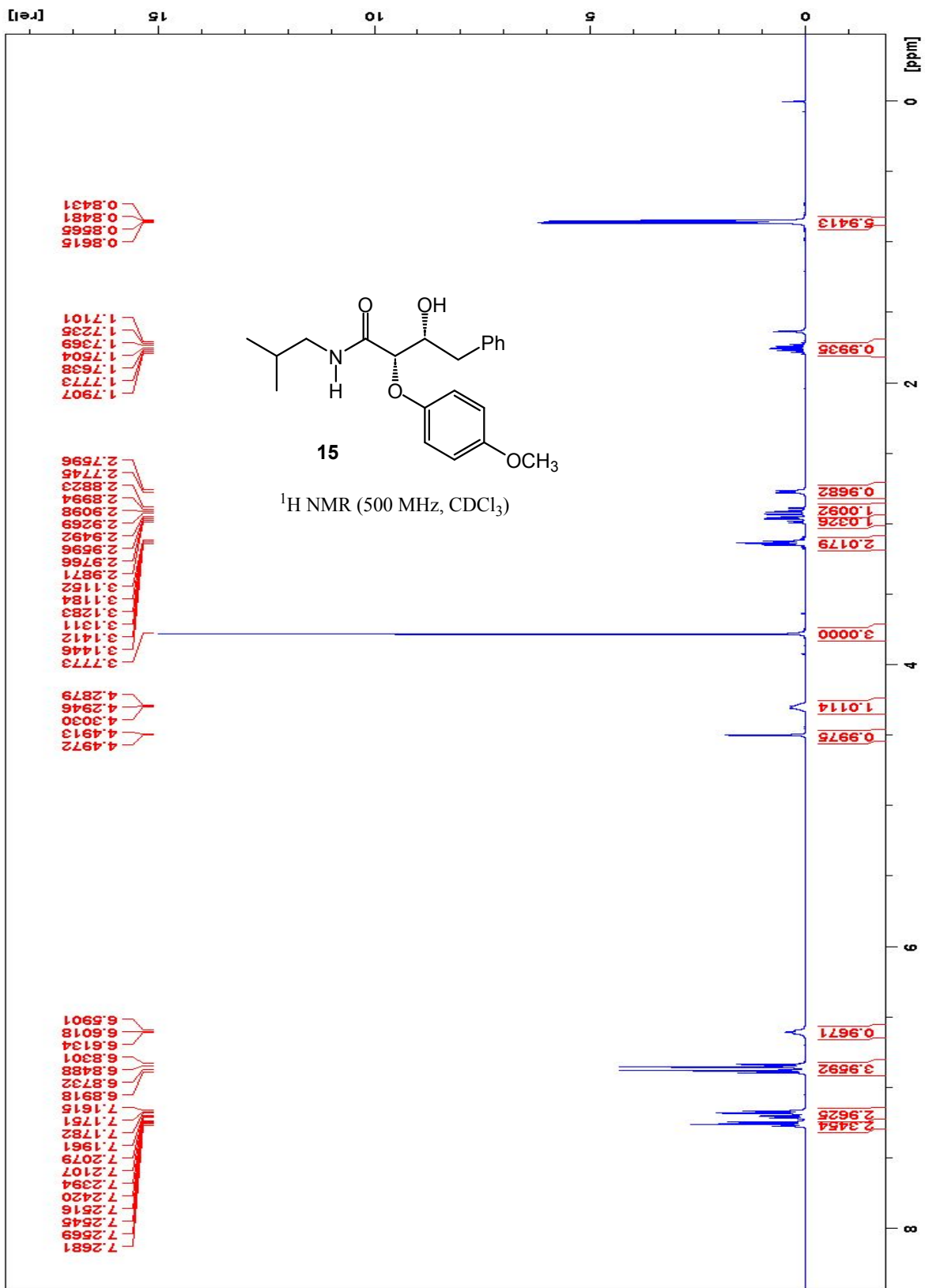


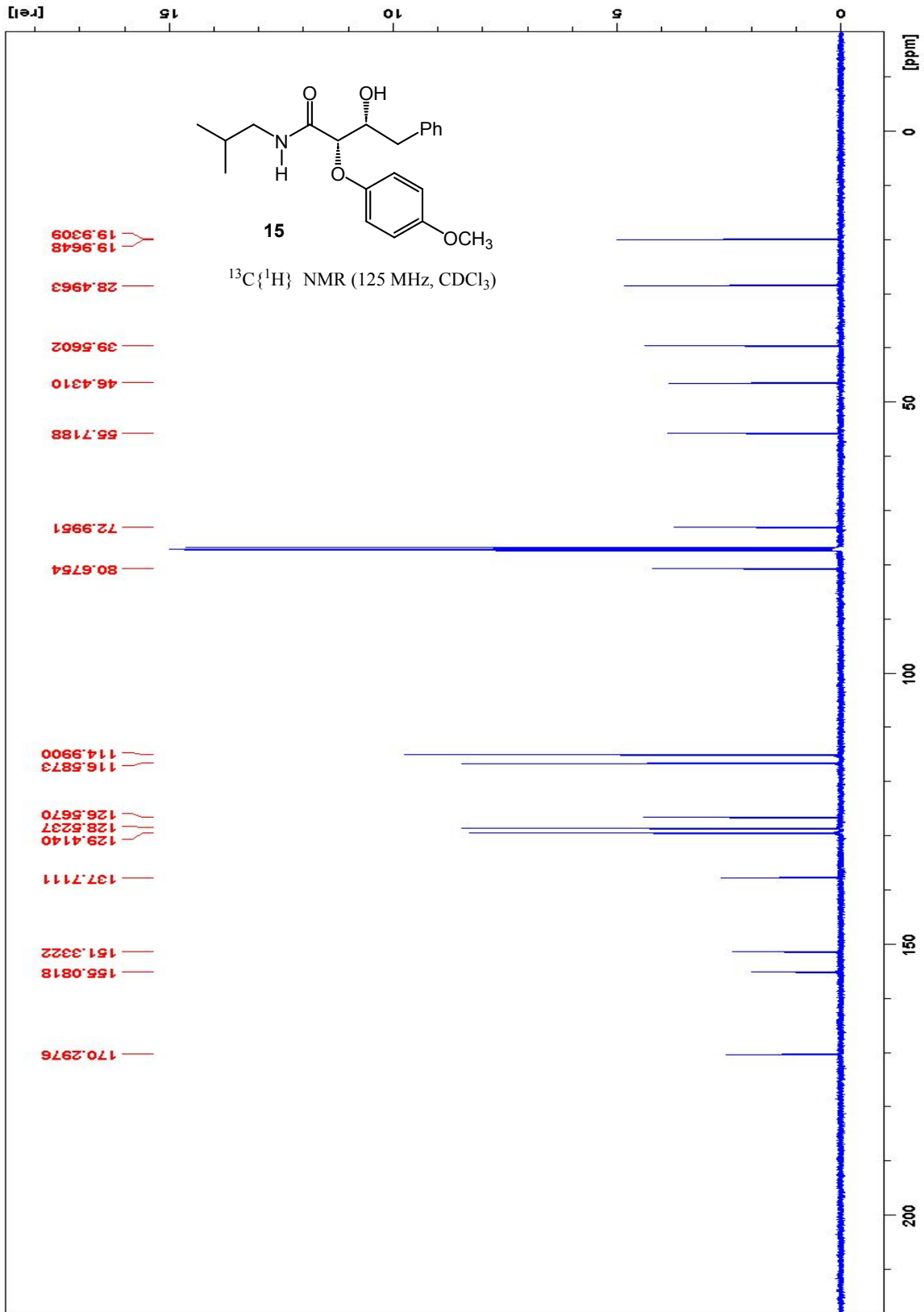


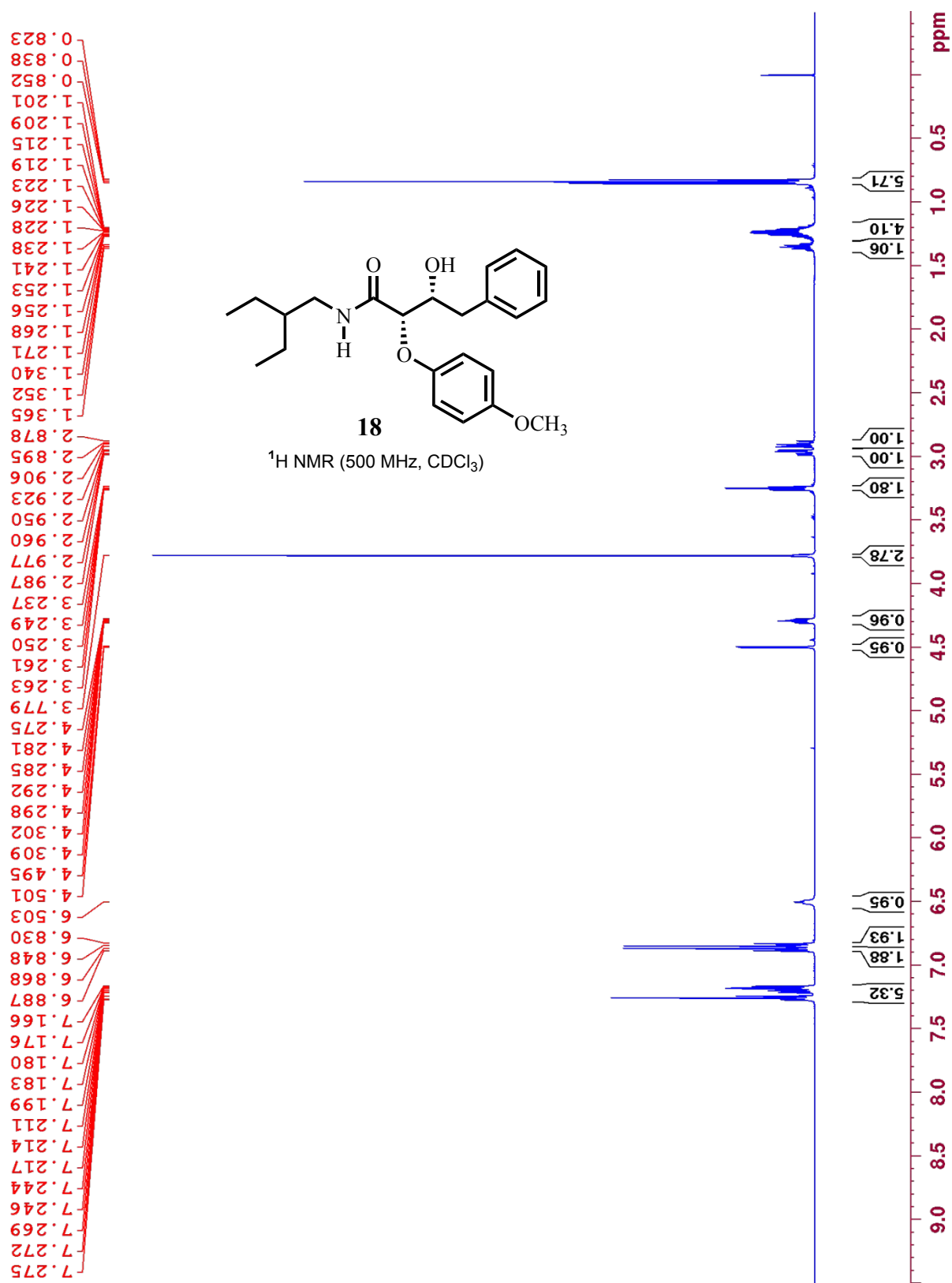


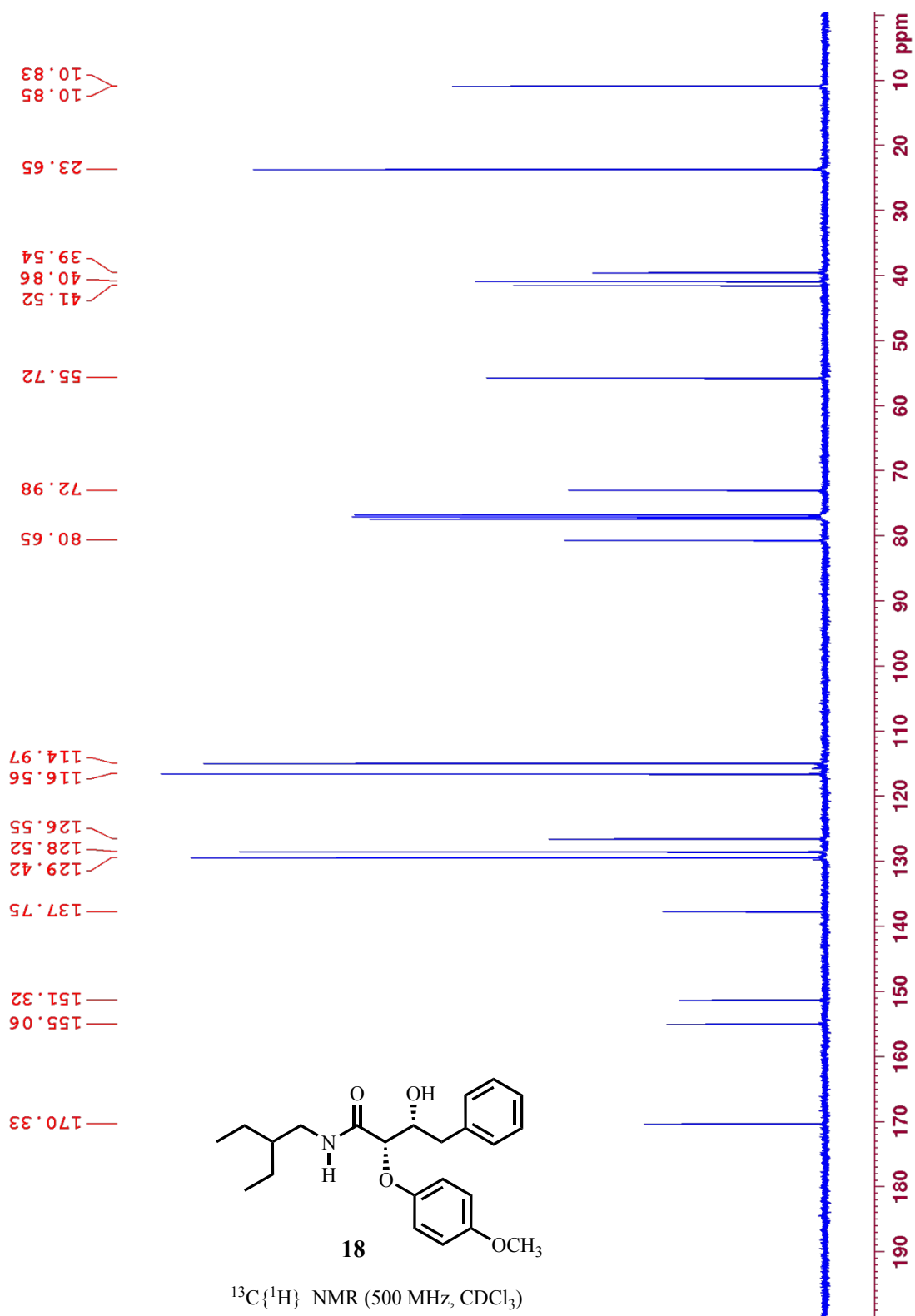


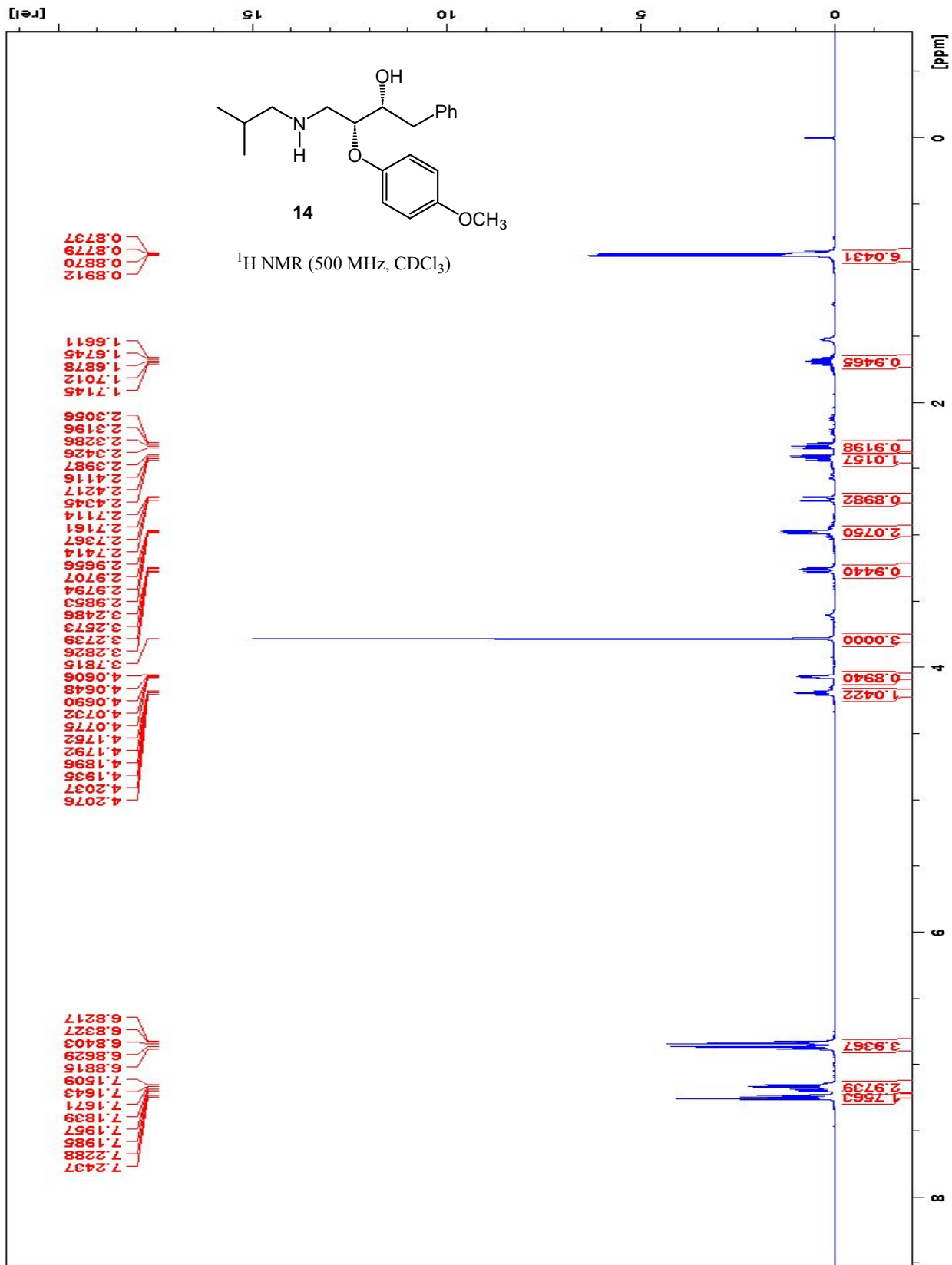




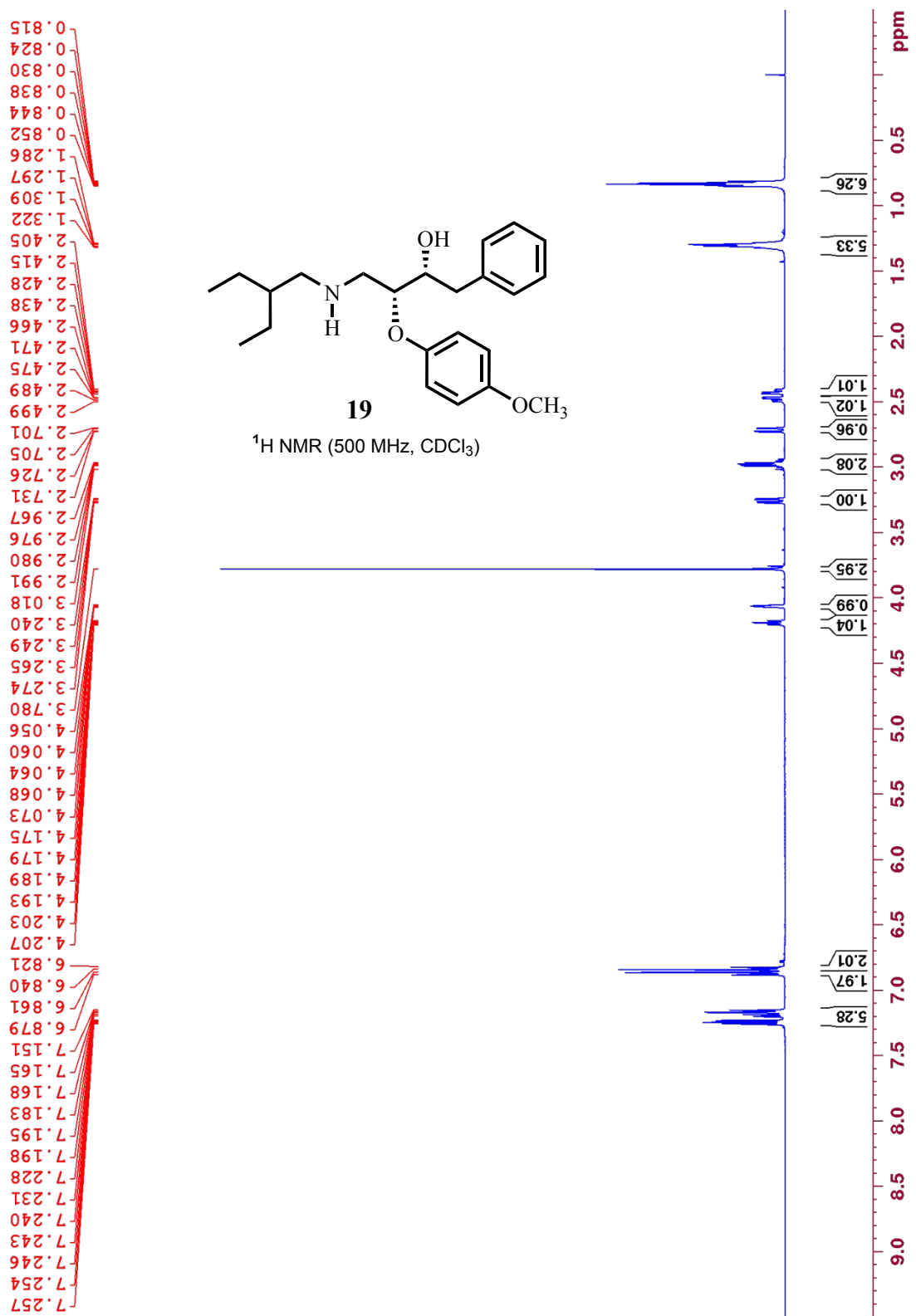


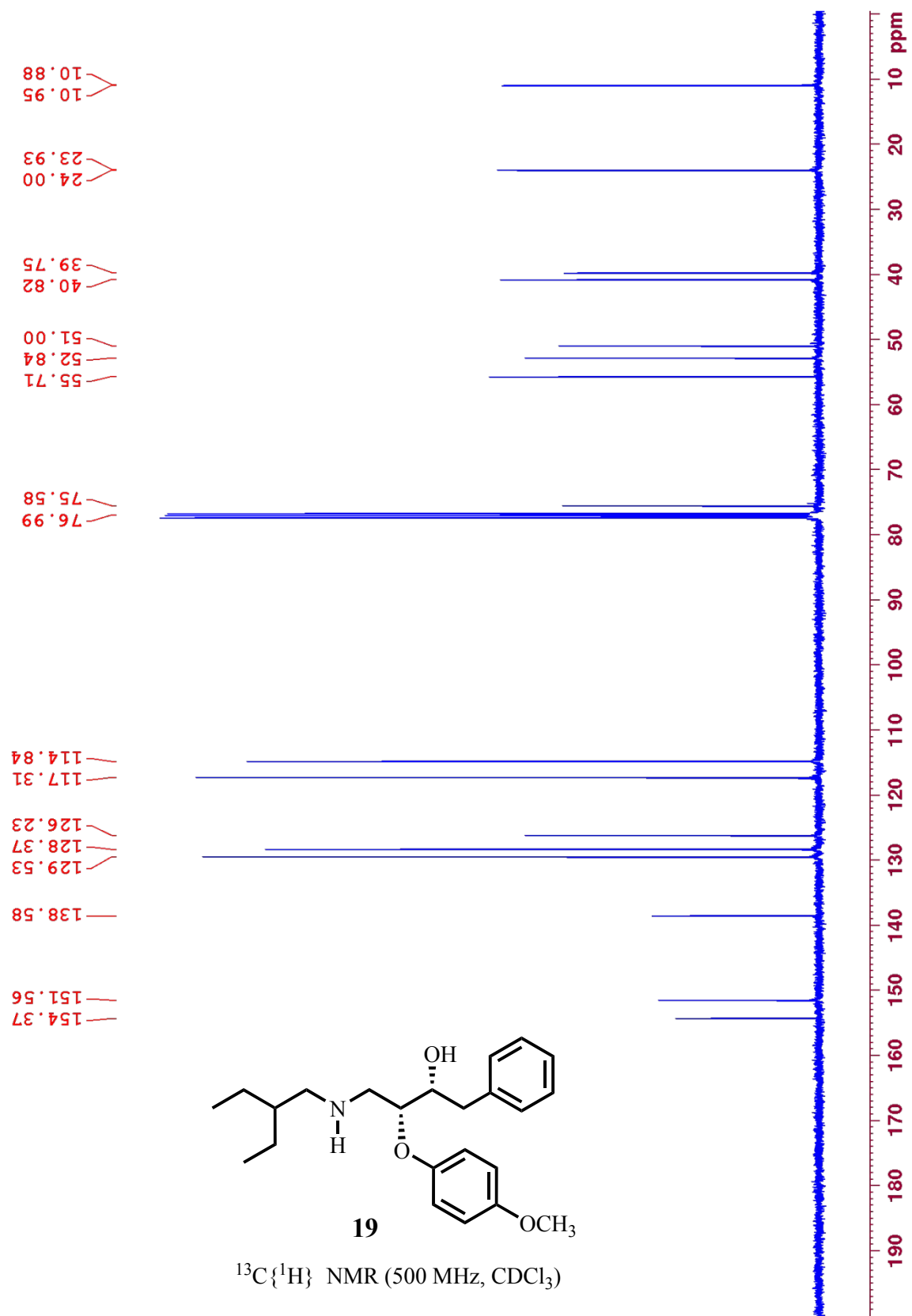


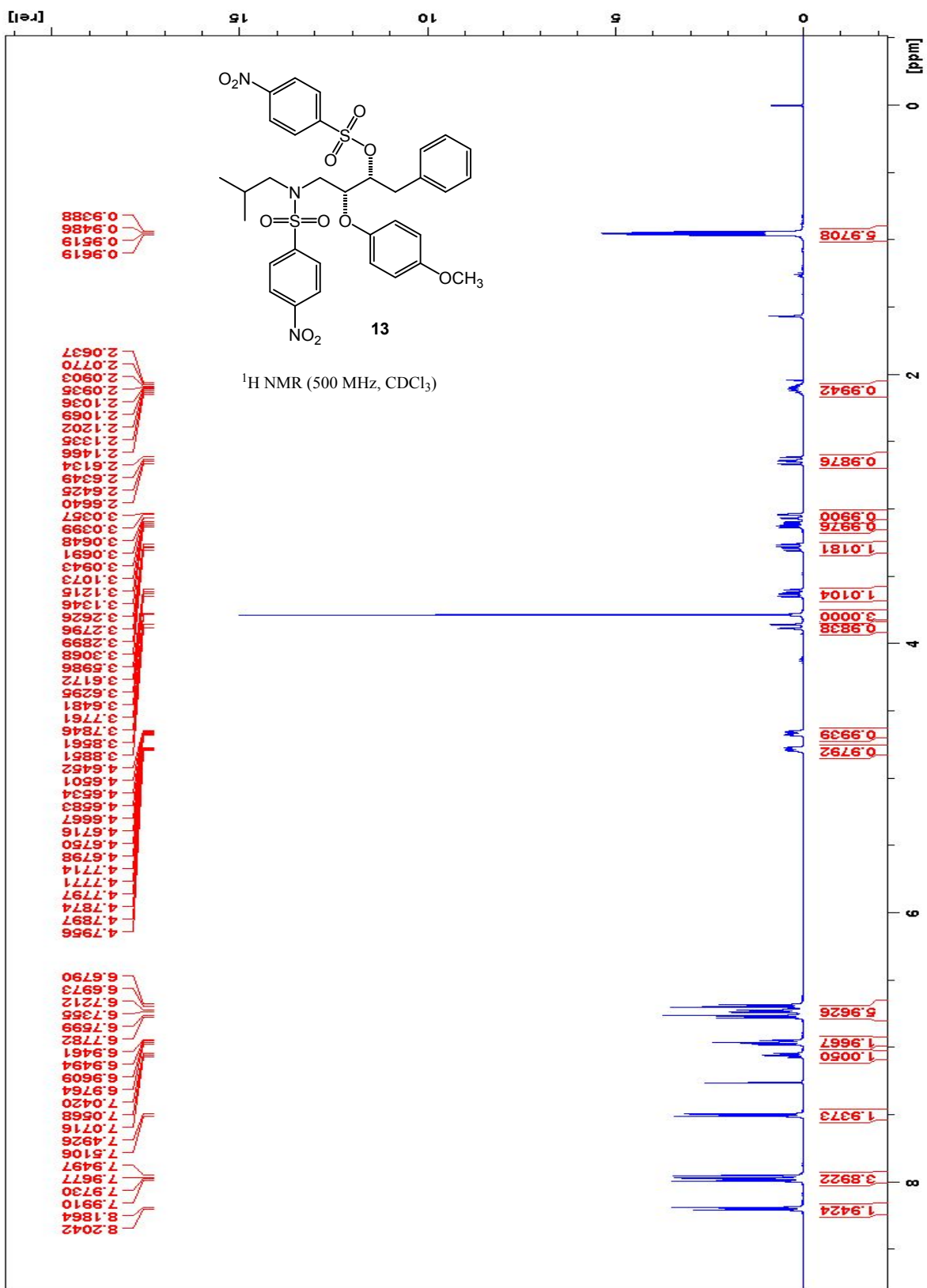


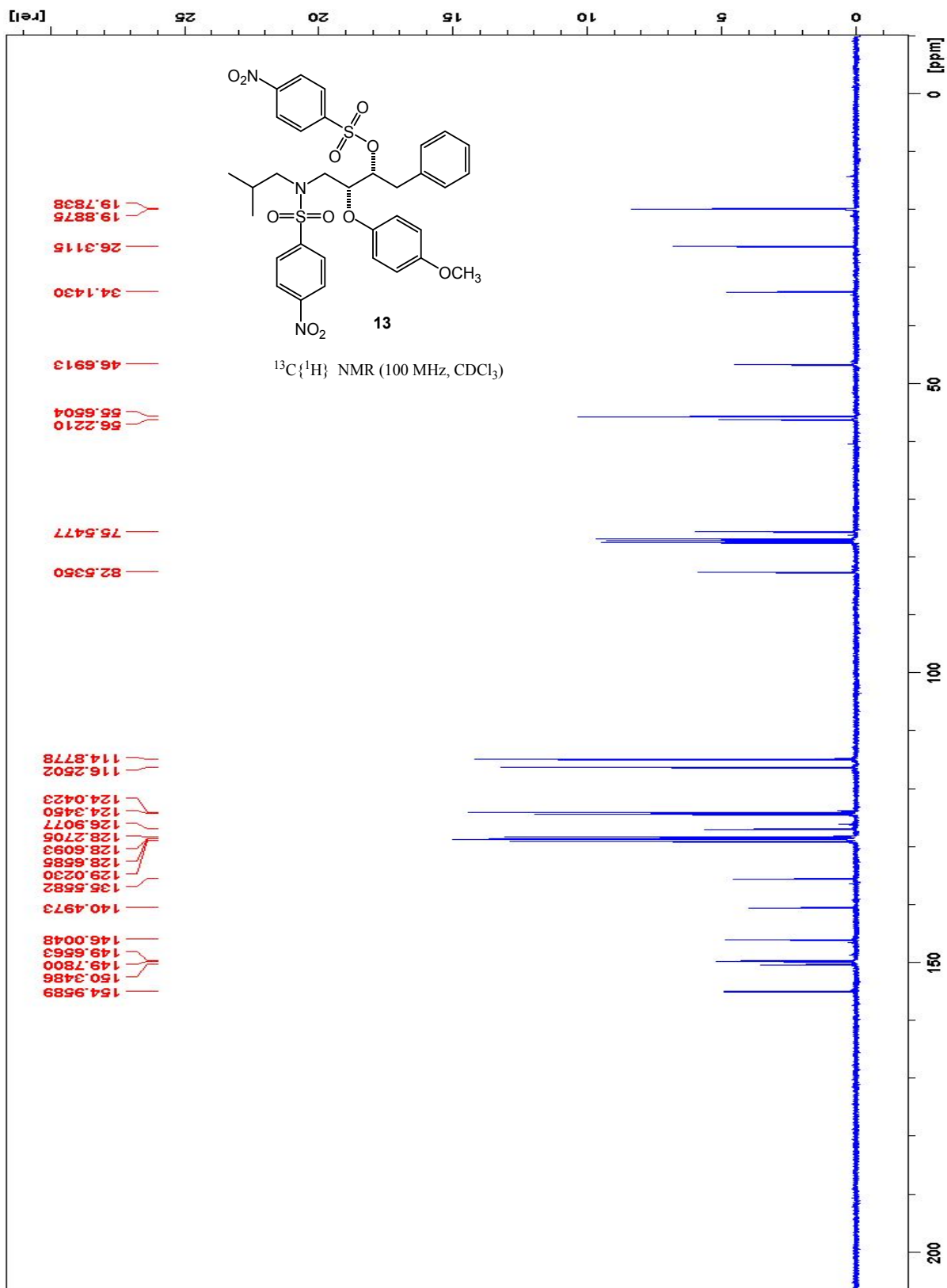


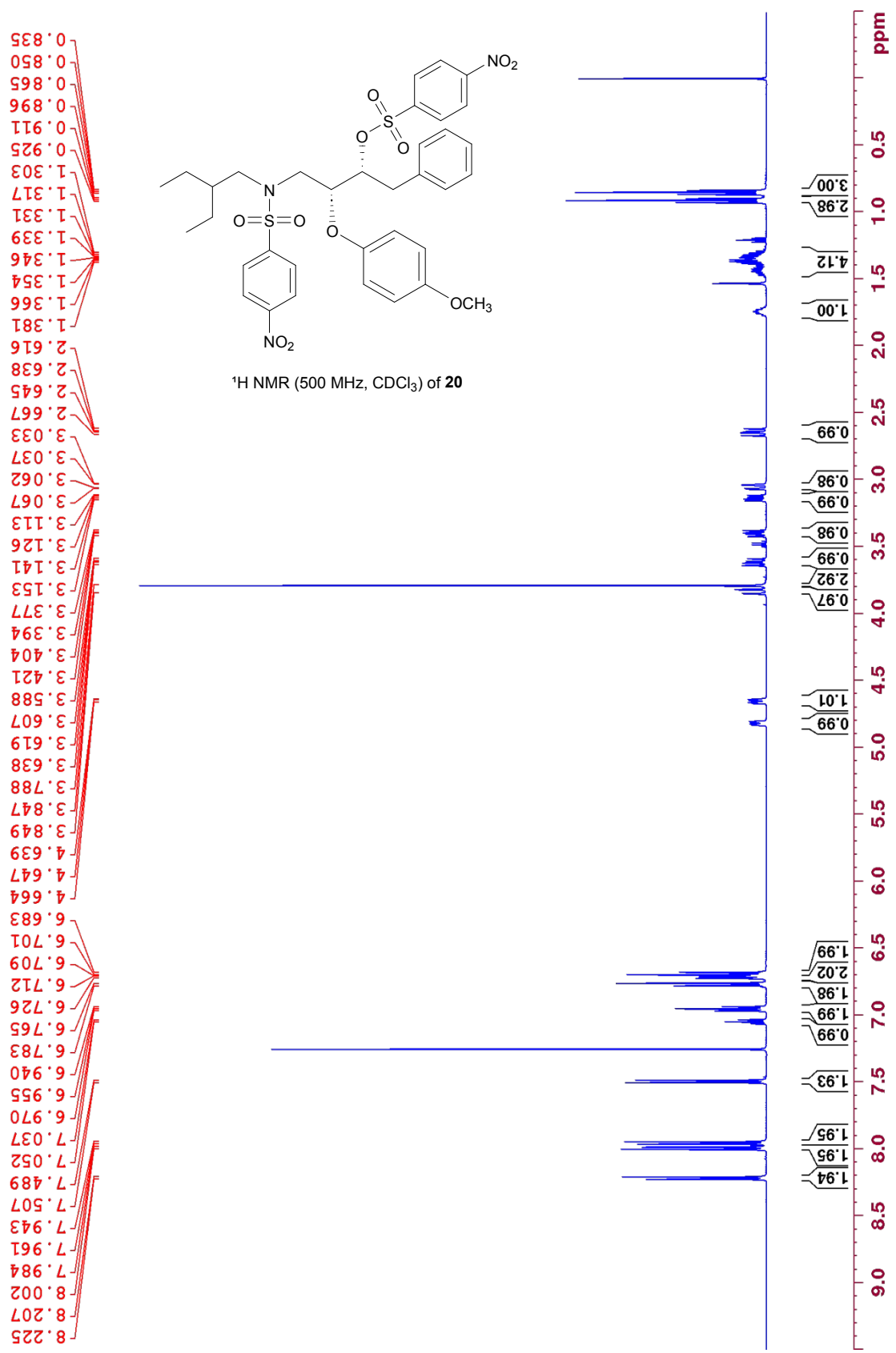


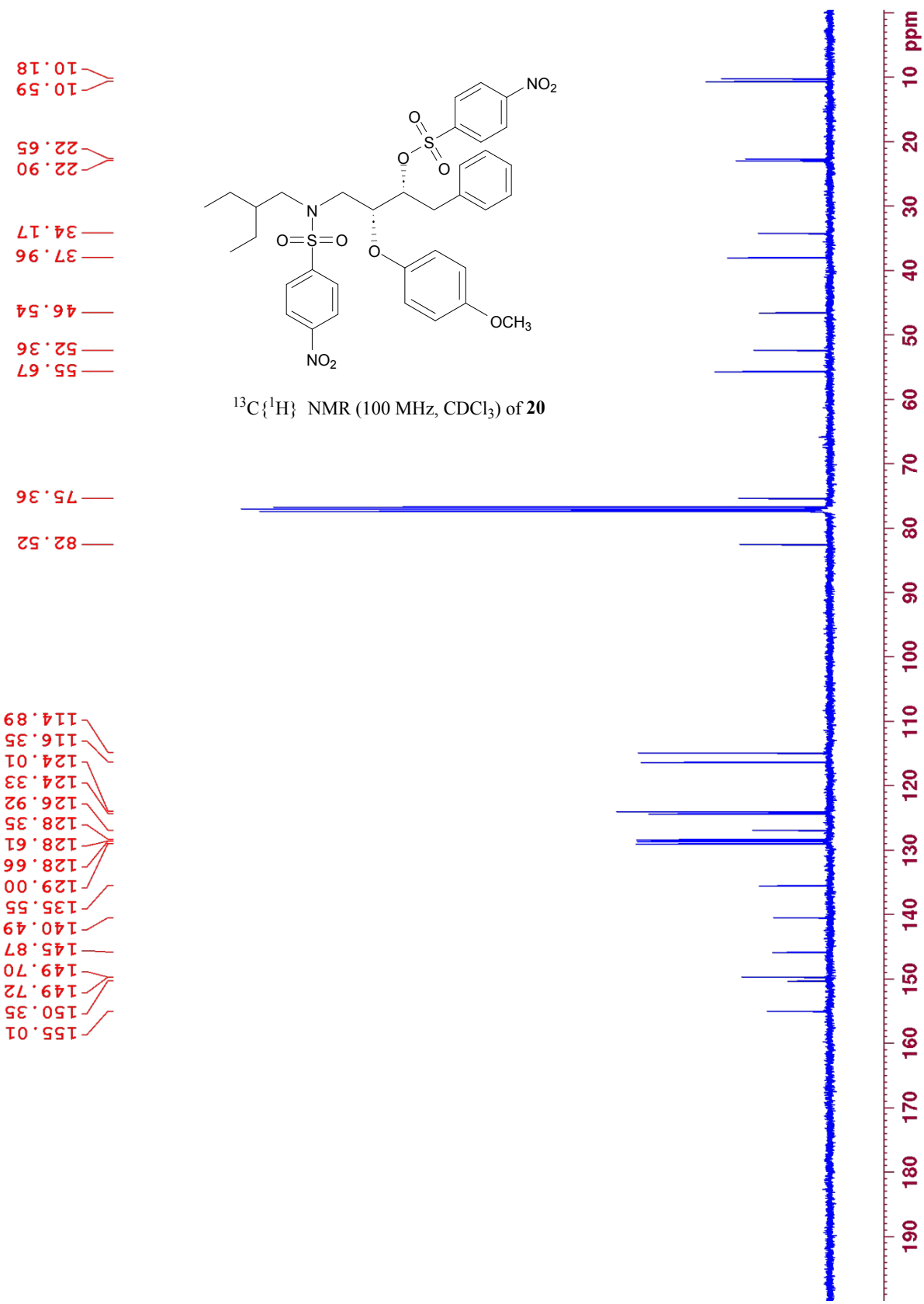


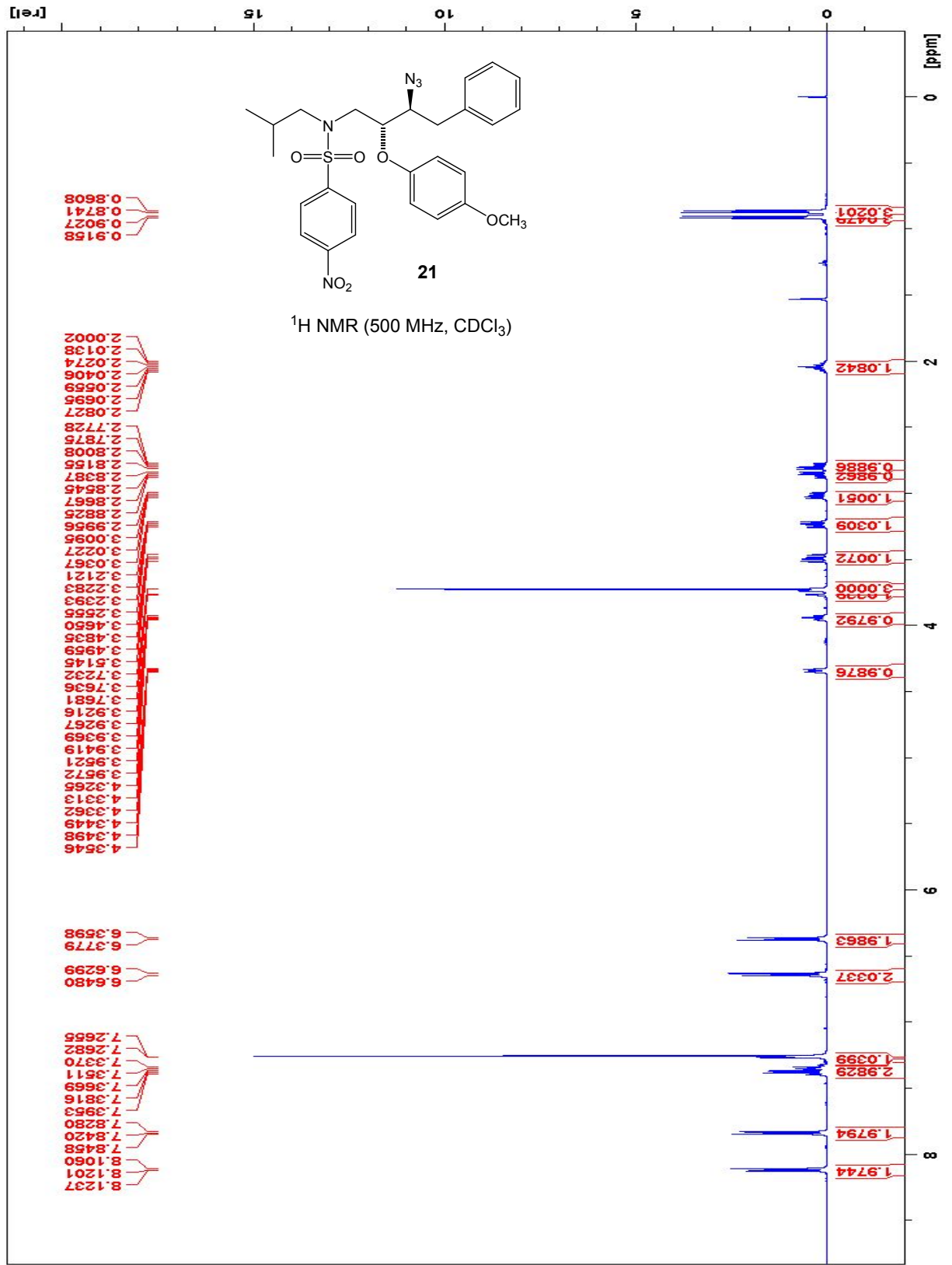


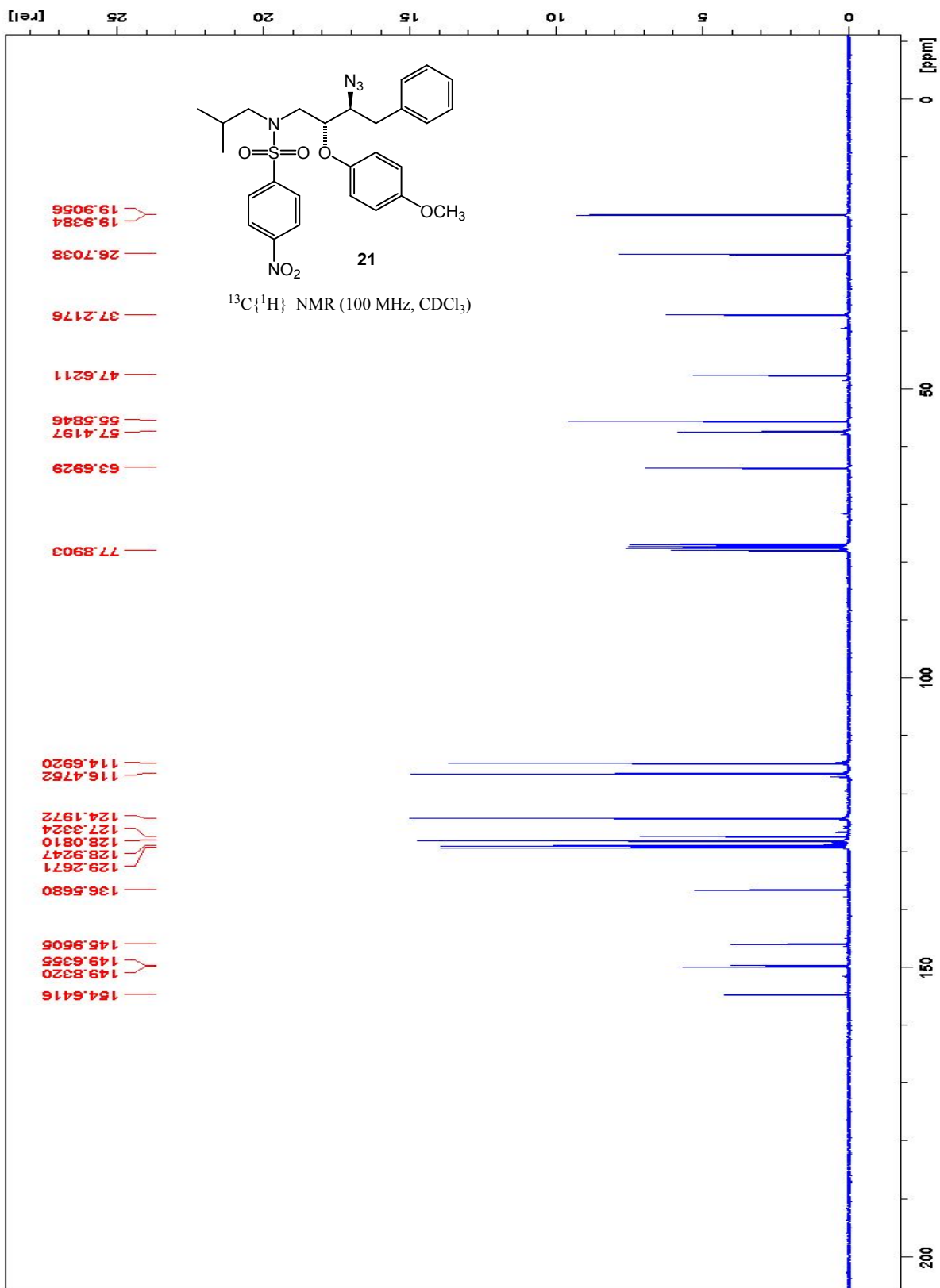


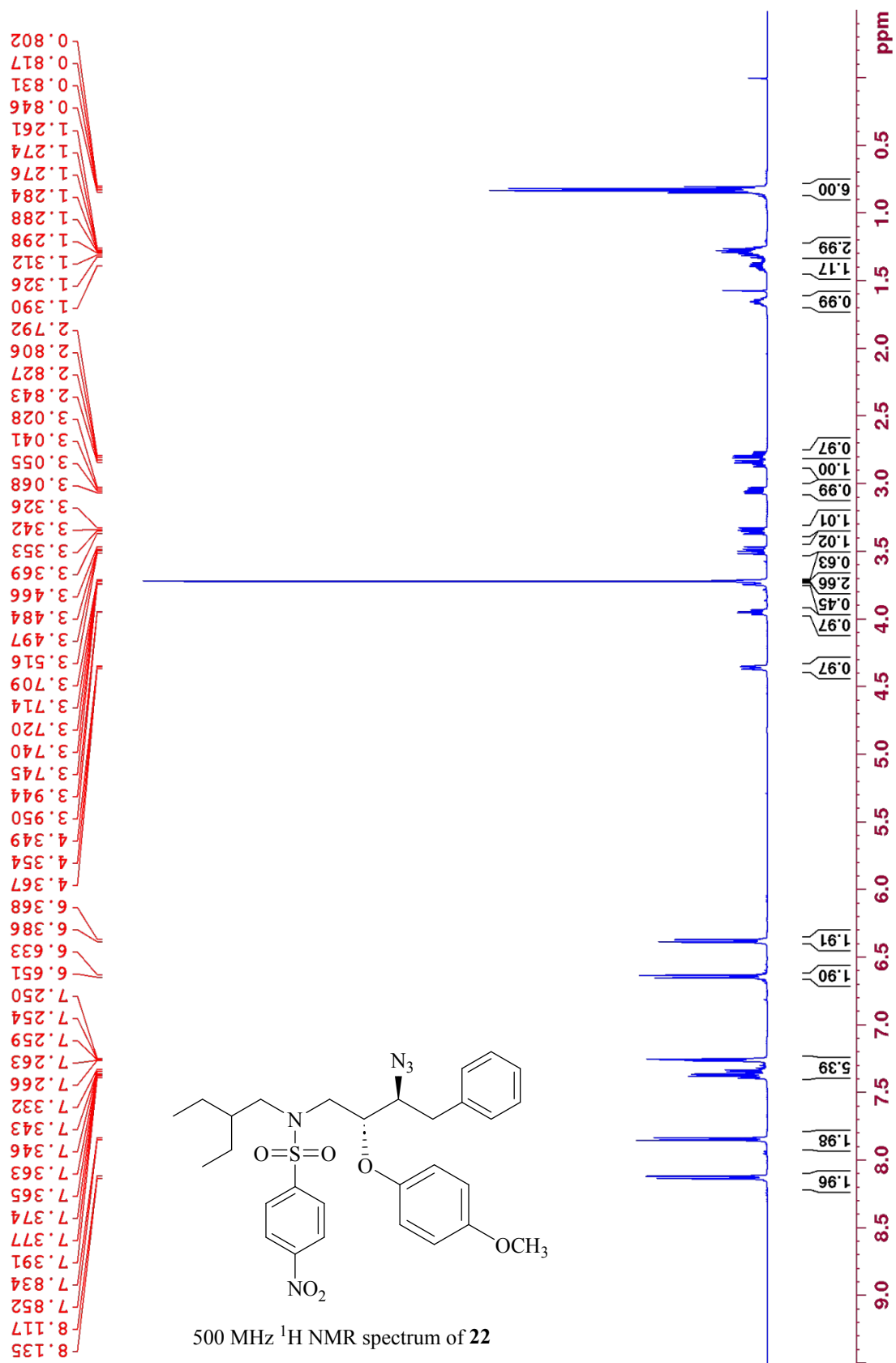


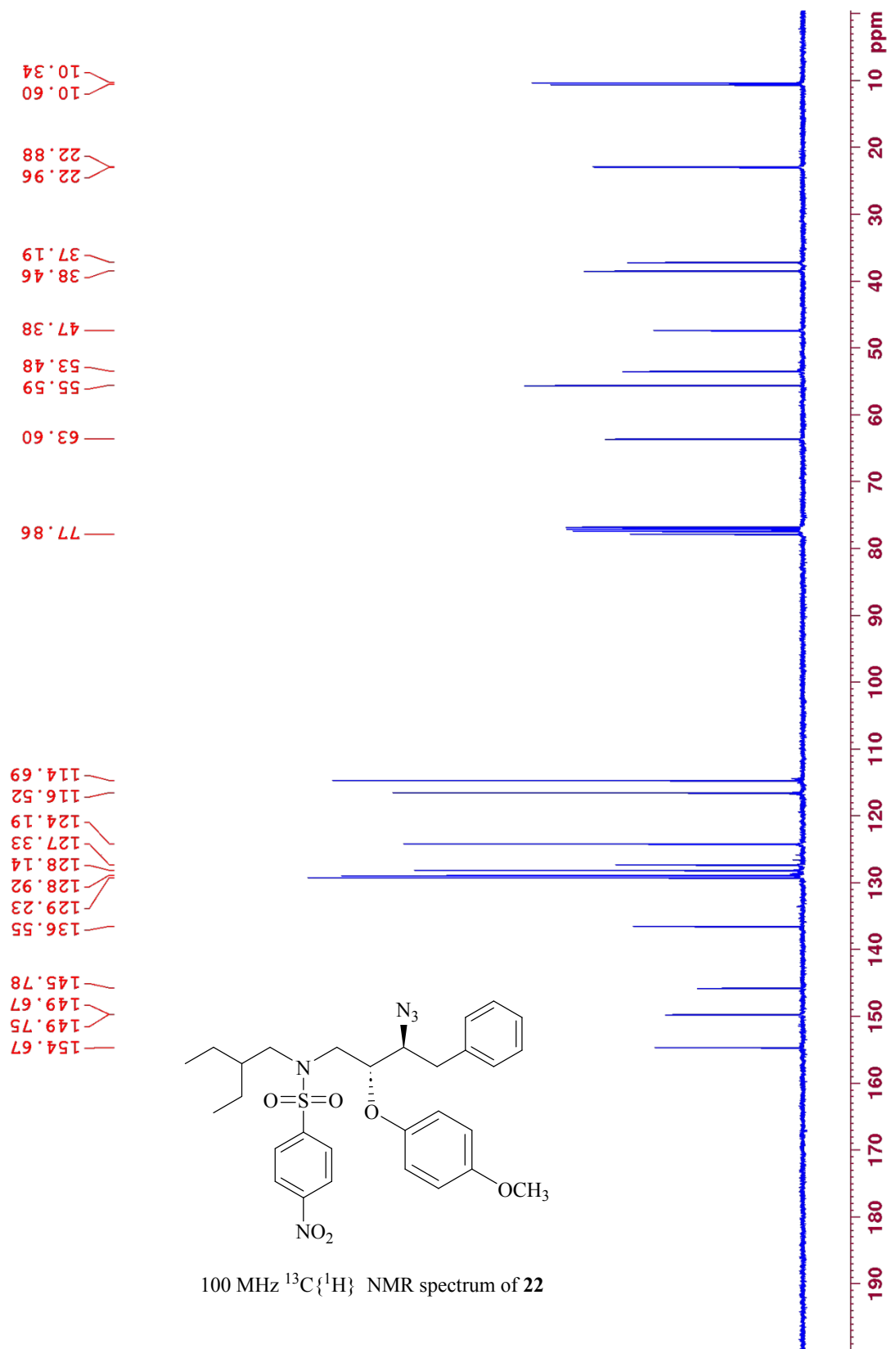


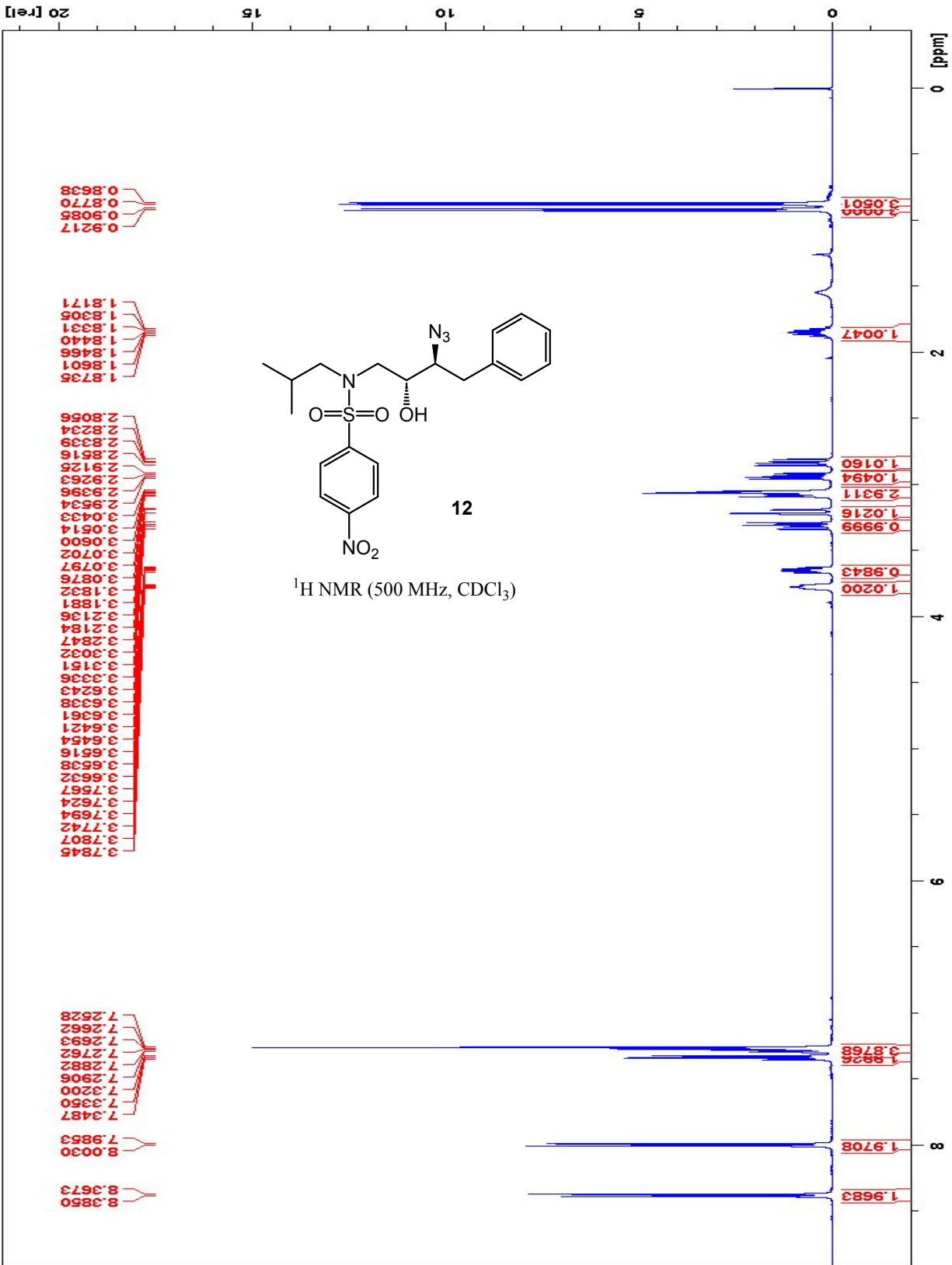


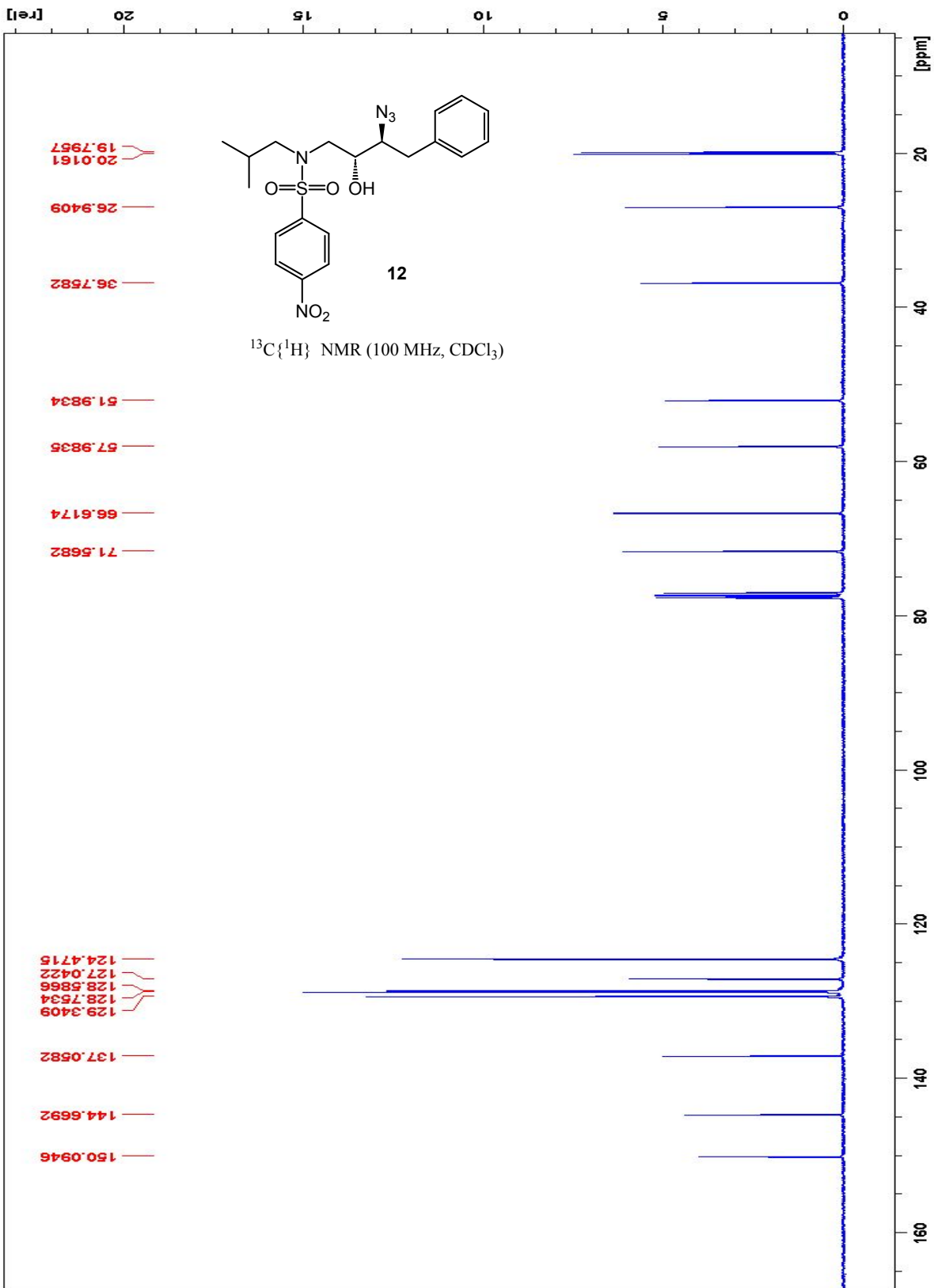


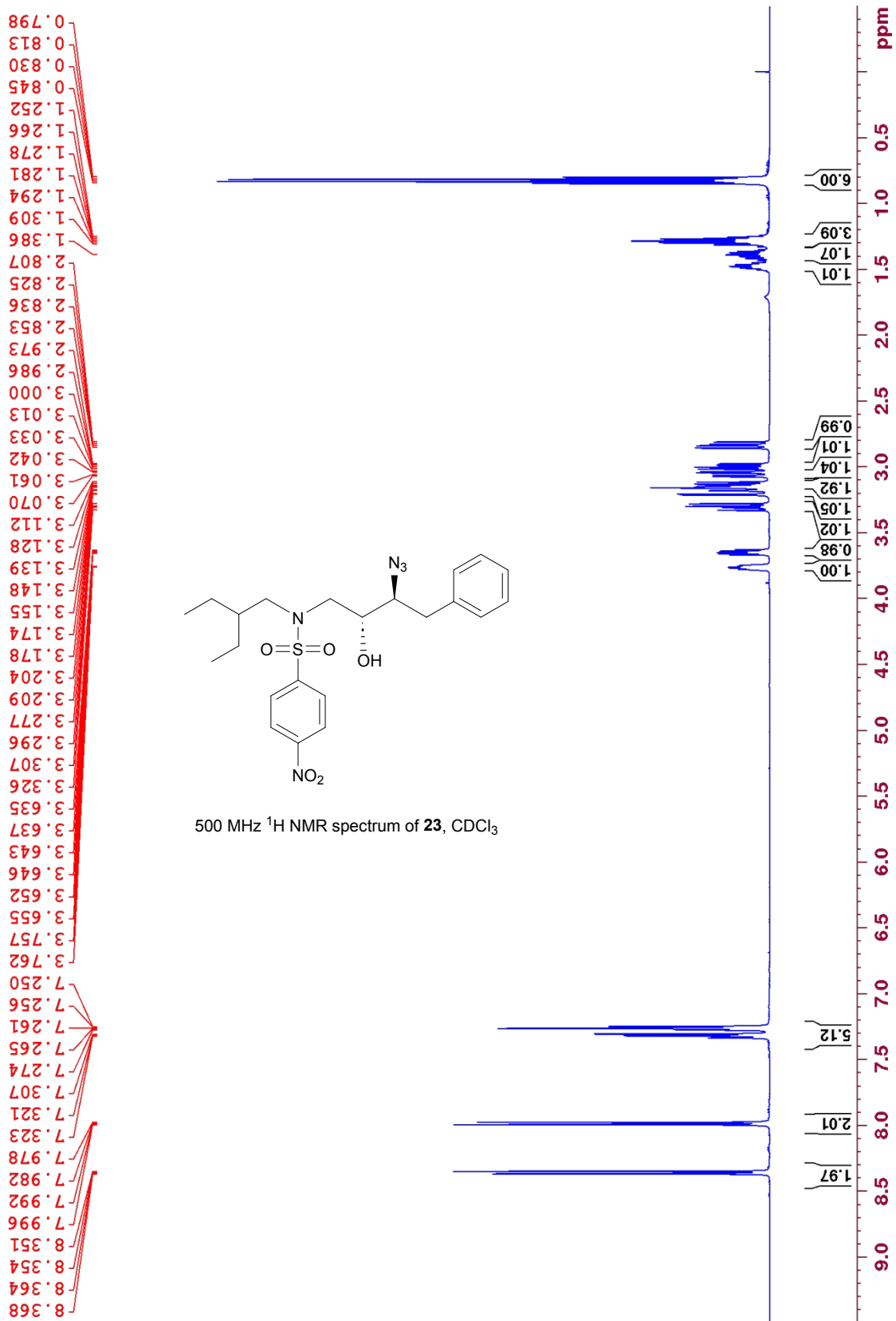


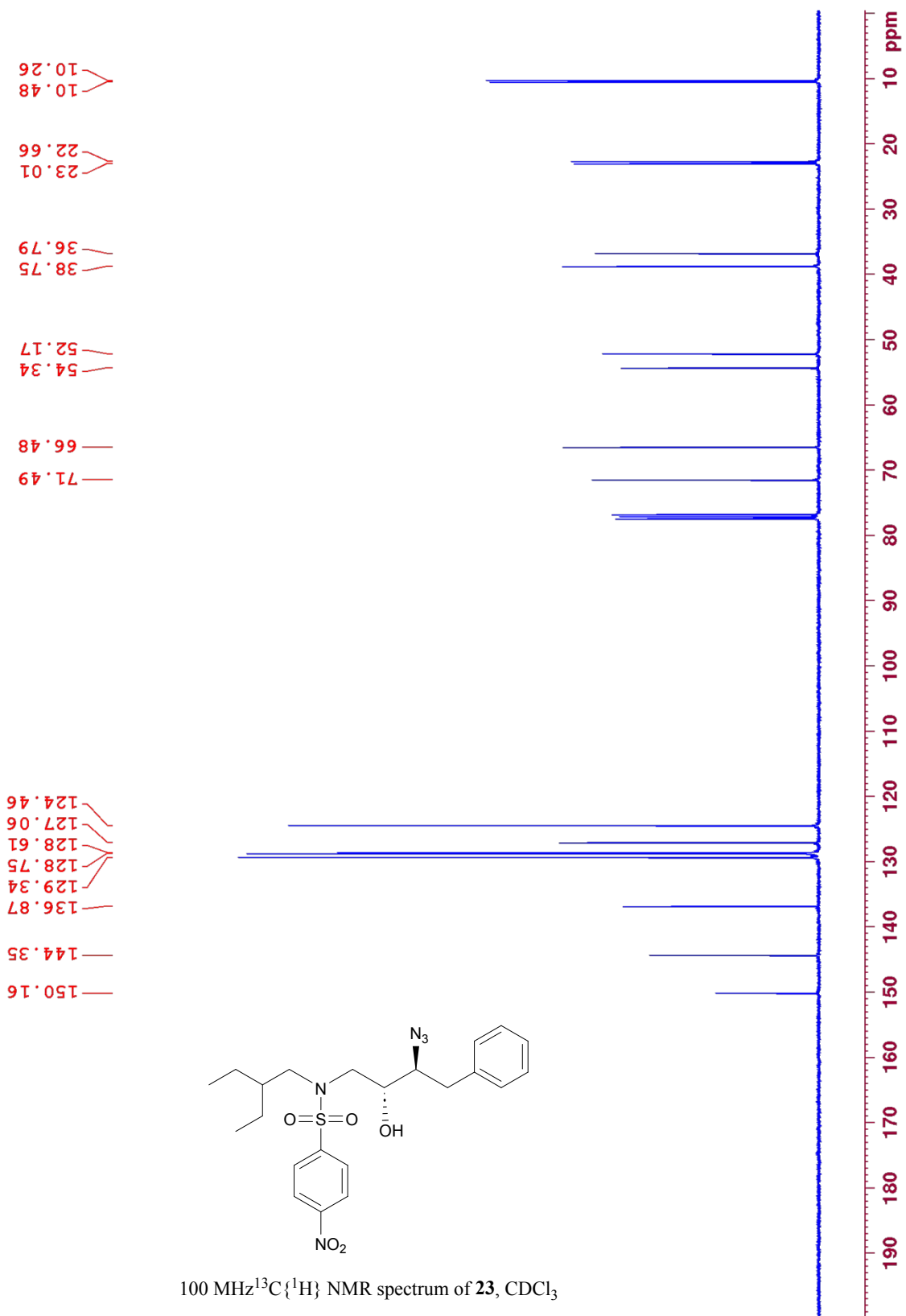


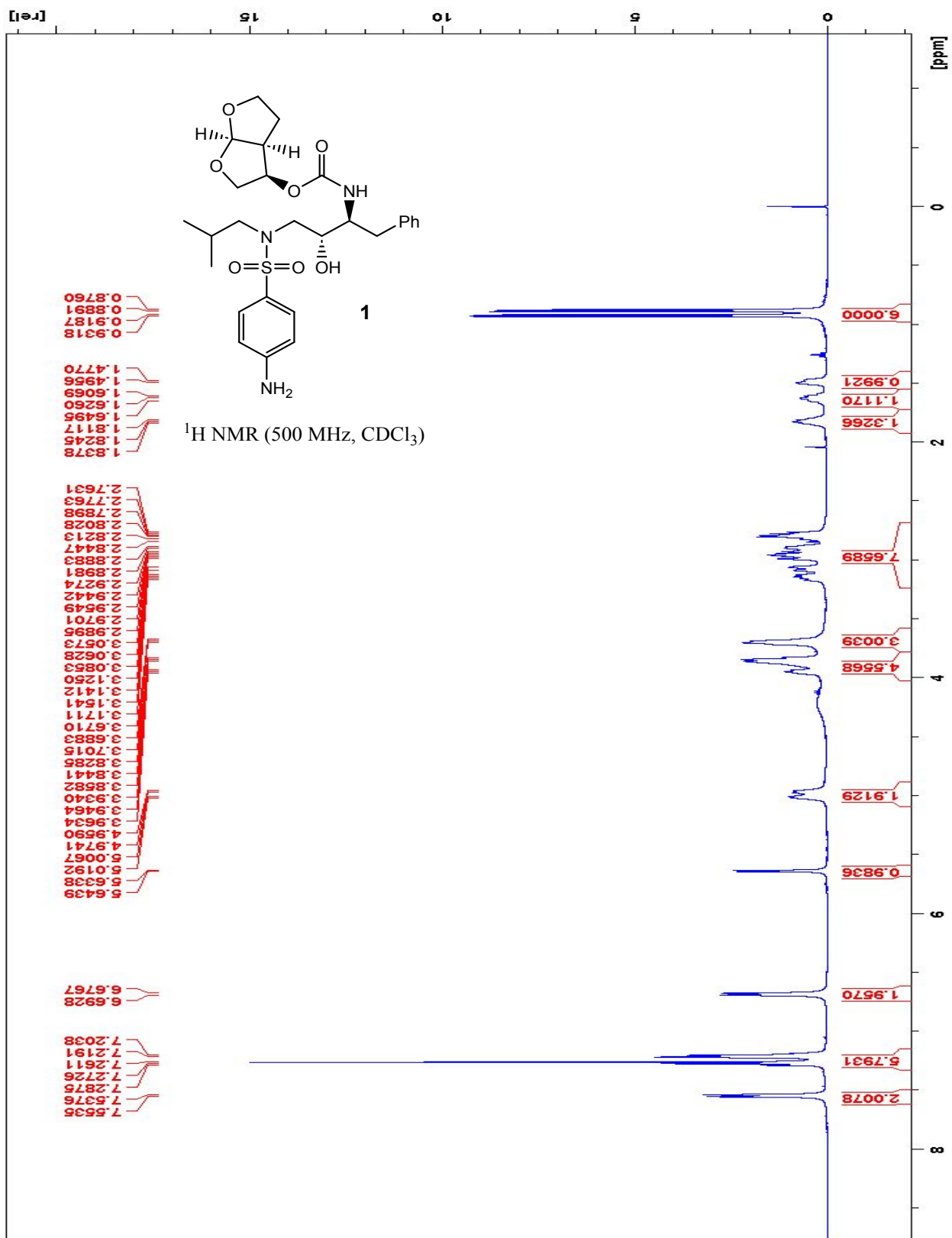


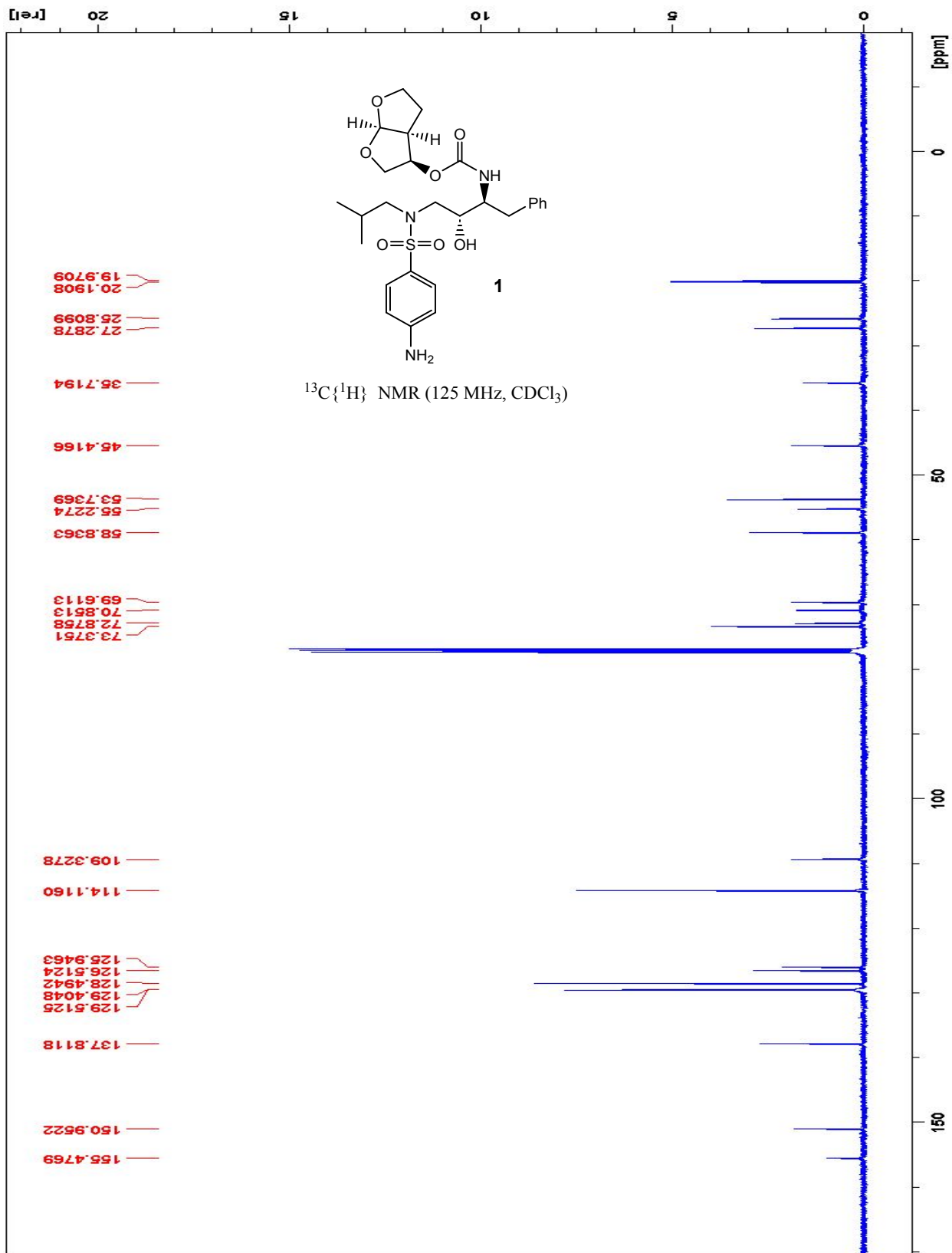


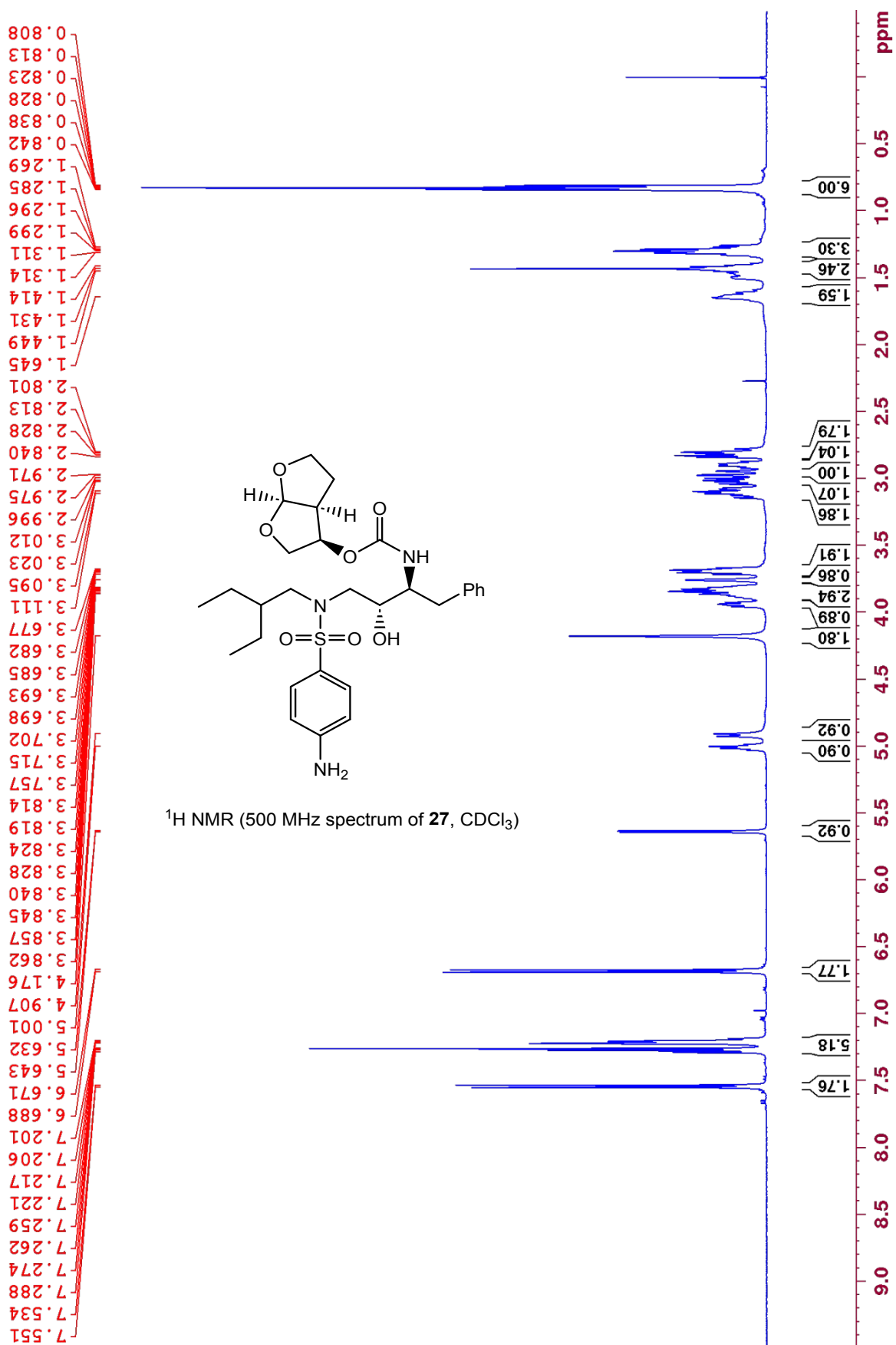




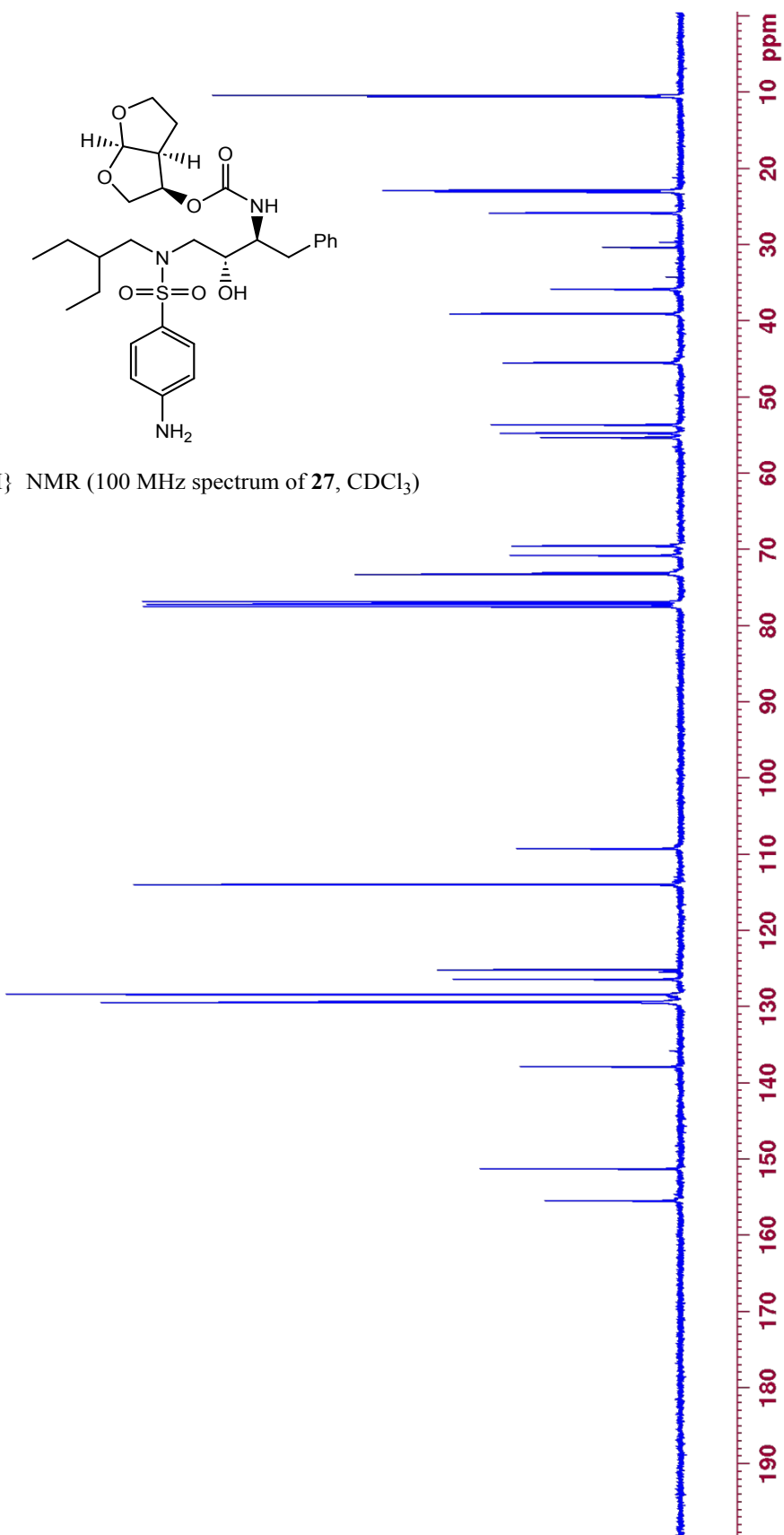






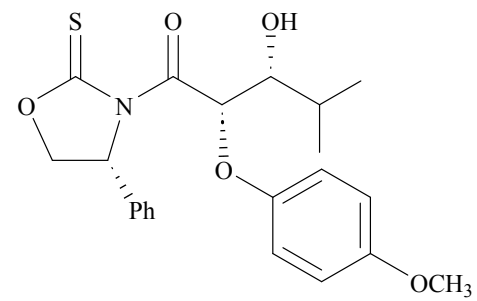


10.35
 10.54
 22.83
 23.03
 25.80
 35.80
 39.02
 45.46
 53.59
 54.70
 55.26
 69.60
 70.84
 73.11
 73.31
 109.32
 114.02
 125.22
 126.46
 128.45
 129.40
 129.50
 137.92
 151.32
 155.52

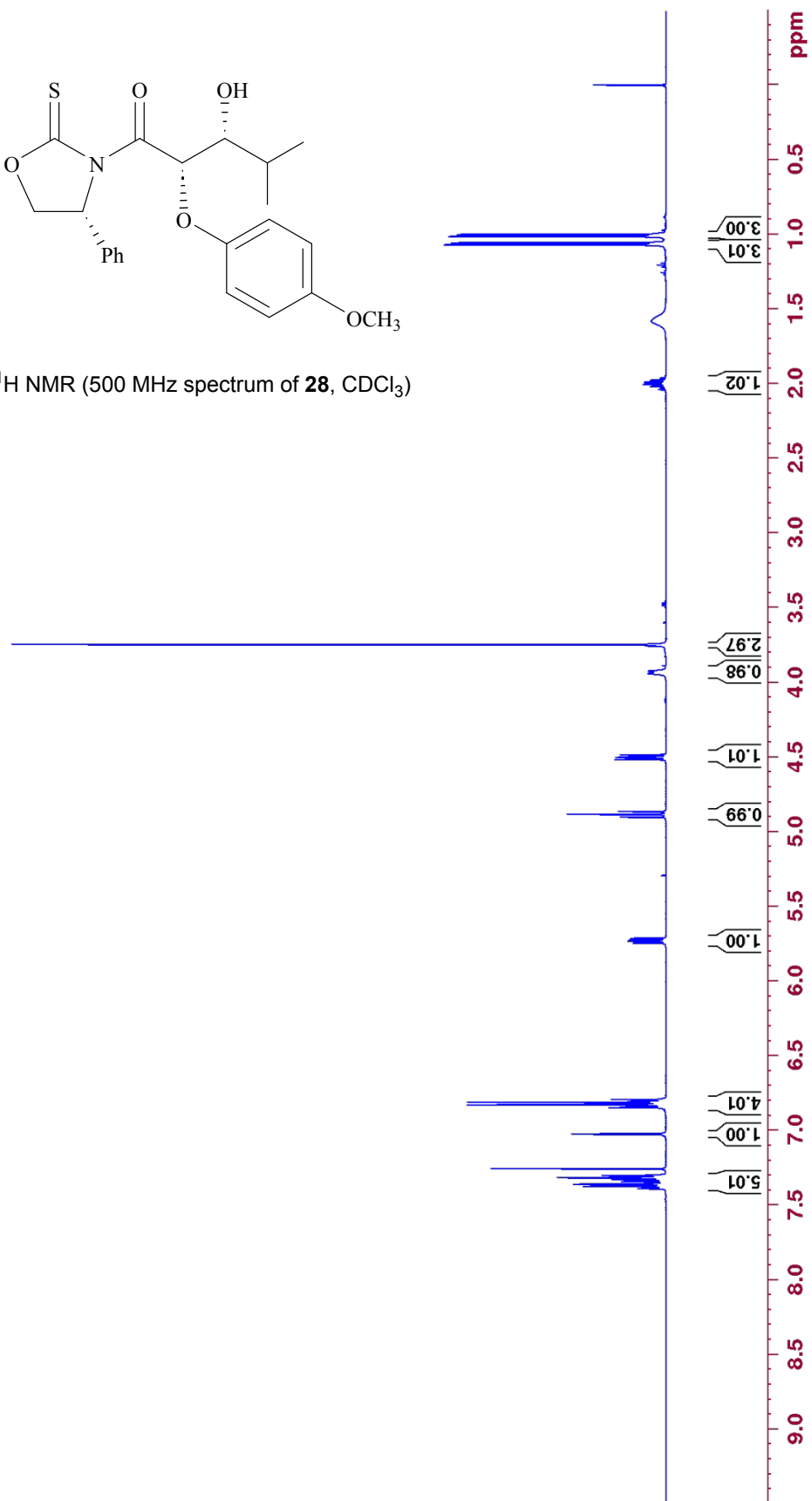


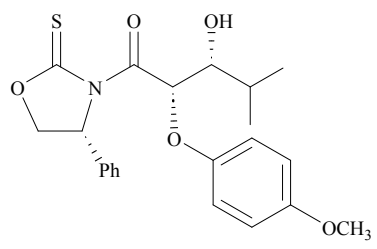
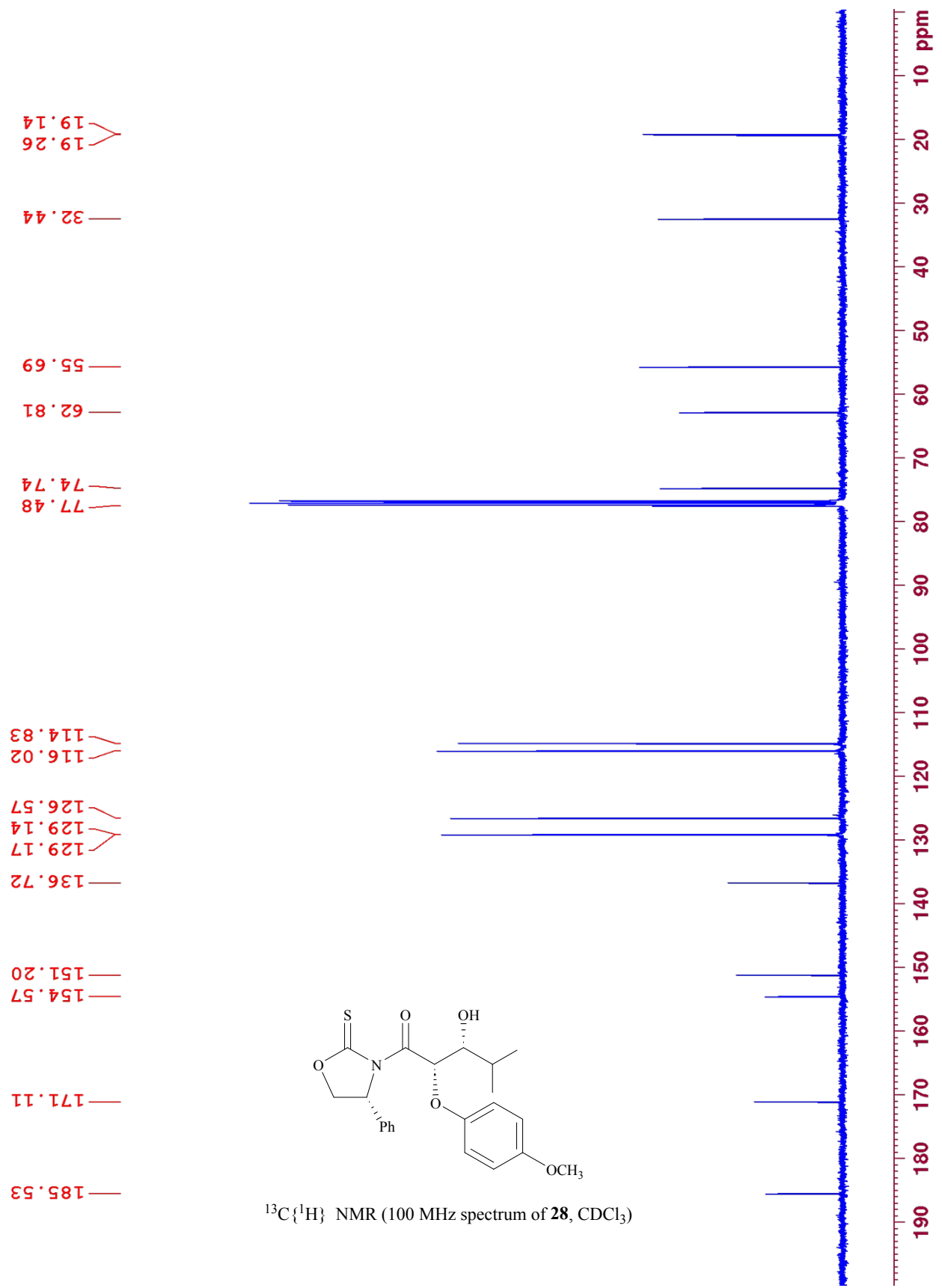
2.039
2.033
2.020
2.006
2.003
1.992
1.989
1.976
1.963
1.069
1.055
1.013
1.000

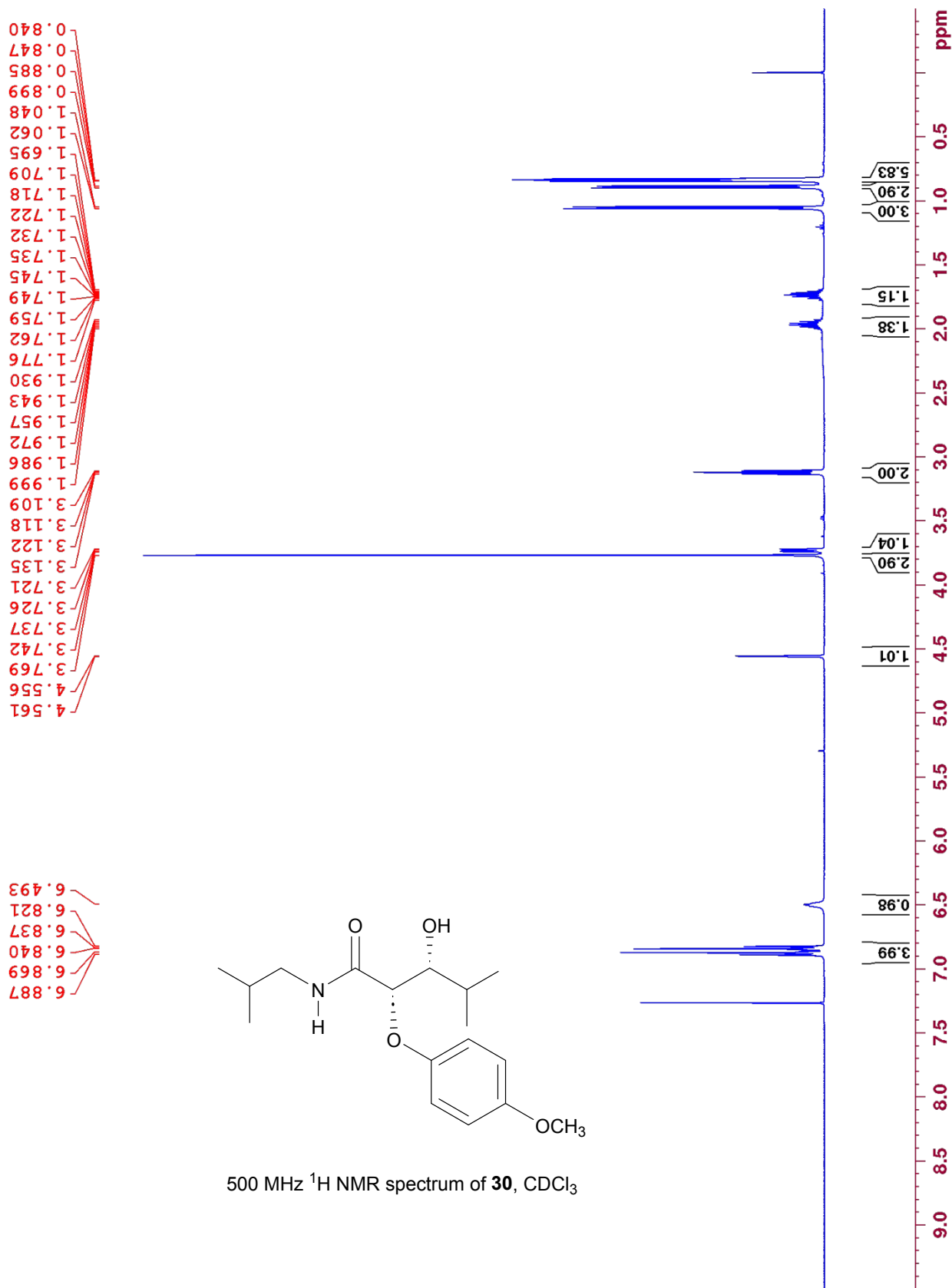
7.385
7.378
7.375
7.371
7.362
7.360
7.346
7.343
7.340
7.334
7.329
7.319
7.316
7.311
7.306
7.303
7.300
7.025
7.022
6.847
6.834
6.828
6.817
6.811
6.805
6.792
5.745
5.732
5.726
5.713
4.902
4.884
4.865
4.516
4.503
4.497
4.484
3.940
3.925
3.746

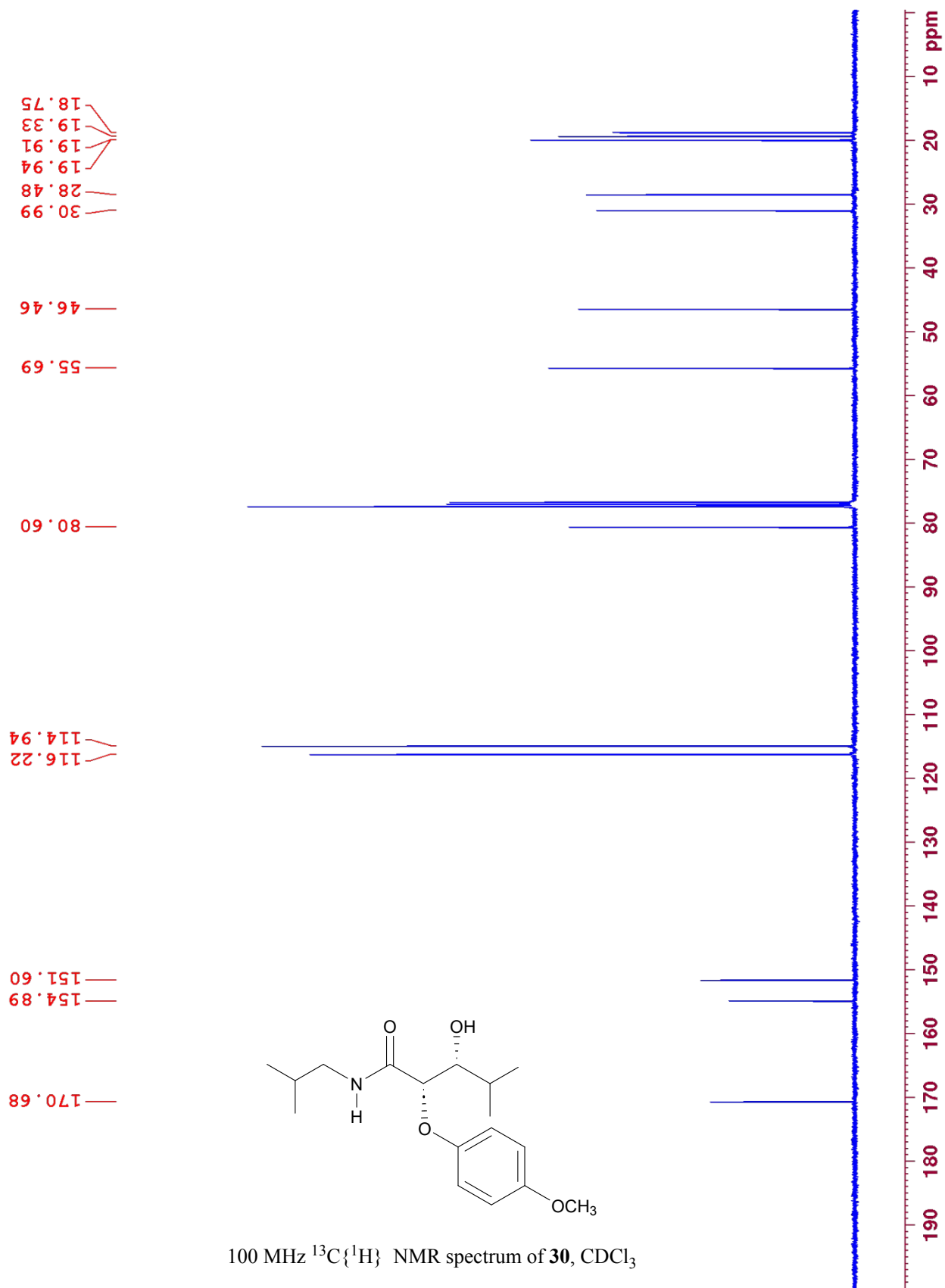


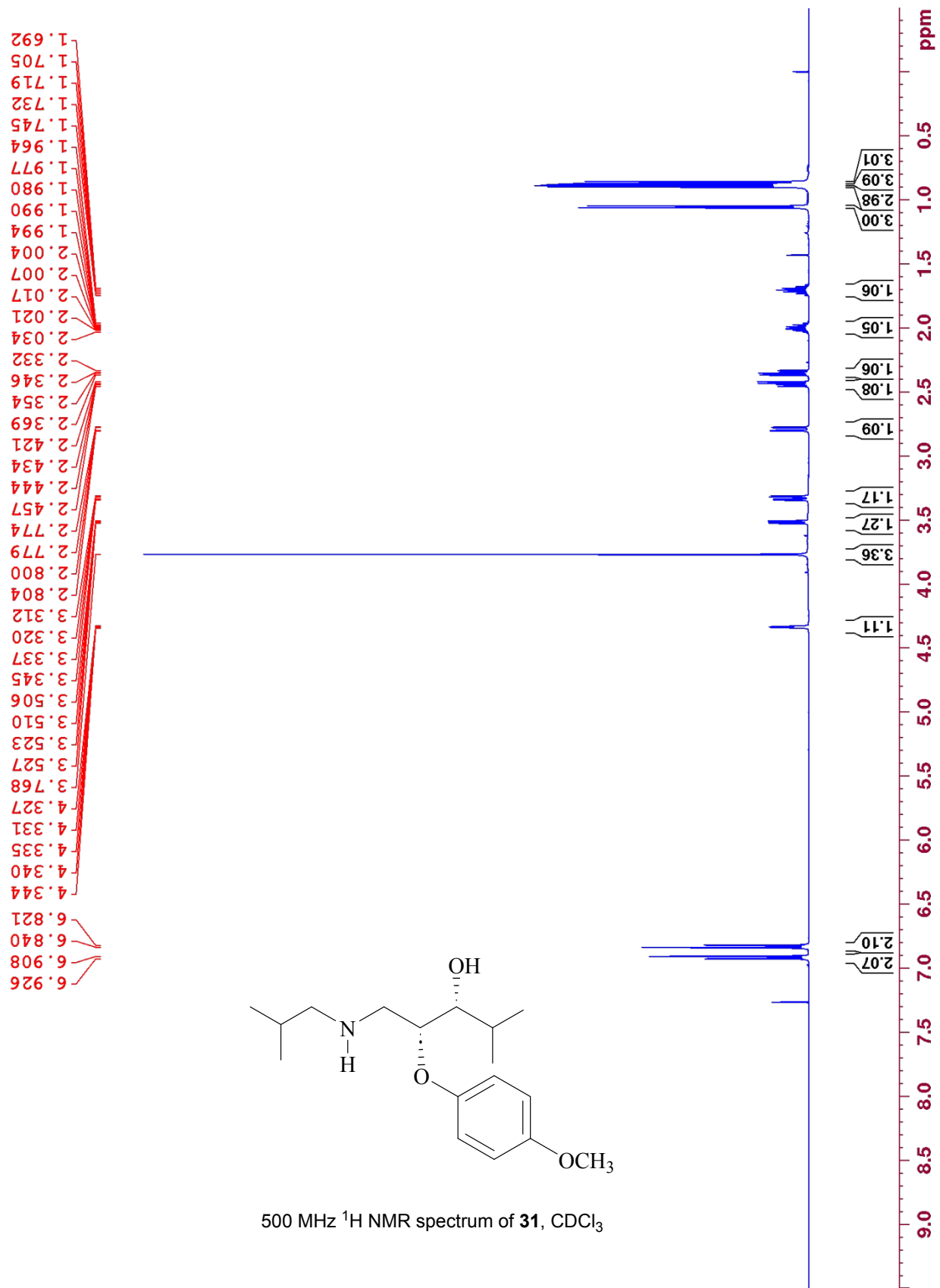
^1H NMR (500 MHz spectrum of **28**, CDCl_3)

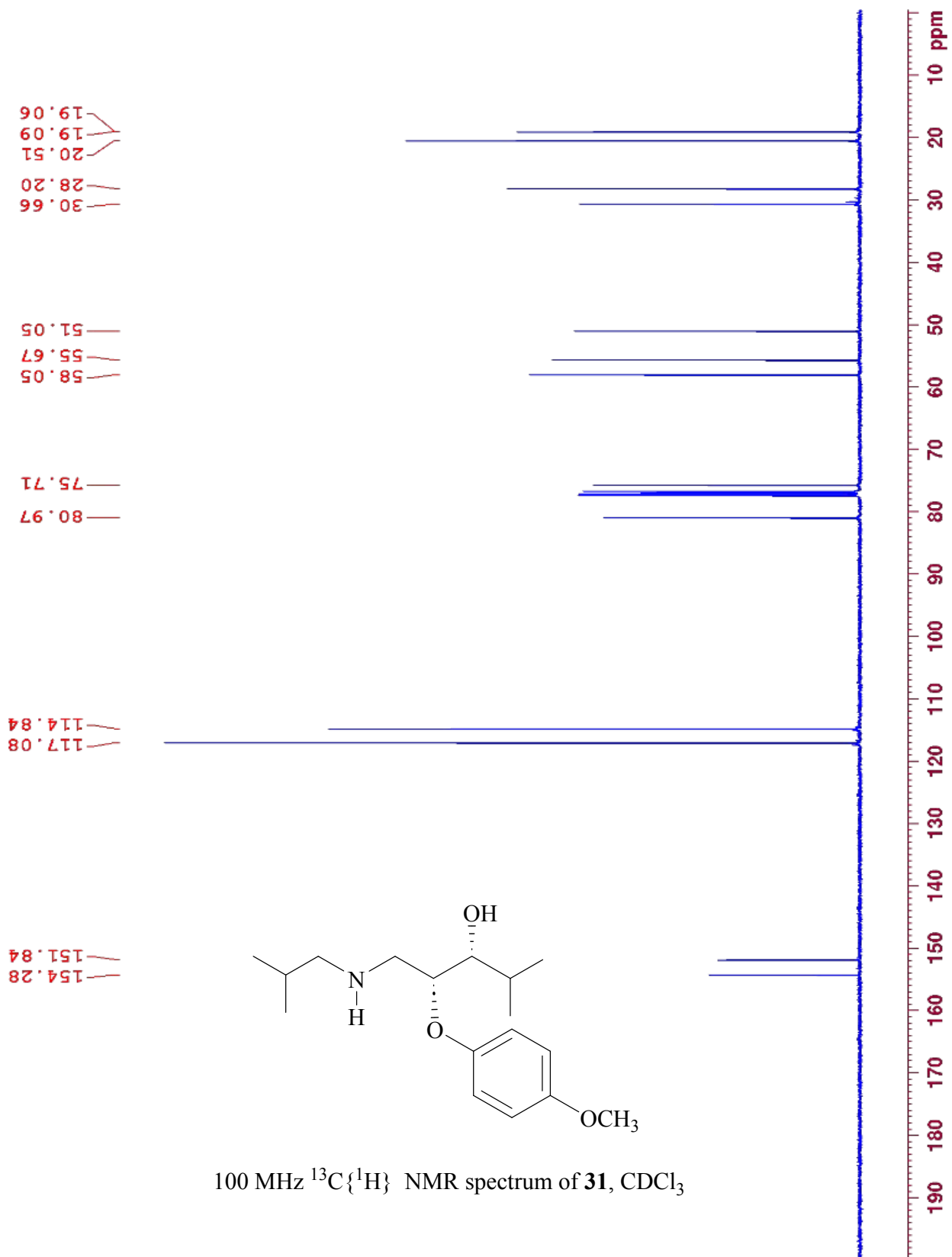


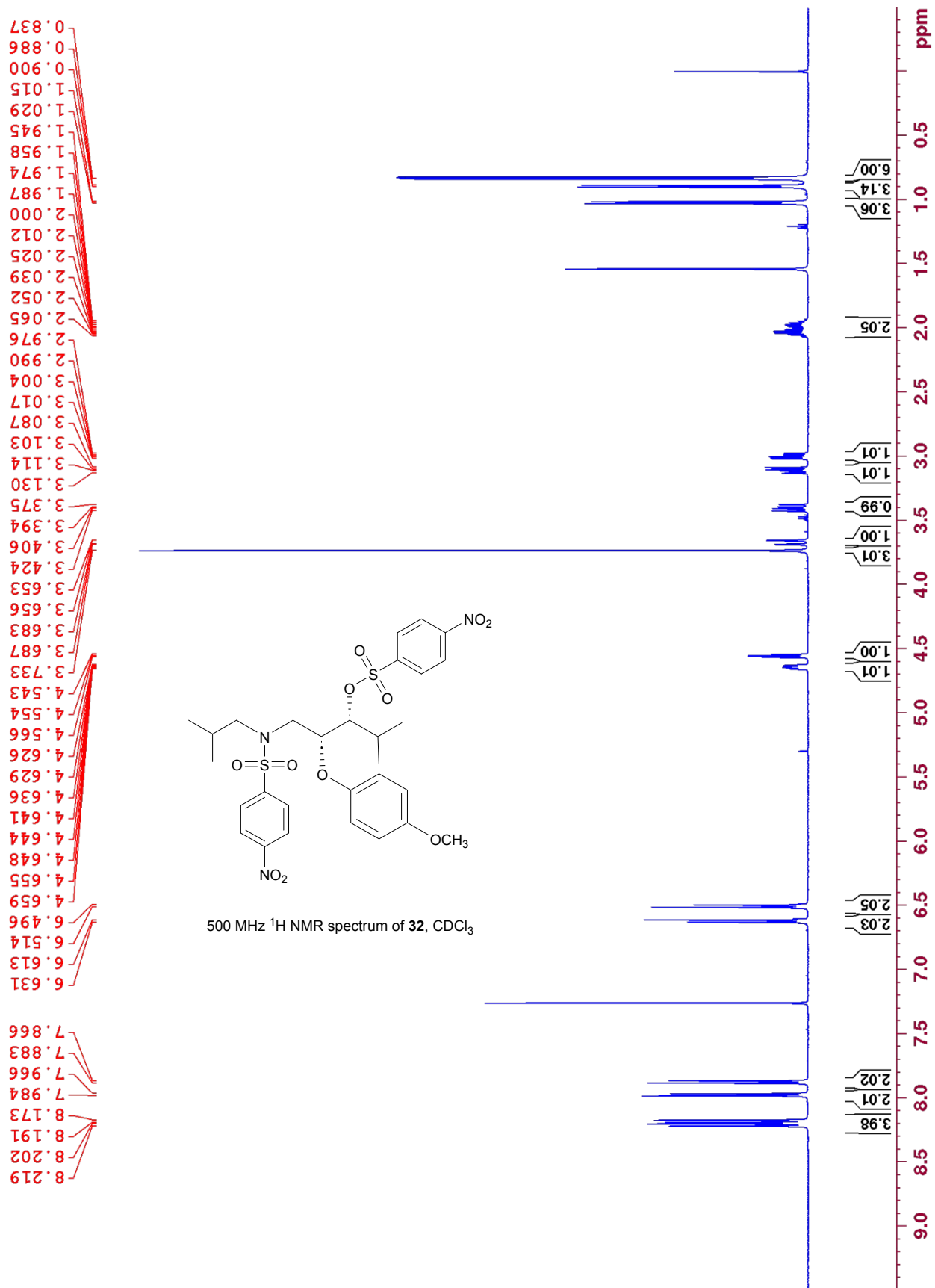


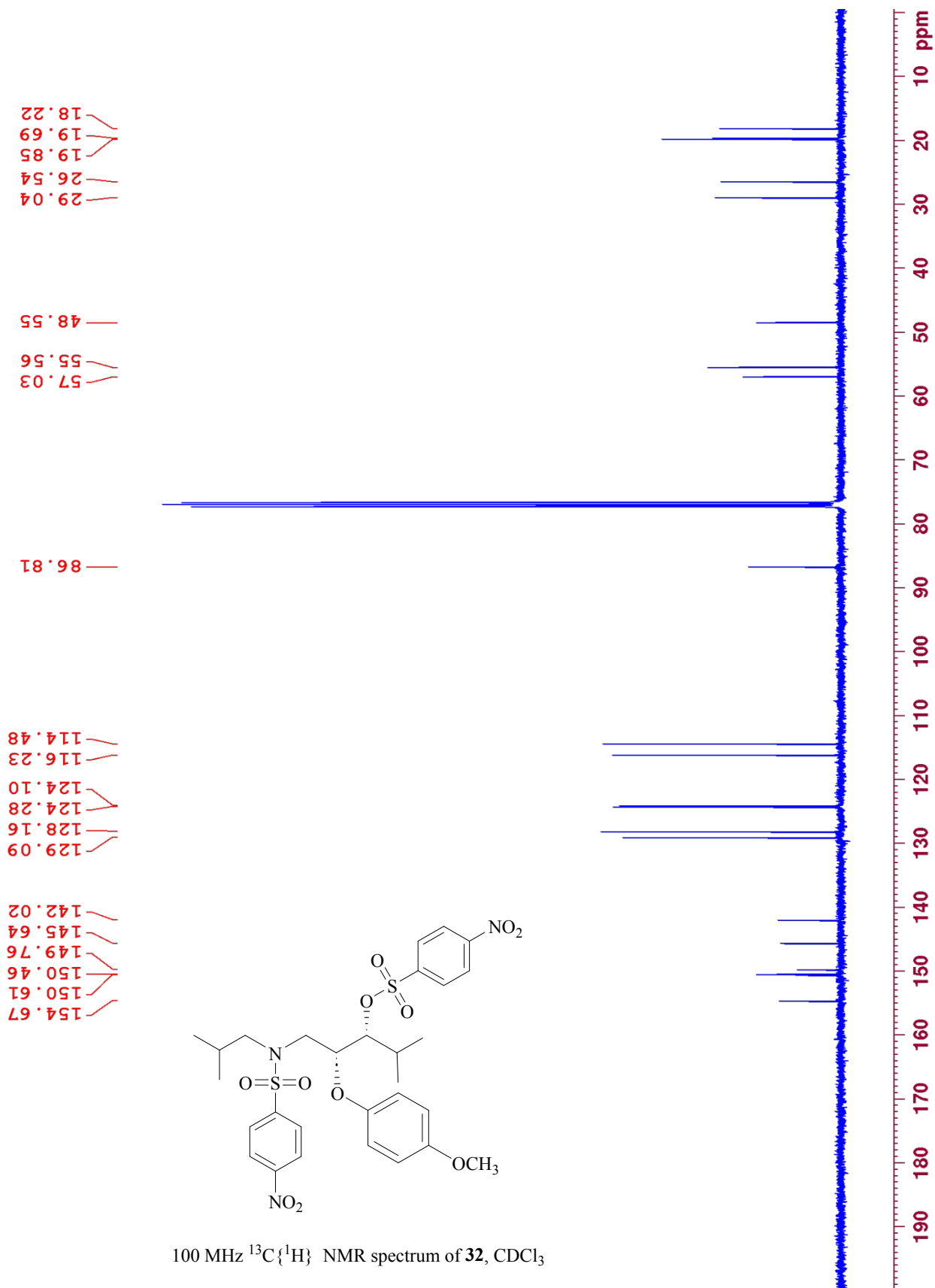


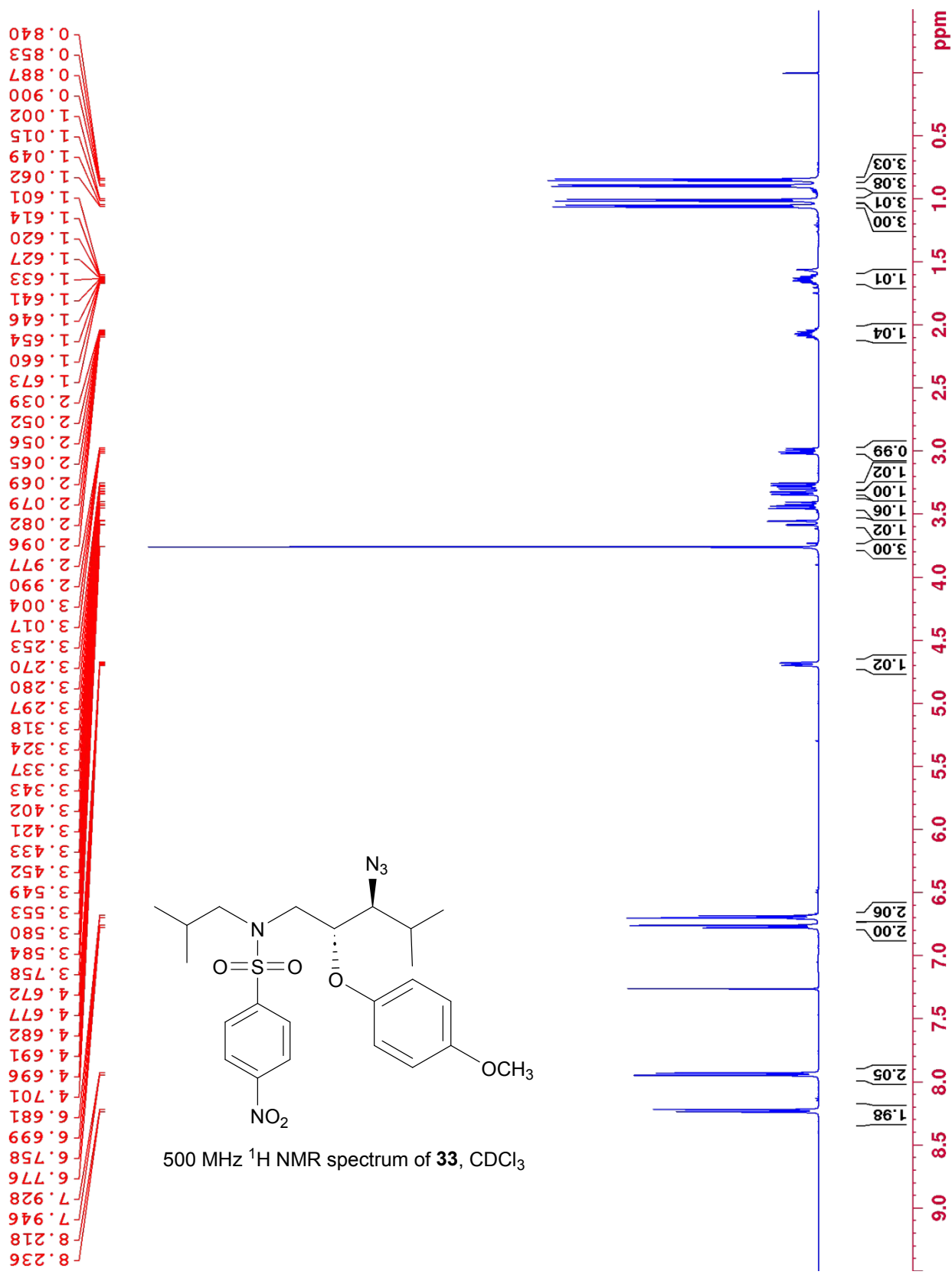


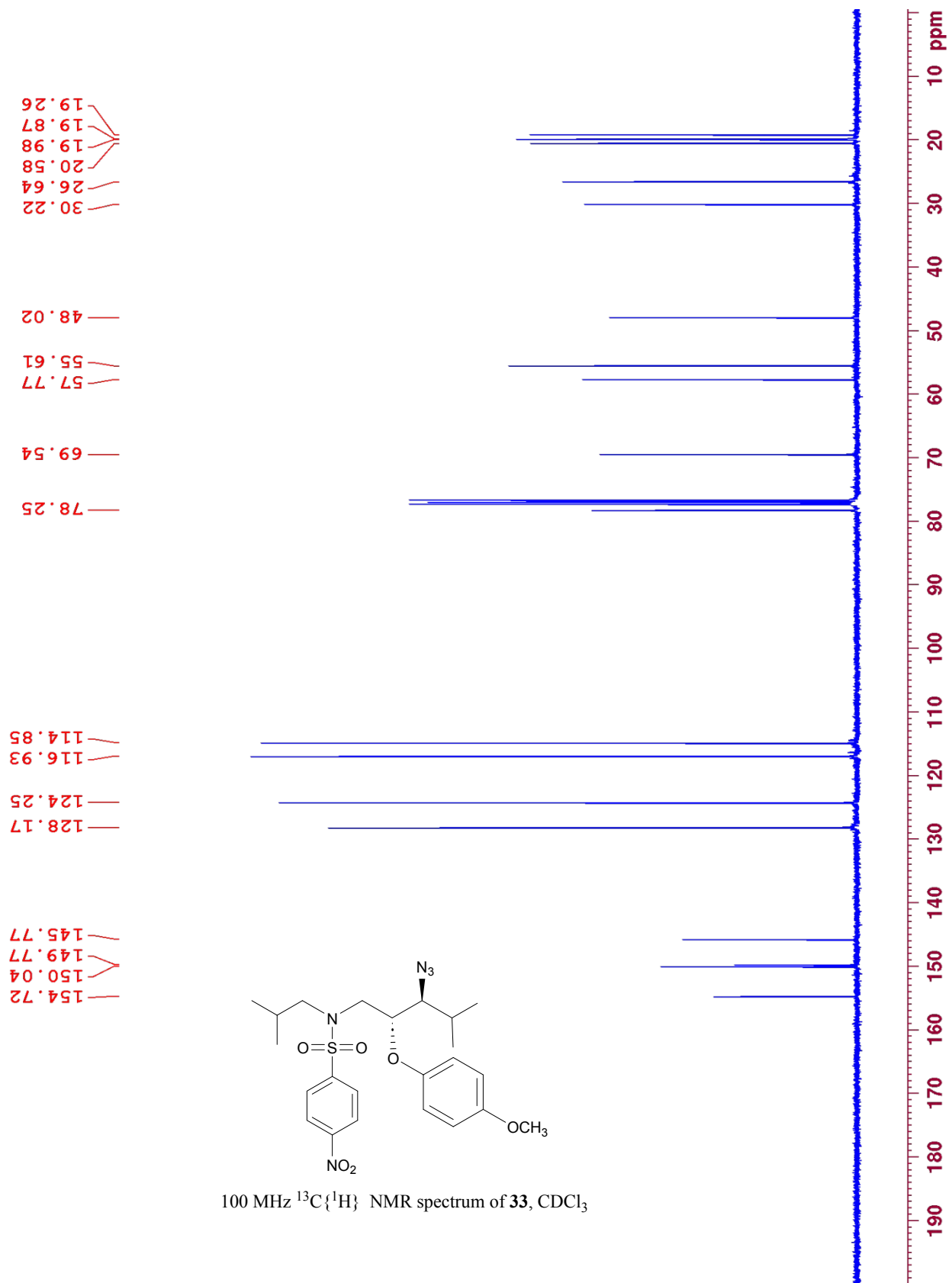


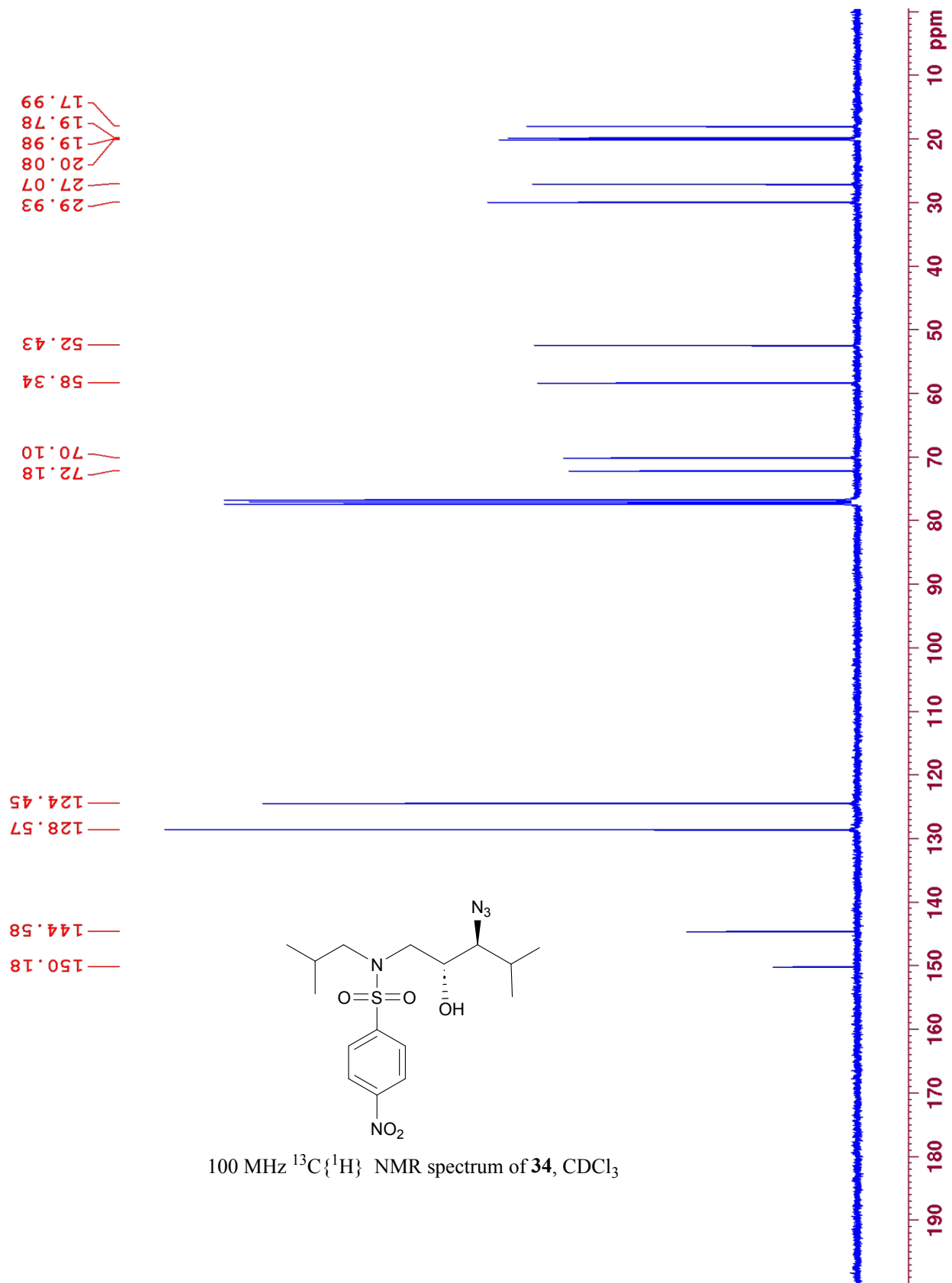


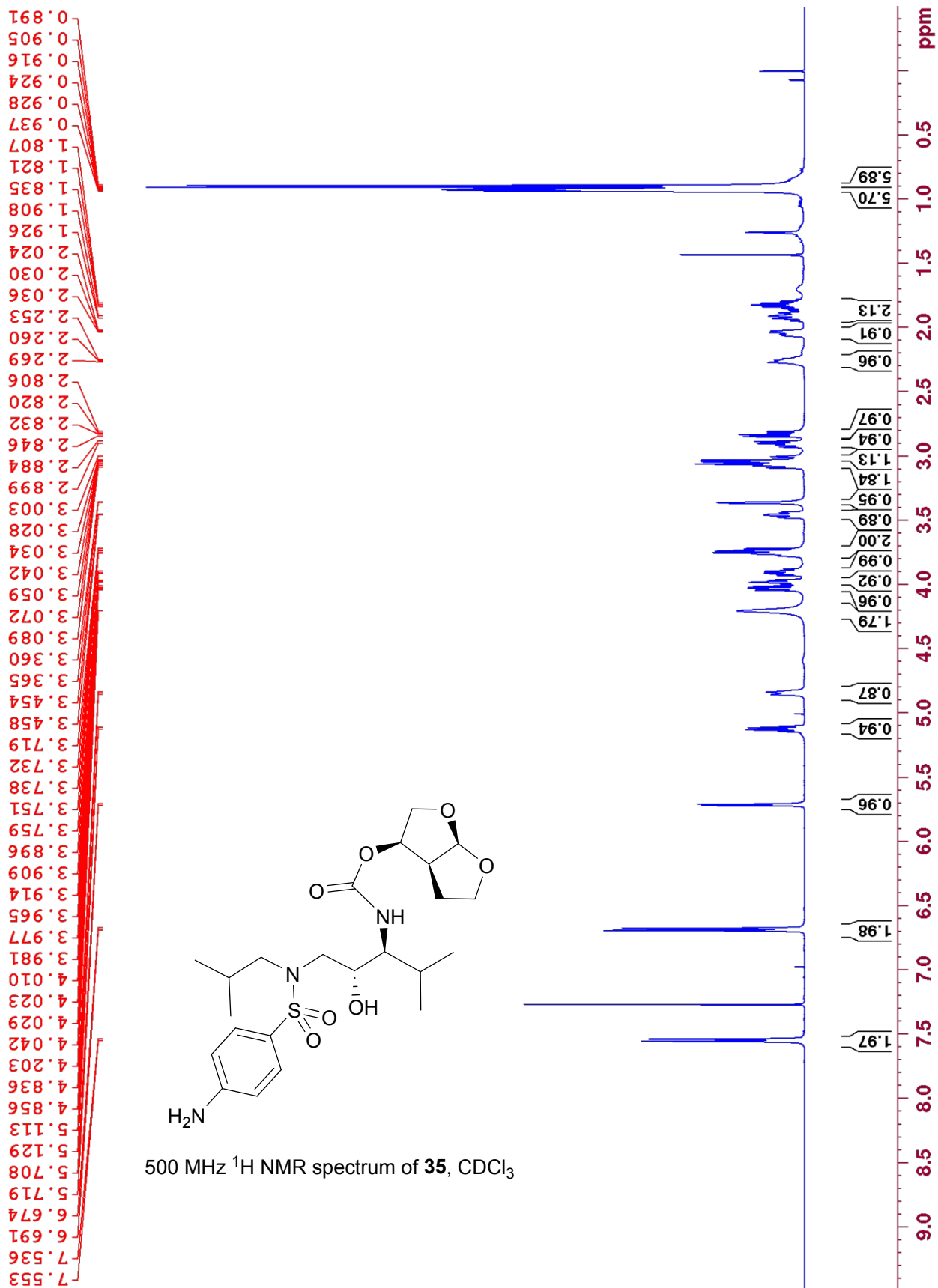


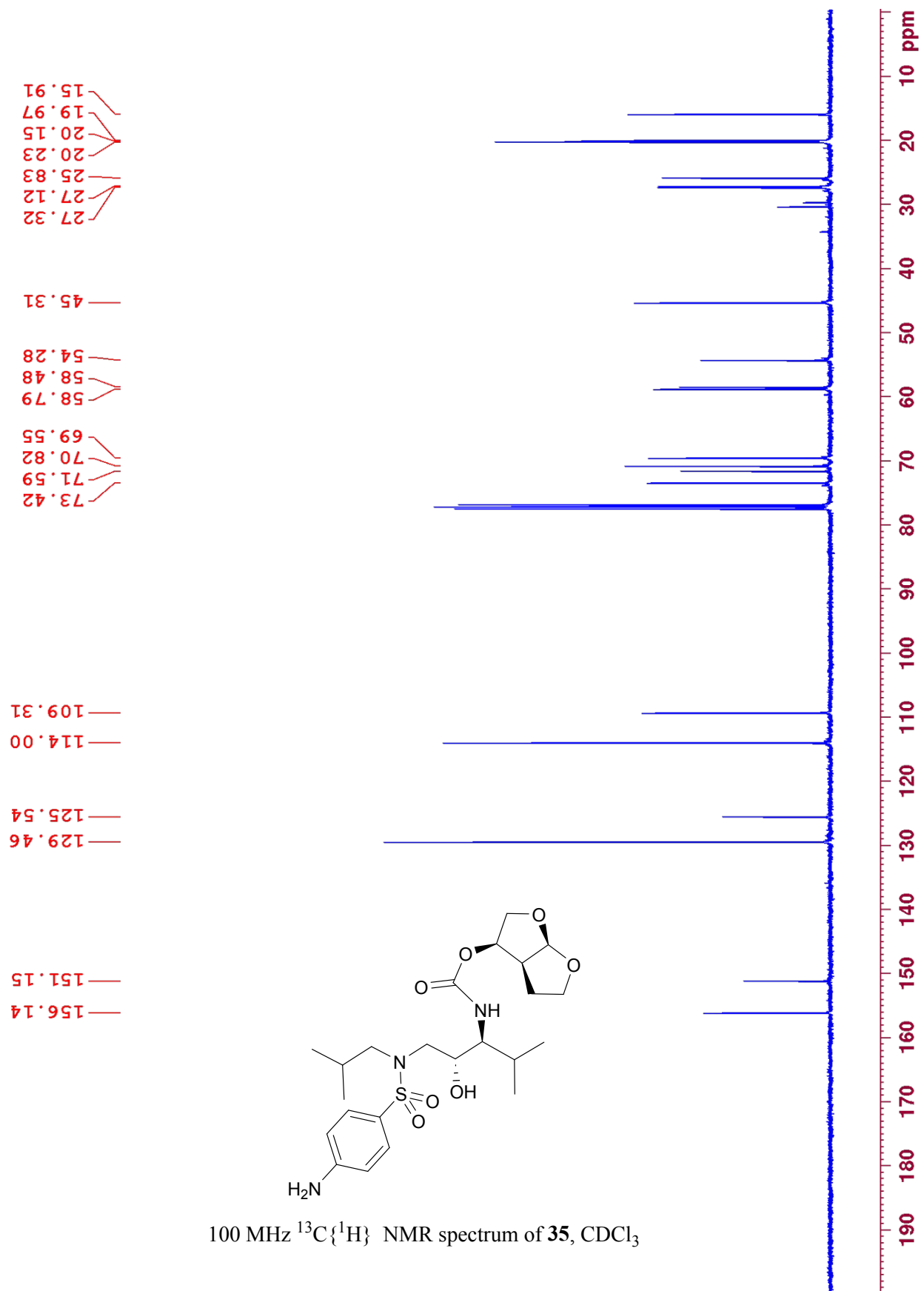


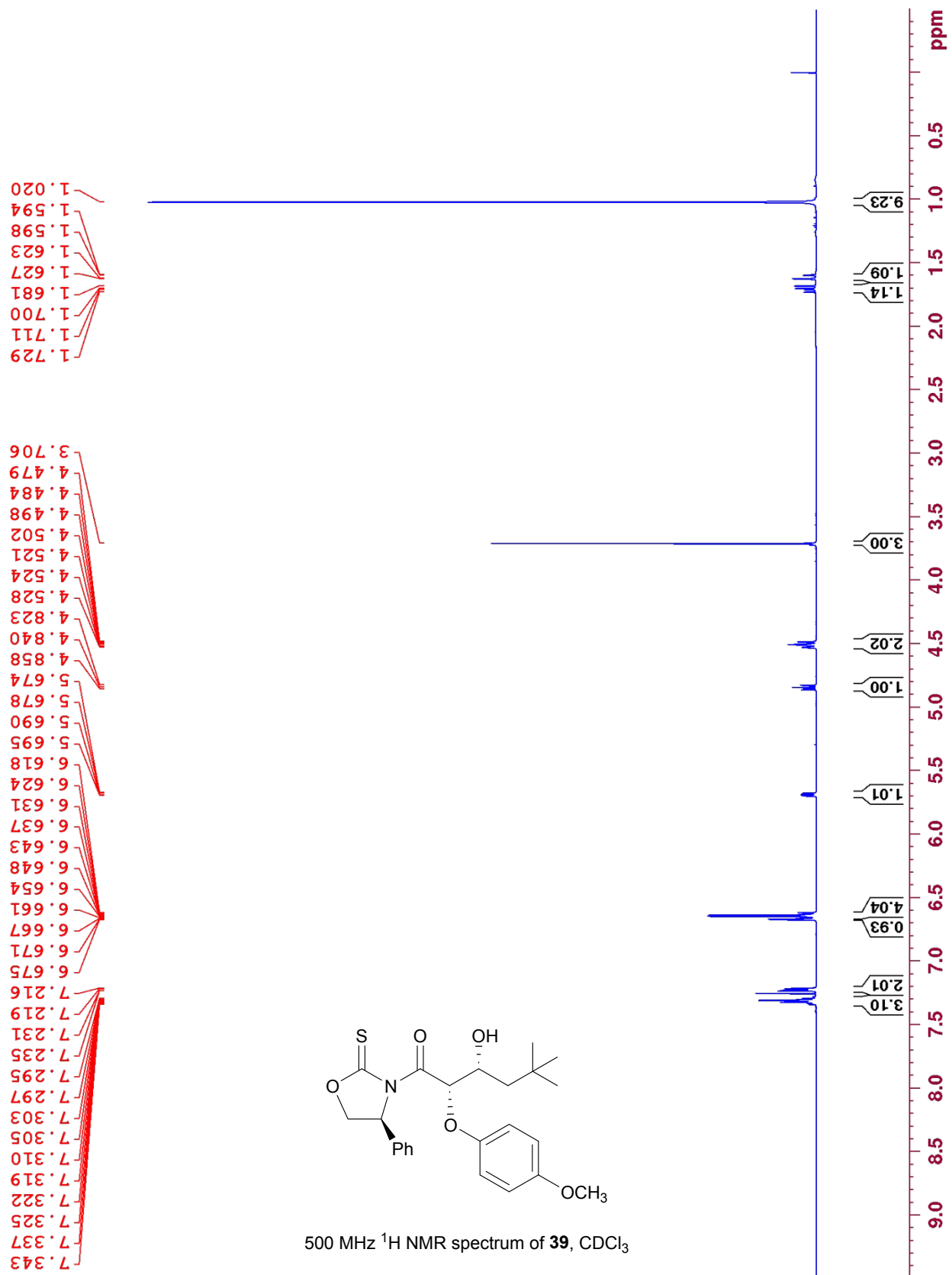


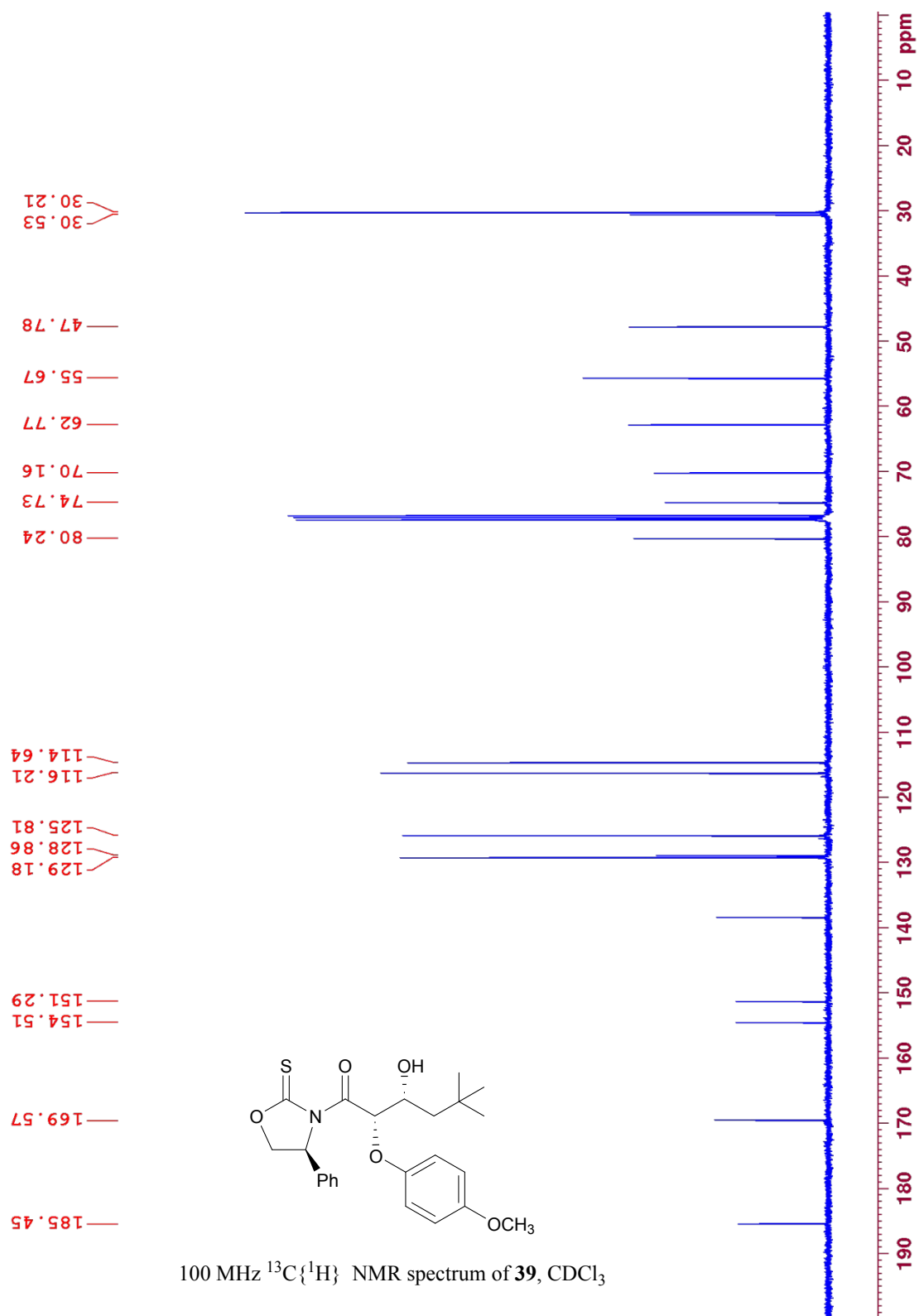


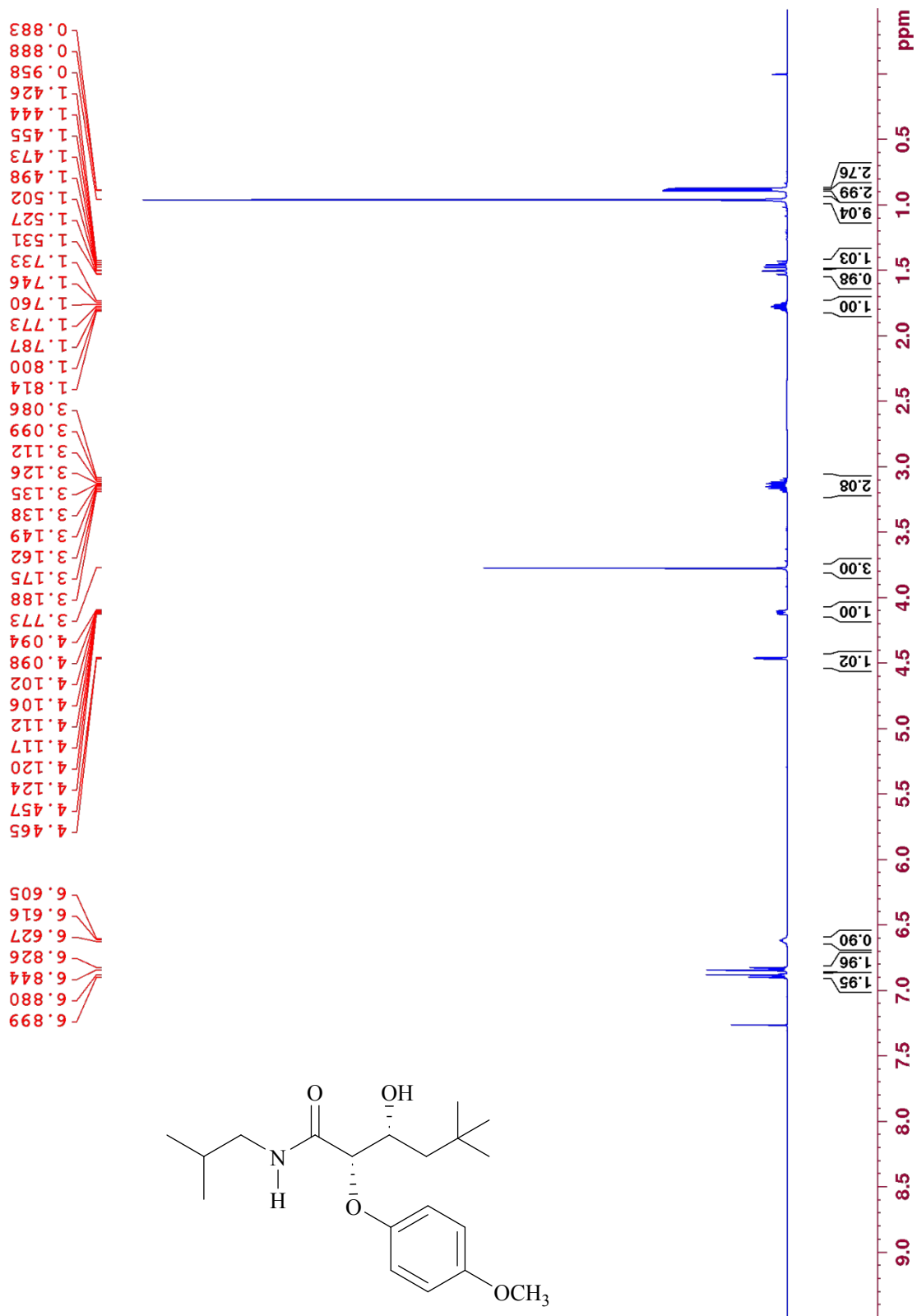




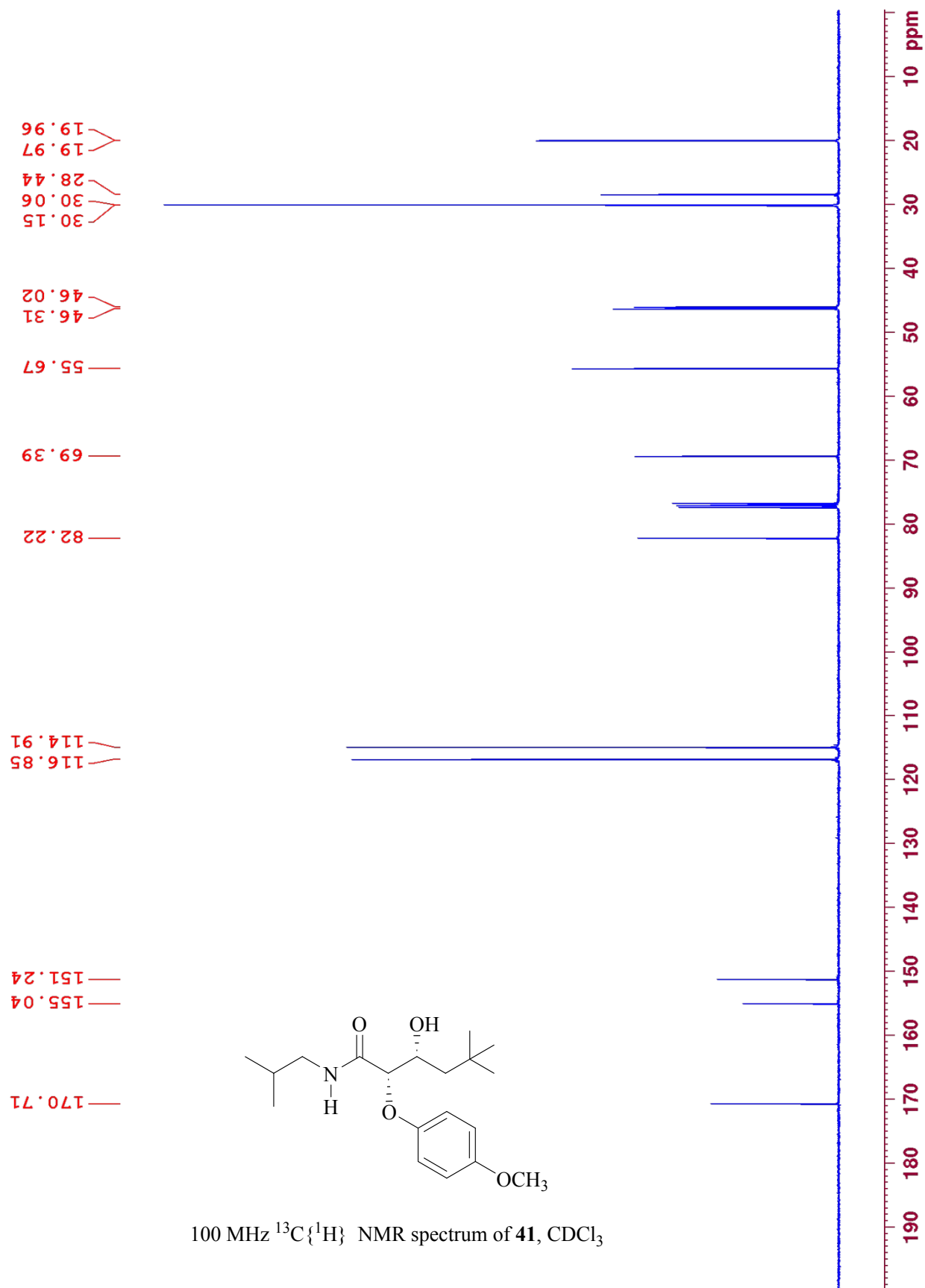


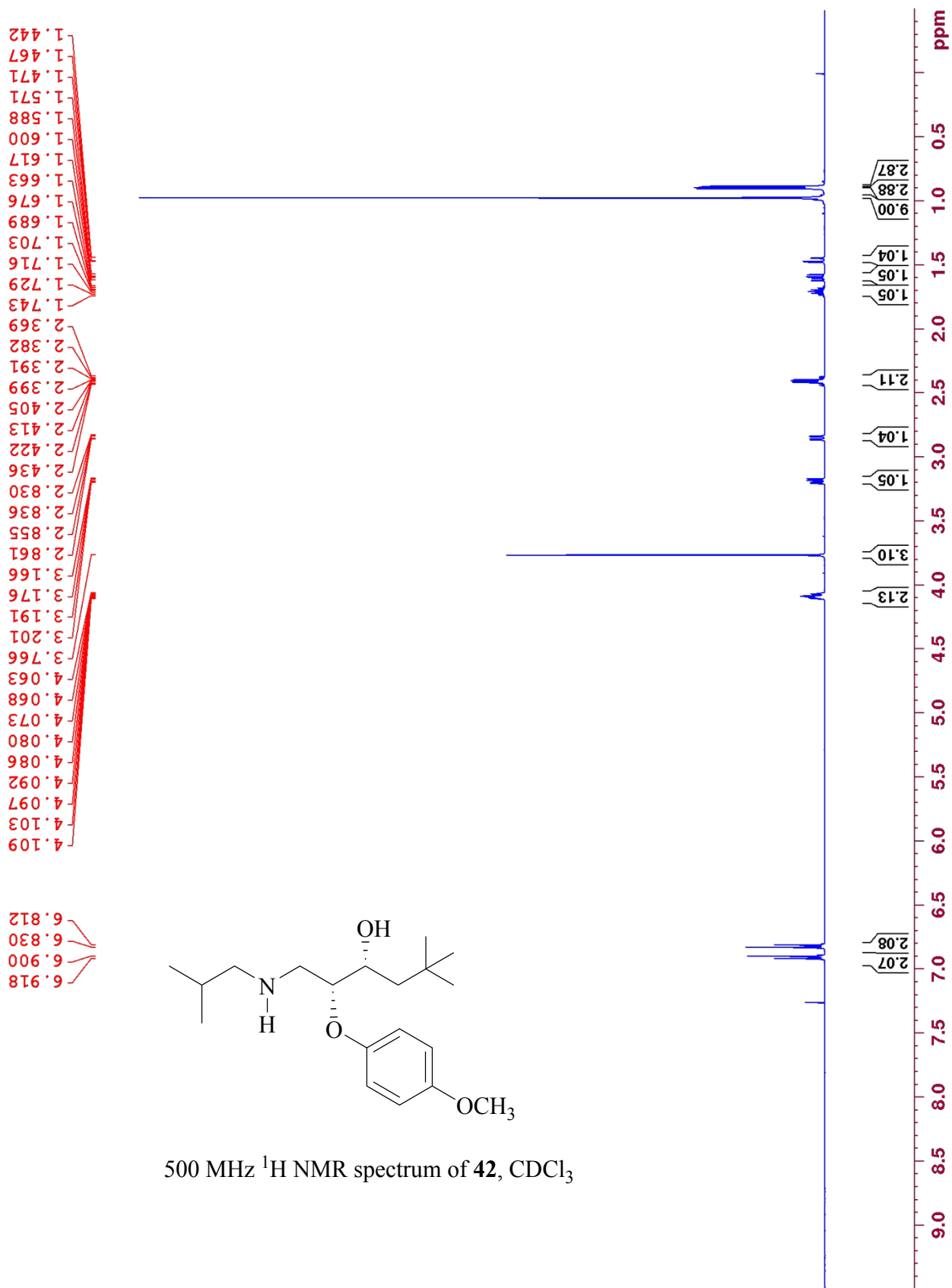


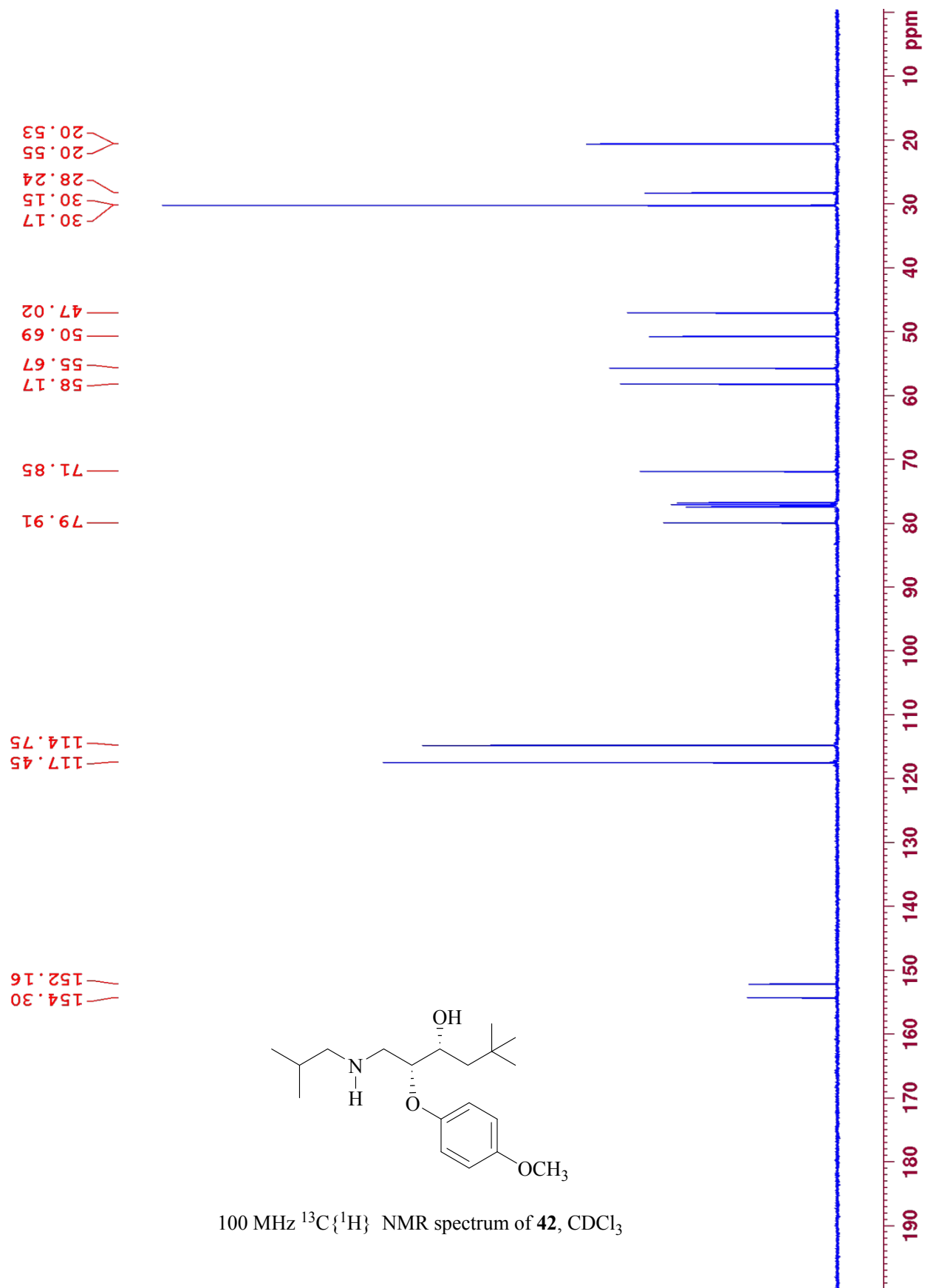




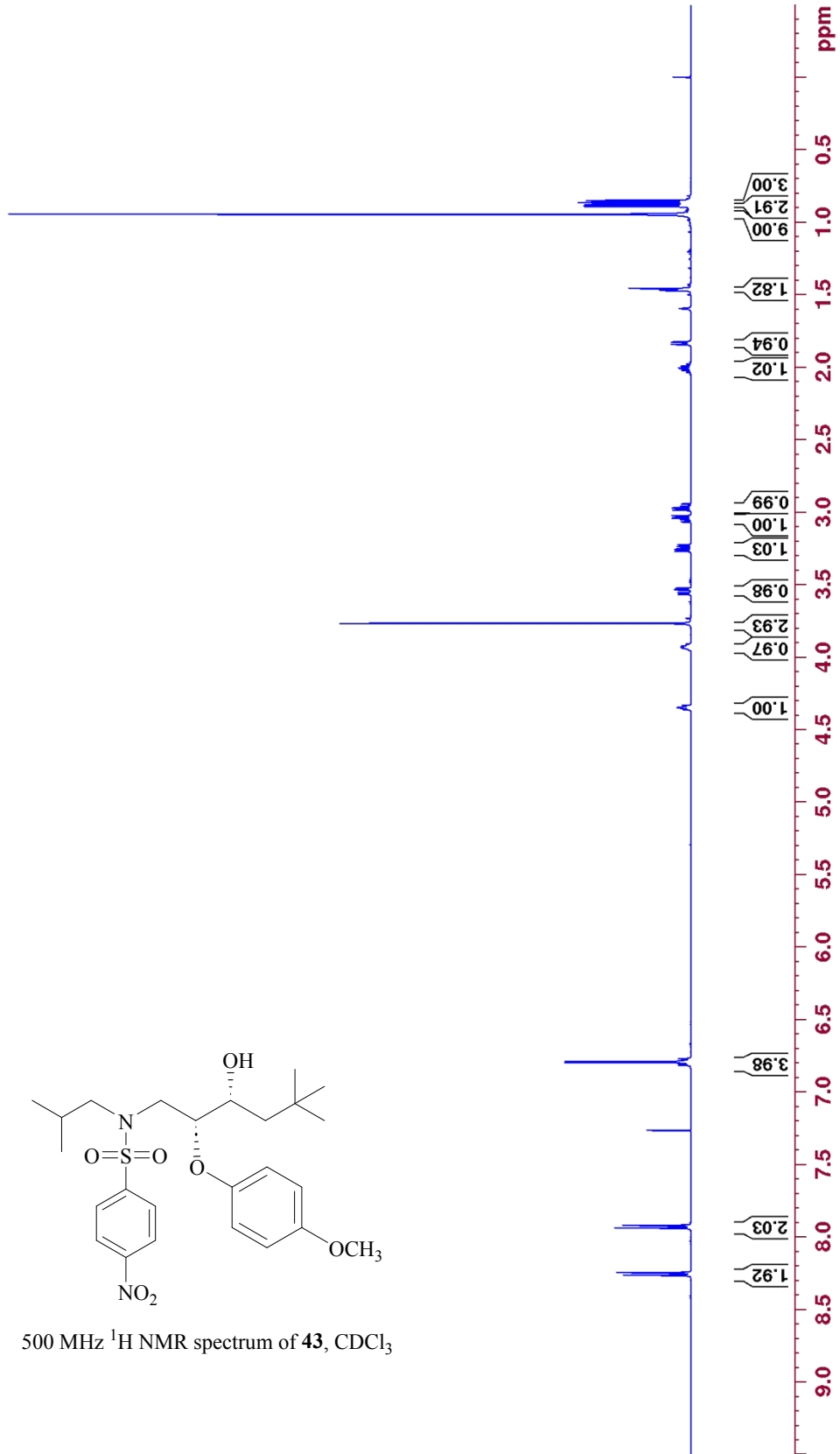
500 MHz ^1H NMR spectrum of **41**, CDCl_3



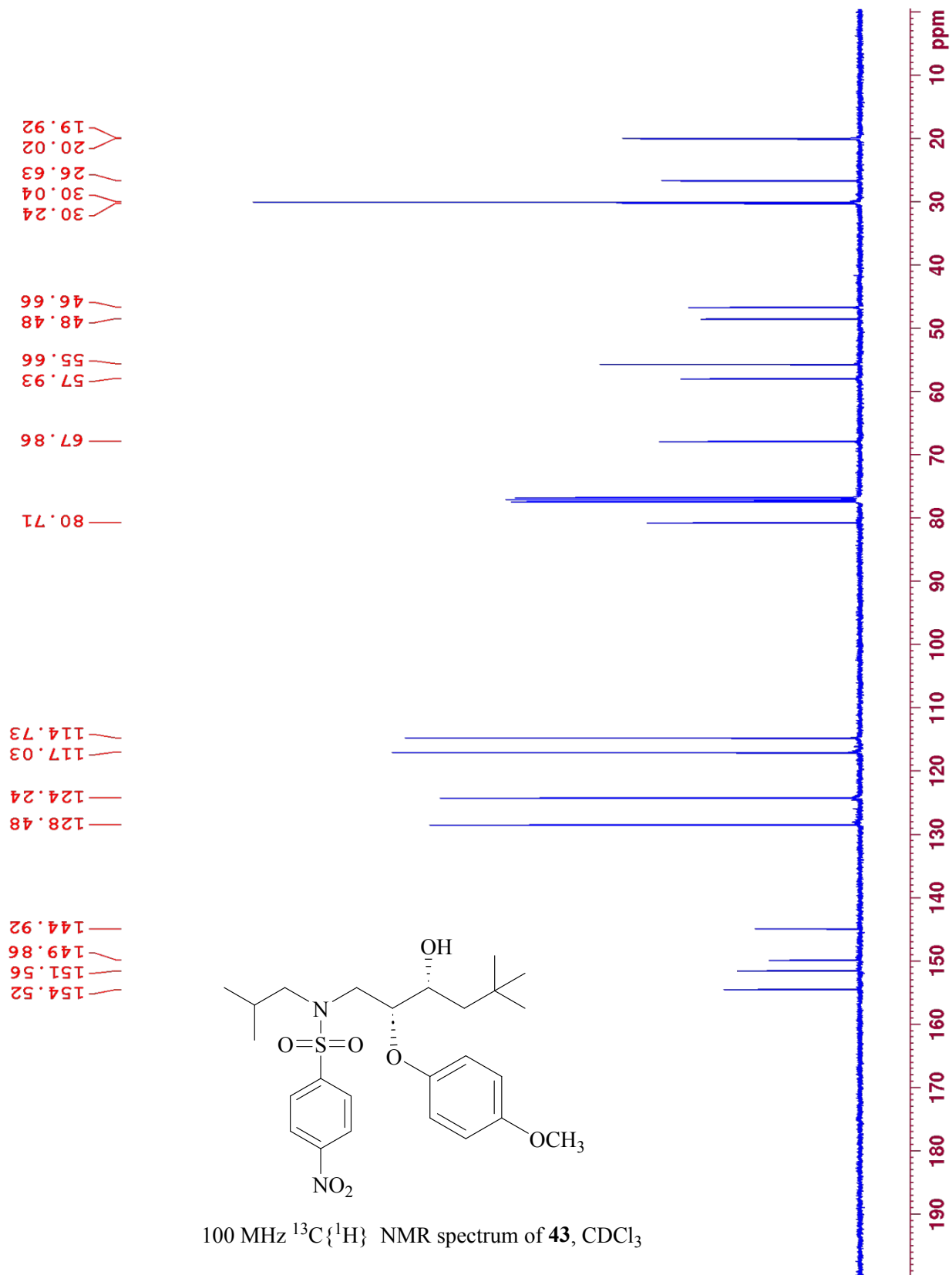


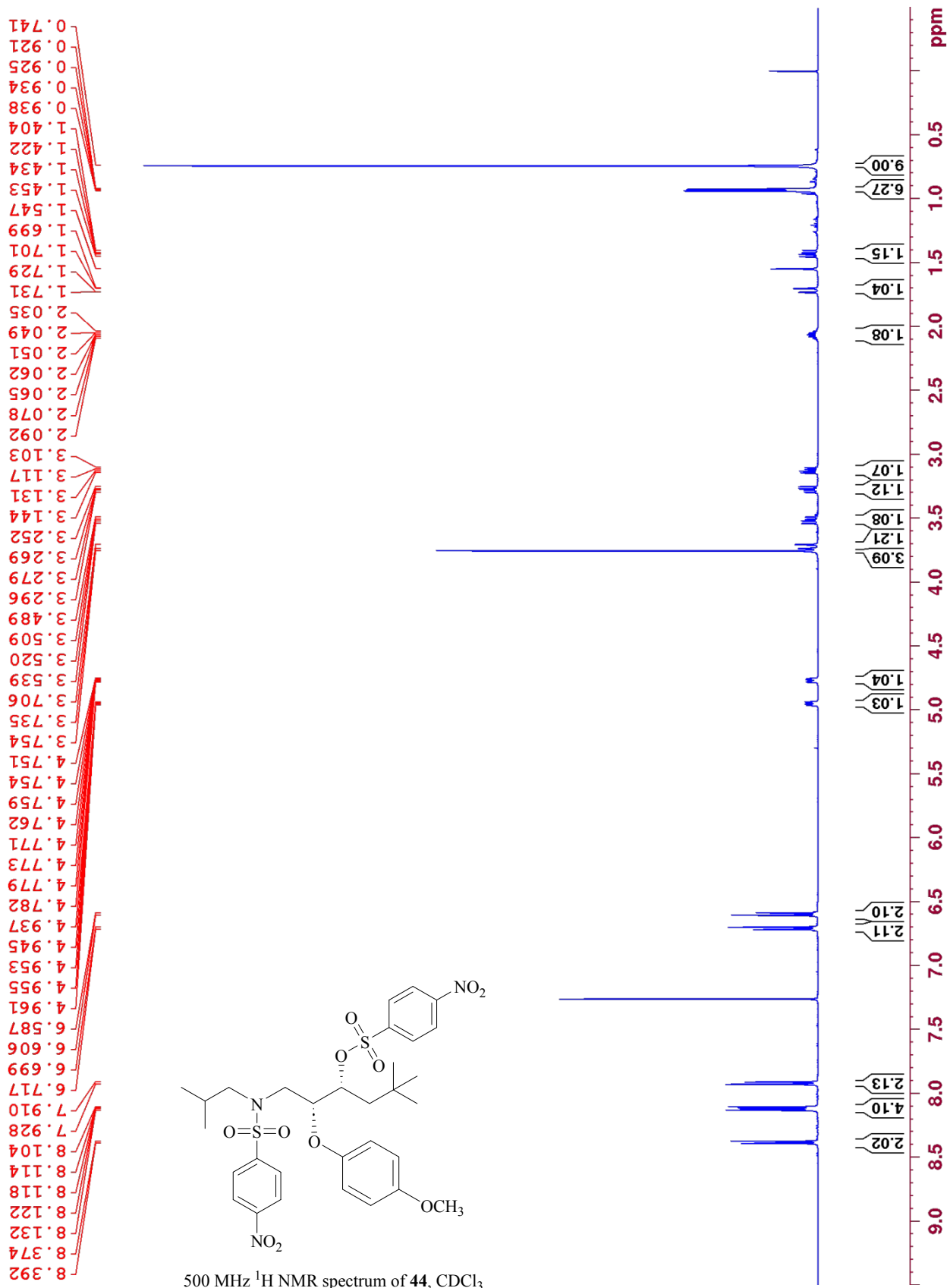


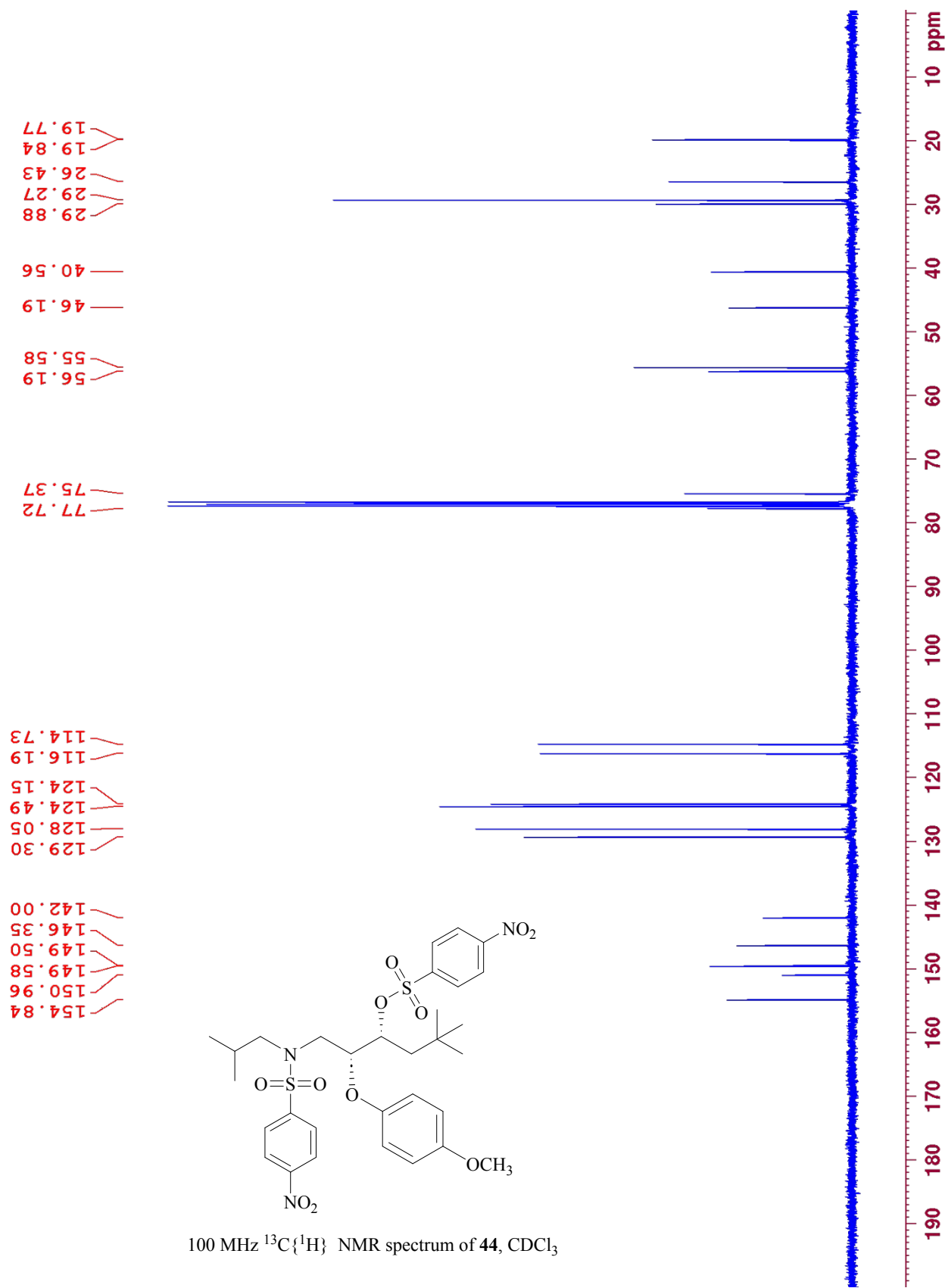
0.946
 1.458
 1.466
 1.472
 1.828
 1.843
 1.967
 1.981
 1.994
 2.008
 2.021
 2.035
 2.049
 2.945
 2.960
 2.972
 2.987
 3.026
 3.041
 3.053
 3.068
 3.226
 3.240
 3.257
 3.270
 3.526
 3.538
 3.557
 3.568
 3.768
 3.909
 3.917
 3.924
 3.930
 3.938
 3.944
 3.952
 4.334
 4.339
 4.347
 4.351
 4.359
 4.364
 6.772
 6.778
 6.784
 6.790
 6.793
 6.797
 6.803
 6.809
 6.815
 7.922
 7.940
 8.248
 8.266

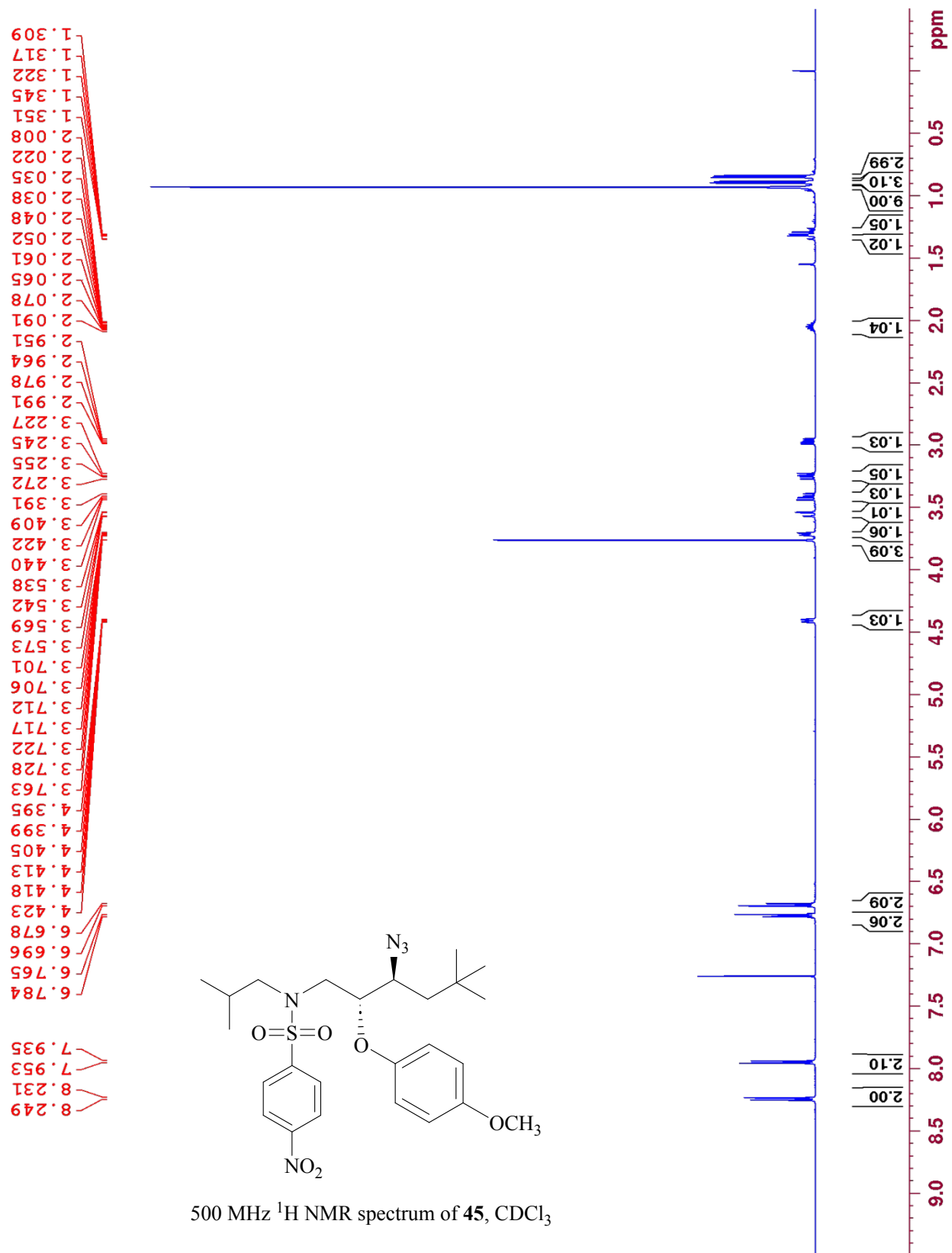


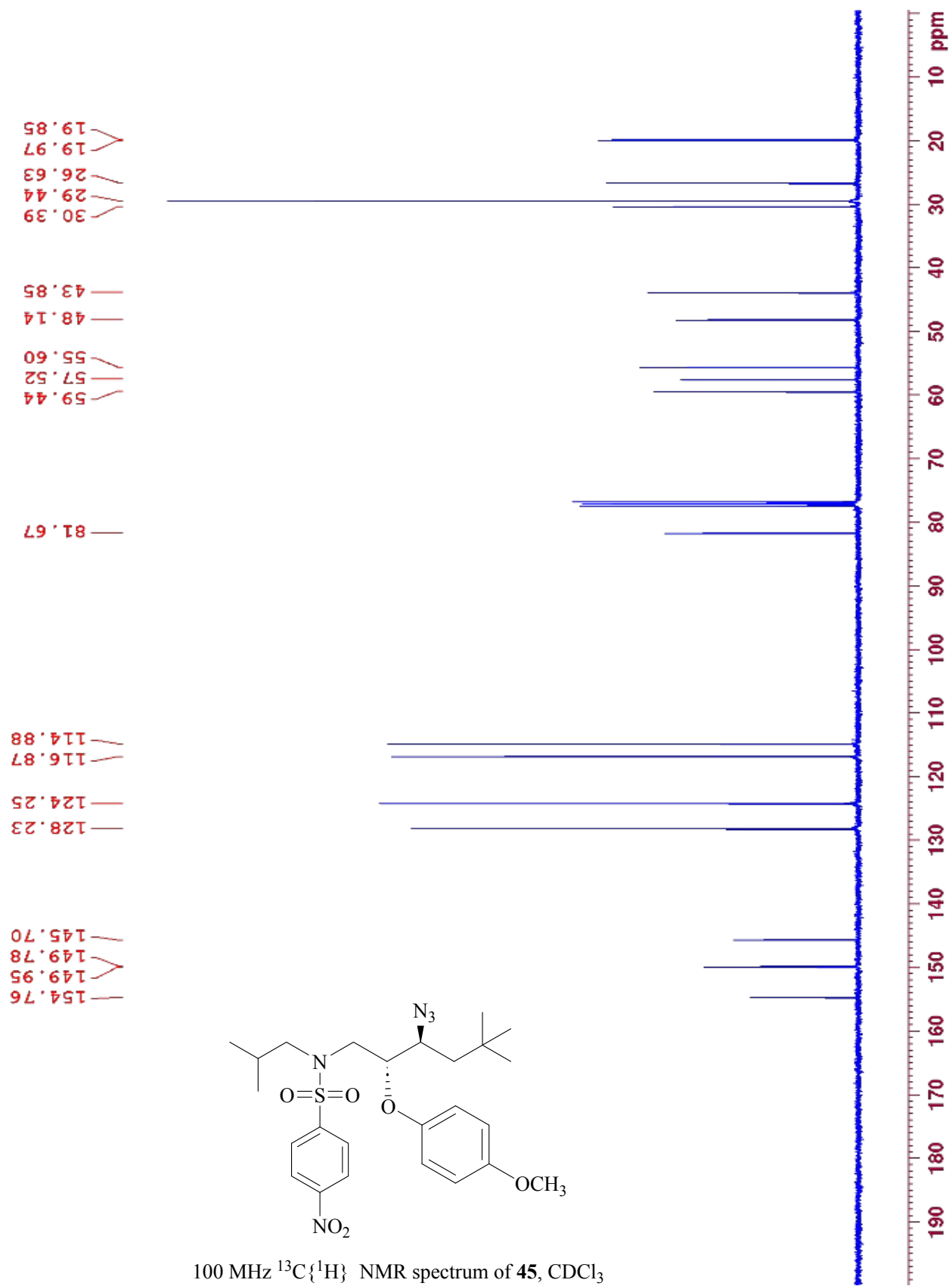
500 MHz ¹H NMR spectrum of **43**, CDCl₃

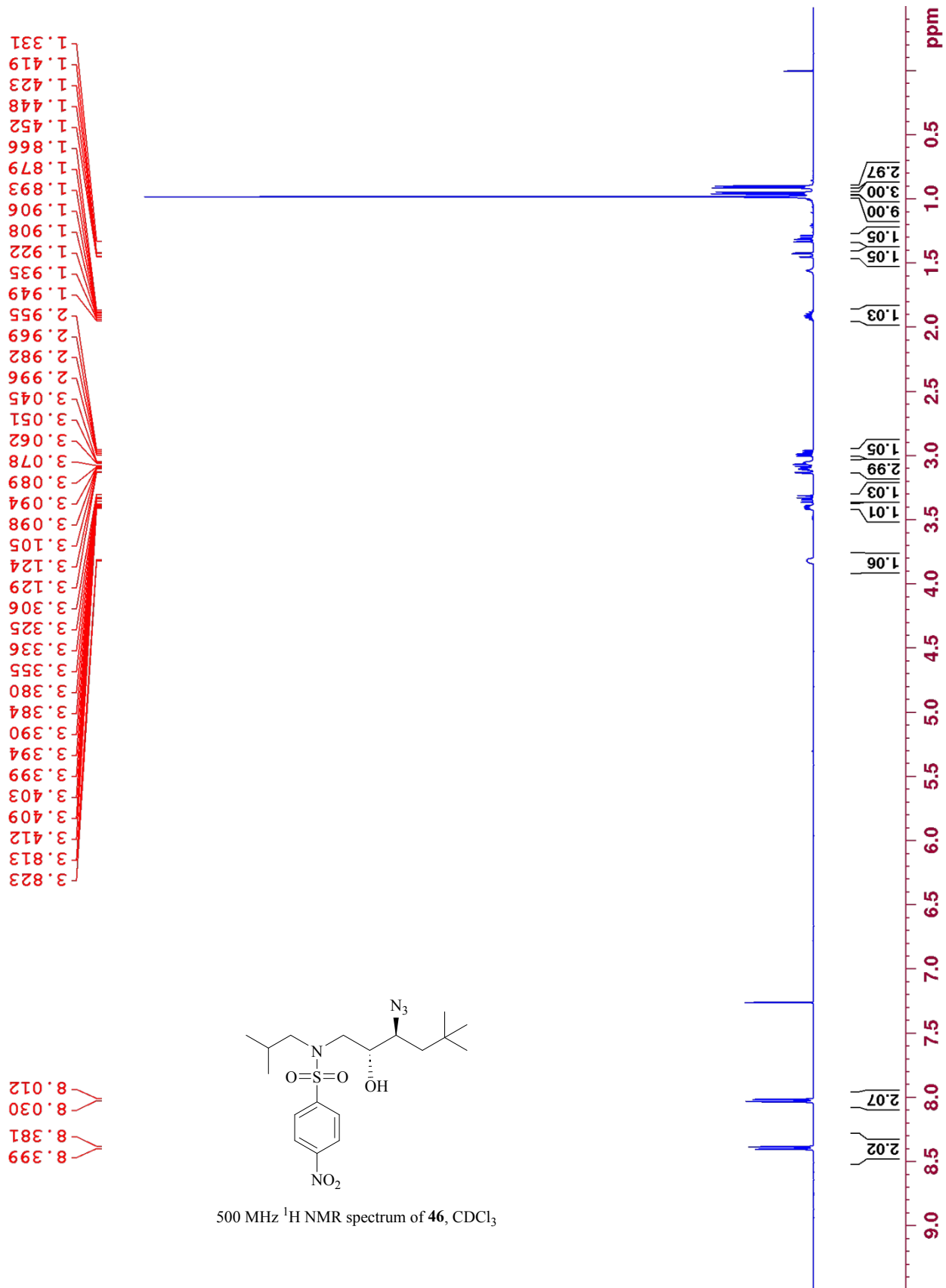


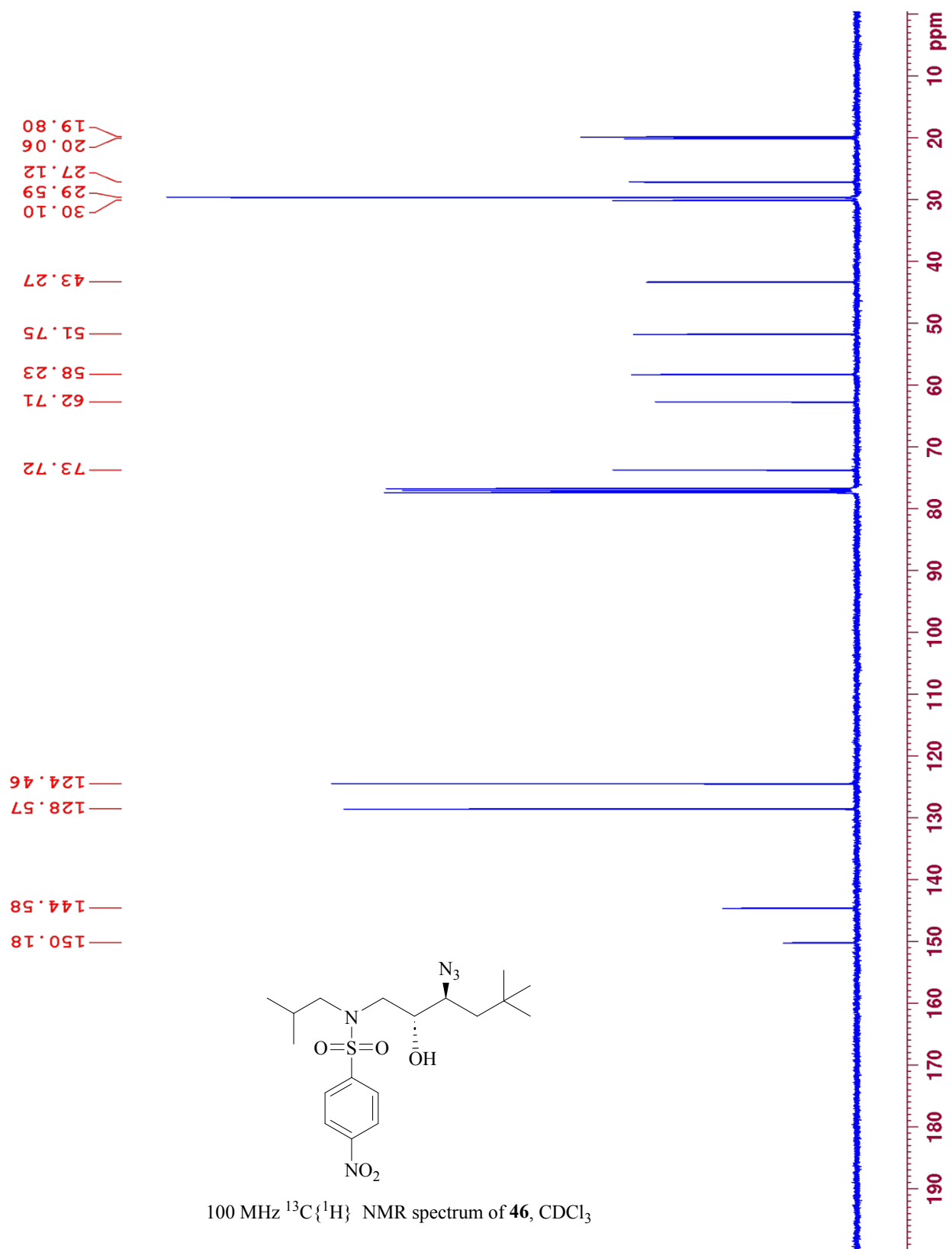


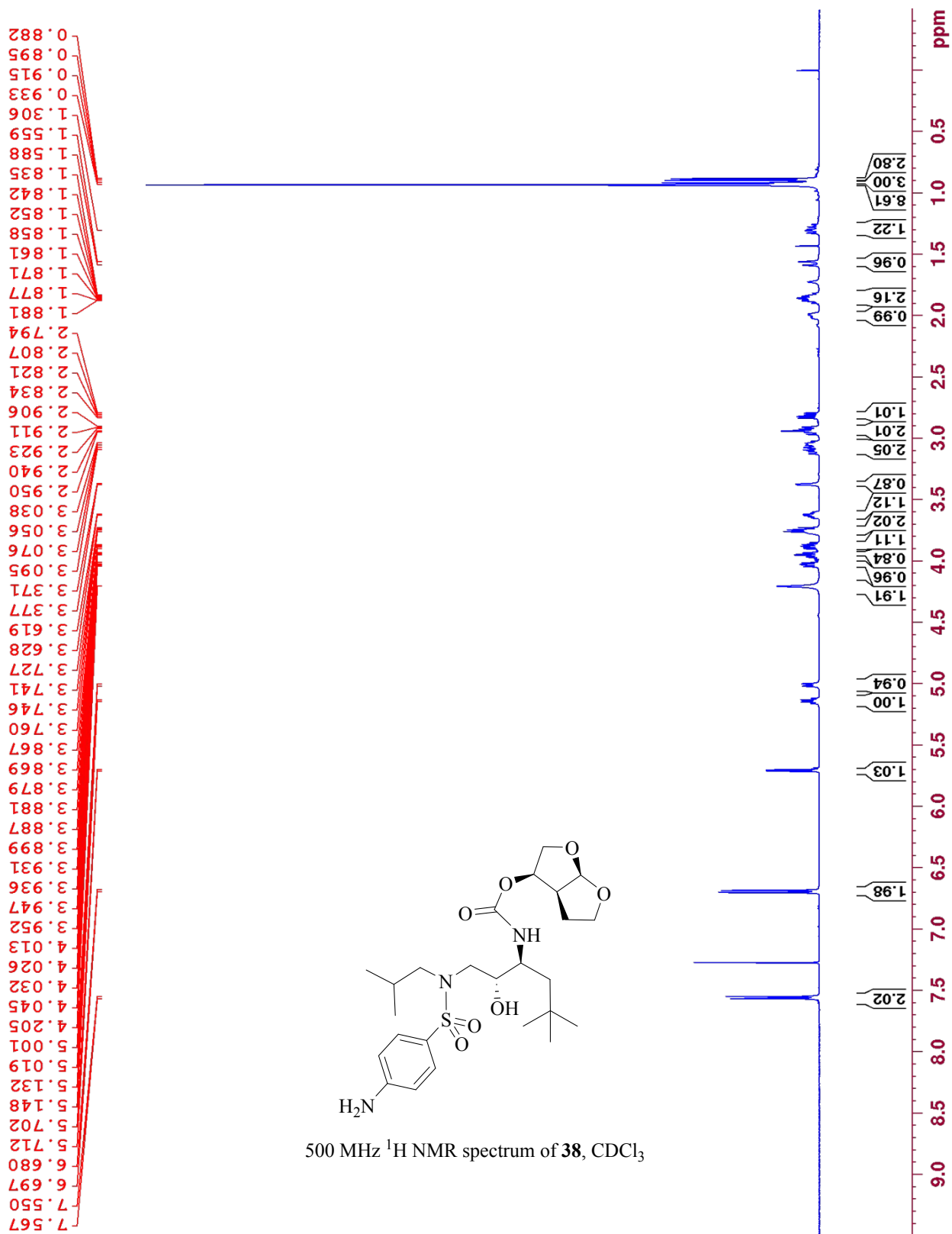


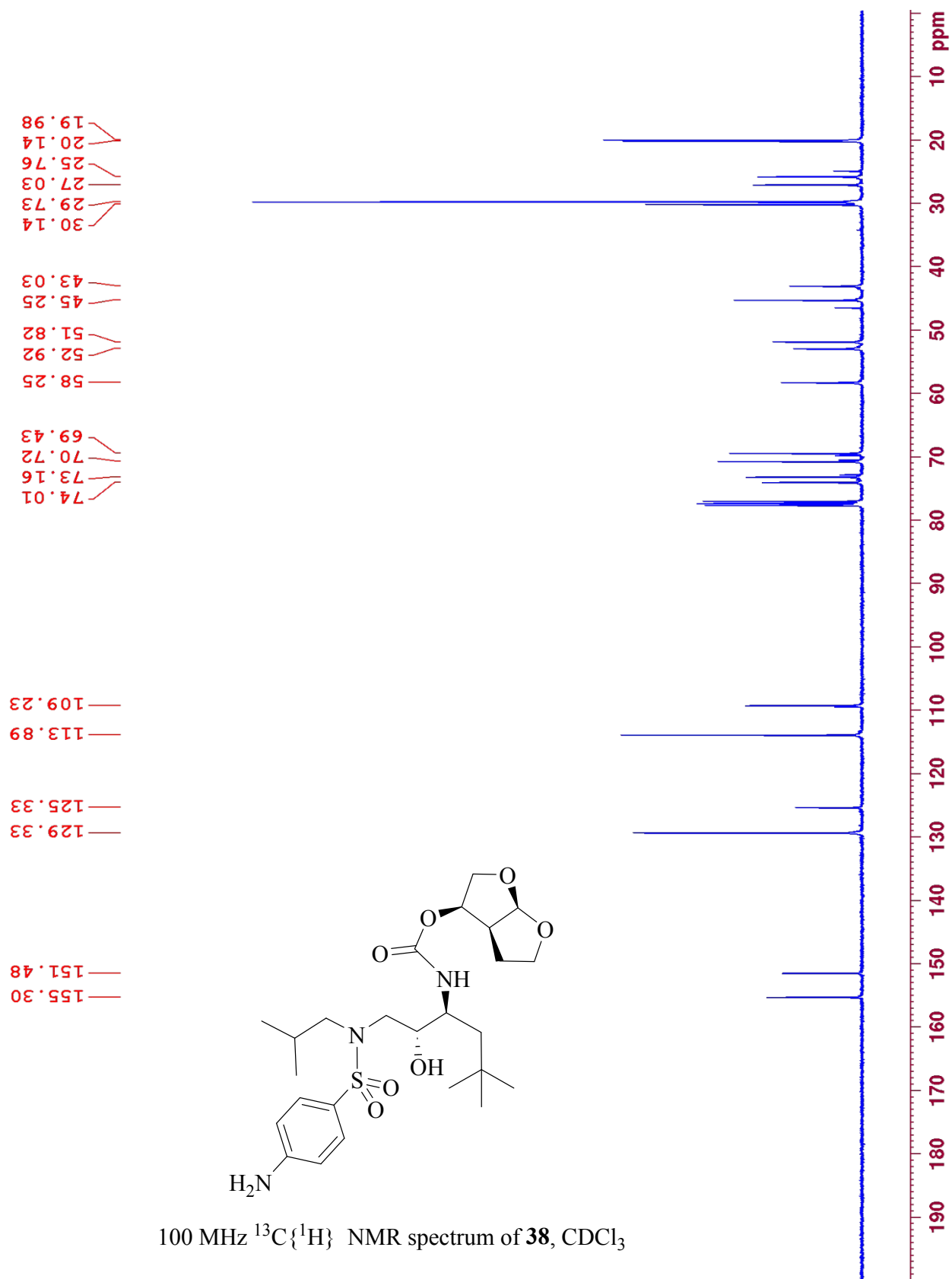












General Crystallographic Experimental Details of (*R,S,R*)-**10**

Samples of X-ray quality crystals were suspended in mineral oil at ambient temperature and a suitable crystal was selected, mounted on a MiTeGen Micromount and transferred to a Bruker AXS SMART APEXII CCD X-ray diffractometer. The X-ray diffraction data were collected at 100(2) K using Mo-K α ($\lambda = 0.71073$ Å) radiation. The frames were integrated with the Bruker SAINT software package using a narrow-frame algorithm.¹ Data were corrected for absorption effects using the Multi-Scan method (SADABS).¹ Structure were solved and refined using the Bruker SHELXTL Software Package,² Molecular diagrams were generated using Mercury.³

Specifically, slow vapor diffusion of pentane into a solution of **10** dissolved in ethyl acetate led to formation of SCXRD quality crystals within 24 hours. A mineral oil coated clear colourless plate-like specimen of **10** (C₂₆H₂₅NO₅S), with approximate dimensions 0.122 mm x 0.273 mm x 0.312 mm, was harvested and placed in the 100(2) K cryogenic stream on the goniometer. The X-ray intensity data were measured. A total of 3672 frames were collected. The total exposure time was 4.08 hours. The integration of the frame data using a triclinic unit cell yielded a total of 45216 reflections to a maximum θ angle of 33.10° (0.65 Å resolution), of which 7908 were independent (average redundancy 5.718, completeness = 95.8%, $R_{\text{int}} = 5.12\%$, $R_{\text{sig}} = 4.41\%$) and 6792 (85.89%) were greater than $2\sigma(F^2)$. The final cell constants of $a = 10.5787(3)$ Å, $b = 10.2358(3)$ Å, $c = 10.8871(3)$ Å, $\beta = 109.878(2)^\circ$, volume = 1108.63(6) Å³, are based upon the refinement of the XYZ-centroids of 7908 reflections above $20 \sigma(I)$ with $4.638^\circ < 2\theta < 59.13^\circ$. Data were corrected for absorption effects. The ratio of minimum to maximum apparent transmission was 0.938. The calculated minimum and maximum transmission coefficients (based

on crystal size) are 0.9440 and 0.97800. The structure was solved and refined using the space group $P2_1$, with $Z = 2$ for the formula unit, $C_{26}H_{25}NO_5S$. All non-H atoms were refined anisotropically. All H atoms were identifiable in the difference Fourier, but with the exception of the H atom attached to O, were included in the final refinement using the riding-model approximation. $d(C-H) = 0.93 \text{ \AA}$, $U_{iso} = 1.2U_{eq}(C)$ for aromatic, 0.97 \AA , $U_{iso} = 1.2 U_{eq}(C)$ for methylene, 0.98 \AA , $U_{iso} = 1.2 U_{eq}(C)$ for methine, and 0.96 \AA , $U_{iso} = 1.5 U_{eq}(C)$ for methyl H atoms. Coordinates of the H atom attached to the O atom were freely refined with $U_{iso} = 1.5U_{eq}(O)$. The final anisotropic full-matrix least-squares refinement on F^2 with 302 variables converged at $R_1 = 4.01\%$, for the observed data and $wR_2 = 9.35\%$ for all data. The goodness-of-fit was 1.026. The largest peak in the final difference electron density synthesis was $0.545 \text{ e}^-/\text{\AA}^3$ and the largest hole was a $-0.393 \text{ e}^-/\text{\AA}^3$ with an RMS deviation of $0.053 \text{ e}^-/\text{\AA}^3$. On the basis of the final model, the calculated density was 1.389 g/cm^3 and $F(000)$, 488 e^- . The absolute configuration was confirmed using 2811 quotients in determination of a Flack parameter of 0.10(2). All residual electron density was within accepted norms and was deemed of no chemical significance.

CCDC-2285488 contains the supplementary crystallographic data for this structure. These data can be obtained free of charge from the Cambridge Crystallographic Data Centre via

<https://summary.ccdc.cam.ac.uk/structure-summary?ccdc=2285488>.

1. Bruker, *APEX4 v2021.10-0*, Bruker AXS Inc., Madison, Wisconsin, USA, 2021.
2. Sheldrick, G. M. Crystal Structure Refinement with SHELXL. *Acta Cryst.* **2015**, *C71*, 3-8.
3. Macrae, C. F.; Sovago, I.; Cottrell, S. J.; Galek, P. T. A.; McCabe, P.; Pidcock, E.; Platings, M.; Shields, G. P.; Stevens, J. S.; Towler, M.; Wood, P. A. Mercury 4.0: from Visualization to Analysis, Design and Prediction. *J. Appl. Cryst.* **2020**, *53*, 226-235.

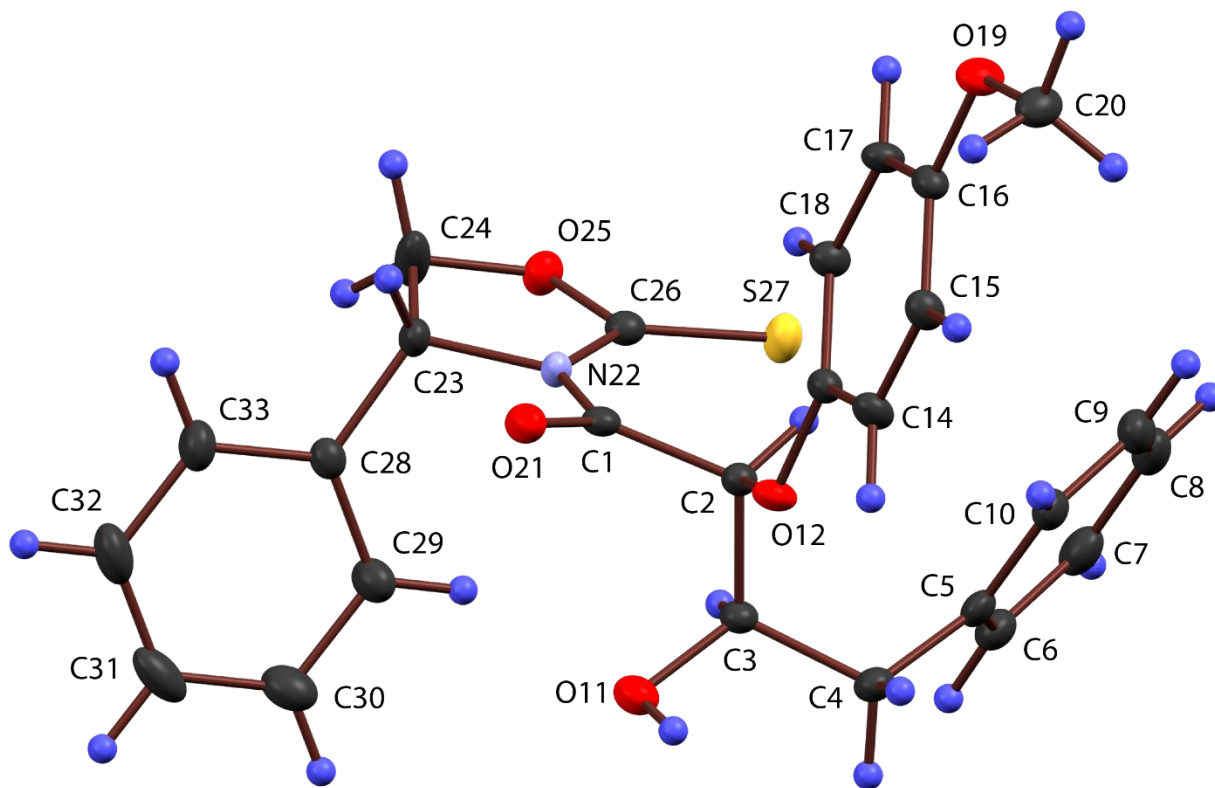


Figure S-1: X-ray crystal structure ORTEP rendering of **10**. The ellipsoids of all non-hydrogen atoms are shown at the 50% probability level; hydrogen atoms are drawn arbitrarily small.